UNIVERSITY OF VAASA

FACULTY OF TECHNOLOGY

COMMUNICATIONS AND SYSTEMS ENGINEERING

Olaobaju Abdulrahman

DEVICE-TO-DEVICE COMMUNICATION IN 5G CELLULAR NETWORKS

Master's thesis for the degree of Master of Science in Technology submitted for assessment, Vaasa, February 10, 2018.

Supervisor Professor Mohammed Elmusrati

Instructor Professor Tapani Ristaniemi

ACKNOWLEDGEMENTS

In the Name of Allah, the Most Beneficent, the Most Merciful. All praise and adoration are due to Almighty Allah (SWT). May the peace and blessing of Allah be upon the noble Prophet Muhammed (SAW), his household, his companions and those who follow his path till the day of resurrection.

I would like to seize this opportunity to express my heartfelt gratitude to my supervisor, Professor Mohammed Elmusrati, for his guidance, support, encouragement, and knowledge imparted during the period of my master's degree program and towards the success of this thesis work. I acknowledge the support and effort of my instructor, Professor Tapani Ristaniemi, towards the completion of this thesis work. My sincere appreciation also goes to the entire member of the Communications and Systems Engineering Group of the University of Vaasa for their immense contributions and support towards the successful completion of my master's degree program.

My profound appreciation goes to my family for their love, prayers, encouragements, and supports throughout my master's degree program. I pray that Almighty Allah continues to bless, guide, and protect you all, and grant you your hearth desires. Finally, a warm appreciation goes to all my friends and classmates for their support and advice during my studies. May Almighty God bless you all and make your dreams a reality.

TABLE OF CONTENTS

SYMBOLS

α_c	Stackelberg Variable of c
β	Constant Earn Ratio
γ_k	SINR of k
γ_k^{tgt}	Predefined SINR Target of k
Γ_c	Candidate Set of c
δ_j	SIR of Receiver j
Δ_c	Reuse Set of c
ΔC_k	Increase in Capacity of k
ΔP_k	Increase in Transmit Power of k
ζ_k	Effective Interference of k
η	Power Efficiency
λ	Wavelength of the Transmitted Signal
$\xi_{i,j}$	Exponentially Distributed Fast Fading Gain between Transmitter i and Receiver j
ρ	Path Loss Exponent
σ_k^2	Additive White Gaussian Noise at k
$\chi_{i,j}$	Log-normal Distributed Slow Fading Gain between Transmitter i and Receiver j
$\mathbf{\Phi}_k$	Covariance Matrix
$\mathbf{\Phi}_k^{\text{red}}$	Reduced Covariance Matrix
$\lambda_{c,\Delta_c}(d)$	Pairwise Throughput
Λ_c	Nominees for Reuse Election
$\Lambda_c^{'}$	Unelected Nominees
A_r^e	Effective Aperture Area of the Receiving Antenna

A_t^e	Effective Aperture Area of the Transmitting Antenna
B	Base Station
c	CUE
b_k	Benefit Value
C	Channel Capacity
C^{sum}	Predefined Sum Capacity Target
d	DUE
$d_{i,j}$	Distance between Transmitter i and Receiver j
$d_{D2D_{\max}}$	Predefined Maximum Distance for D2D Transmission Mode
E_c	Set of Edges in CG_c
f	Carrier Frequency
$g_{i,j}$	Channel Gain between Transmitter i and Receiver j
CG_c	Conflict Graph of c
G_r	Receiving Antenna Gain
G_t	Transmitting Antenna Gain
$\mathbf{H}_{k,j}$	Cross-channel Matrix of the Link between Receiver k and Transmitter j
$\mathbf{H}_{k,k}$	Channel Matrix of the Link between Transmitter k and Receiver k
$\mathbf{I}_{N\times N}$	$N\times N$ Identity Matrix
I_k	Maximum Tolerable Interference of k
I_{rec}	Received Interference Power
K	Path Loss Constant
L_{FSL}	Free-space Path Loss
M	Number of CUEs
M_k	Interference Margin of k

N	Number of DUE Pairs
N_r	Number of Receiving Antenna
N_t	Number of Transmitting Antenna
$P^{\max}$	Maximum Transmit Power of DUE
P_d^{init}	Initial Transmit Power of d
$P_d^{\min}$	Lower Transmit Power Bound of d
$P_d^{\max}$	Upper transmit Power Bound of d
P_r	Received Power at the Receiving Antenna
P_t	Transmitted Power at the Transmitting Antenna
P_T	Total Power Consumed
$PL_{i,j}$	Path Loss between Transmitter i and Receiver j
r	Distance between the Transmitting and Receiving Antenna
$r_{(c,d)}$	Share Rate between c and d
Rx	Receiving DUE
S_j	Sensitivity of Receiver j
T	Overall System Throughput
$\mathbf{T}_k$	Power Loading Matrix of Link k
Tx	Transmitting DUE
$U_c(\alpha_c, P_d)$	Utility of c
V_c	Set of Vertices in CG_c
W	Bandwidth

ABBREVIATIONS

3GPP	3rd Generation Patnership Project
AP	Access Point
BS	Base Station
CDMA	Code Division Multiple Access
CG	Conflict Graph
CoMP	Coordinated Multipoint
CSI	Channel State Information
CUE	Cellular User Equipment
D2D	Device-to-Device
DUE	D2D User Equipment
E2E	End-to-End
EDGE	Enhanced Data Rate for GSM Evolution
EPC	Evolved Packet Core
E-UTRAN	Evolved UTRAN
eNB	Evolved NodeB
FBMC	Filter Bank Multicarrier
FDD	Frequency Division Duplexing
FFT	Fast Fourier Transform
GFDM	Generalized Frequency Division Multiplexing
GPRS	General Packet Radio Service
GRA	Greedy Resource Allocation
GSM	Global Systems for Mobile Communications
GTM+	Greedy Throughput Maximization Plus
HetNet	Heterogenous Network

HTs	Horizon Topics
ICIC	Inter-Cell Interference Coordination
IMT	International Mobile Telecommunications
IoT	Internet of Things
ISI	Inter-symbol Interference
ITU	International Telecommunication Union
KPIs	Key Performance Indicators
LTE	Long Term Evolution
LTE-A	Long Term Evolution Advanced
M2M	Machine-to-Machine
METIS	Mobile and Wireless Communications Enablers for Twenty-twenty Information Society
MIMO	Multiple Inputs Multiple Outputs
MiSo	Maximum Independent Set-based and Stackelberg Game-based Resource Allocation and Power Control
MMB	Millimeter-wave Mobile Broadband
MMC	Massive Machine Communication
mmWave	Millimeter-wave
M-MIMO	Massive Multiple Inputs Multiple Outputs
OFDM	Orthogonal Frequency Division Multiplexing
PLMN	Public Land Mobile Network
PRB	Physical Resource Block
ProSe	Proximity Service
QoE	Quality of Experience
QoS	Quality of Service
RAN	Radio Access Network

RB	Resource Block
SIR	Signal-to-Interference Ratio
SINR	Signal-to-Interference-plus-Noise Ratio
SNR	Signal-to-Noise Ratio
TDD	Time Division Duplexing
TDMA	Time Division Multiple Access
UDN	Ultra-dense Networks
UE	User Equipment
UFMC	Universal Filtered Multicarrier
UMTS	Universal Mobile Telecommunications System
UTRAN	UMTS Terrestrial Radio Access Network
WCDMA	Wideband Code Division Multiple Access
WiMAX	Worldwide Interoperability for Microwave Access

LIST OF FIGURES

LIST OF TABLES

UNIVERSITY OF VAASA
Faculty of technology
Author: Olaobaju Abdulrahman
Topic of the Thesis: Device-to-Device Communication in 5G Cellular Networks
Supervisor: Professor Mohammed Elmusrati
Instructor: Professor Tapani Ristaniemi
Degree: Master of Science in Technology
Degree Programme: Communications and Systems Engineering
Year of Entering the University: 2015
Year of Completing the Thesis: 2018 **Pages:** 132

ABSTRACT:

Owing to the unprecedented and continuous growth in the number of connected users and networked devices, the next-generation 5G cellular networks are envisaged to support enormous number of simultaneously connected users and devices with access to numerous services and applications by providing networks with highly improved data rate, higher capacity, lower end-to-end latency, improved spectral efficiency, at lower power consumption. D2D communication underlaying cellular networks has been proposed as one of the key components of the 5G technology as a means of providing efficient spectrum reuse for improved spectral efficiency and take advantage of proximity between devices for reduced latency, improved user throughput, and reduced power consumption. Although D2D communication underlaying cellular networks promises lots of potentials, unlike the conventional cellular network architecture, there are new design issues and technical challenges that must be addressed for proper implementation of the technology. These include new device discovery procedures, physical layer architecture and radio resource management schemes. This thesis explores the potentials of D2D communication as an underlay to 5G cellular networks and focuses on efficient interference management solutions through mode selection, resource allocation and power control schemes. In this work, a joint admission control, resource allocation, and power control scheme was implemented for D2D communication underlaying 5G cellular networks. The performance of the system was evaluated, and comparisons were made with similar schemes.

KEYWORDS: 5G, D2D, Latency, Spectral Efficiency, Interference Management

1. INTRODUCTION

1.1. Background

Over the past few decades, our world has witnessed an evolution of mobile data communication systems from the very first-generation communication networks towards the second, third and the fourth-generation networks. This evolution has been a major driving force behind the advancement and development of our world into an advanced and networked environment. Mobile communication has developed from being a service that is available and affordable for only a few people to become a service that is used abundantly by majority of the world's population. Millions of people around the globe are now interconnected through mobile communication. It has become an integral part of our everyday existence and its applications are ubiquitous in every walk of life. It has been at the forefront of many advancements and breakthroughs in several fields such as healthcare, transportation, energy, manufacturing, architecture, agriculture, engineering, business, education, meteorology, broadcasting, media and entertainment.

The rapid growth in the global market of mobile communication devices has been witnessed in the past few years. Moreover, this growth is continuously being felt and the world will continue to experience the proliferation of mobile communication devices such as smartphones, tablets, wearable devices, notebooks, and laptop computers, together with new and existing services and applications provided by mobile communication systems such as voice call, video conferencing, online gaming, live video streaming and many more. According to the Cisco Visual Networking Index (2017), close to half a billion (429 million) mobile devices and connections were added in 2016 alone, most of which were smartphones, followed by machine-to-machine (M2M) modules. This growth increased the global mobile device figure from 7.6 billion in 2015 to 8.0 billion in 2016.

In the past, wireless communication was mostly about communication between two or more people over mobile communication devices connected to cellular networks. Presently, the communication world is evolving gradually toward the Internet of Things (IoT) era where virtually every device and machine in our environment will be connected

to a communication network. With IoT, communication between devices and machines such as motor vehicles, home appliances, and public infrastructures are being introduced. In 2016, there were 2.3 networked devices per capita, with a total of 17.1 billion devices connected to IP networks and monthly IP traffic was 13 GB per capita. All these figures are expected to increase rapidly over the coming years (Cisco Systems, 2017).

The ever-increasing demand for numerous mobile communication services and applications resulted in the need for a wireless broadband communication network with reduced latency, improved data rate, capacity, coverage, efficiency and quality of service (QoS) to support these bandwidth-hungry, multimedia-rich, and data-intensive applications and services. Because of this, the 3GPP (3rd Generation Partnership Project) came up with a set of new mobile communication standards and technologies called LTE to meet the requirements of the fourth generation (4G) mobile communication networks (Kanchi, Sandilya, Bhosale, Pitkar, & Gondhalekar, 2013: 195–200). Technologies like MIMO, OFDM and Carrier Aggregation enabled LTE to offer communication systems with improved features, better efficiency and higher data rate than the previous generations. Presently, 4G networks have been able to provide for the requirements and expectations of current services and applications (Jimaa, Chai, Chen, & Alfadhl, 2011).

However, it is unlikely that the 4G LTE networks will be enough to serve users need as time goes on as the technology is expected to reach its limits. From the year 2016 to 2021, the global IP traffic is expected to increase by nearly three times and rise at a Compound Annual Growth Rate of 24 percent with monthly IP traffic reaching 35 GB per capita by 2021 from 13 GB per capita in 2016. Also, number of connected devices per capita will reach 3.5 networked devices per capita and the total number of networked device will be 27.1 billion in 2021 (Cisco Systems, 2017). In the long-run, with data traffic explosion and continuous rapid increase in number of users and connected devices, 4G LTE networks will no longer be enough to satisfy the requirements of new services and applications and the massive number of connected devices. Also, researchers are developing new applications that are latency-sensitive which cannot be supported by the current latency provided by 4G (Agiwal, Roy, & Saxena, 2016).

Mobile data traffic explosion has led researchers, designers and developers to begin work on the fifth-generation (5G) networks. The main aim of 5G technology is to develop high capacity networks with very high data rate and low latency to meet the demands of future applications and services. Several research activities in the wireless communication field have been considering, improving, and implementing several emerging technologies for the next generation networks. Technologies like massive multiple-input, multiple-output (M-MIMO), dense small cell deployment (ultra-densification), millimetre-wave, M2M and device-to-device (D2D) communication are the key research areas and will be the major enablers for the 5G networks (Al-Falahy & Alani, 2017: 13).

Device-to-device communication as one of the key research areas in 5G cellular networks offers a lot of opportunities. With D2D communication, devices close to each other can directly communicate with one another in the licenced band without involving the base station (BS) or with limited base station involvement, taking traffic load off the main network. D2D implementation in 5G significantly reduce latency, power consumption and cost. Furthermore, operators can take advantage of D2D for network traffic offloading in congested local areas such as a big mall, stadium or campus (Tehrani, Uysal, & Yanikomeroglu, 2014). However, several technical challenges and design issues such as security, interference management, resource allocation, power control, device discovery, mobility management, and session setup and management still need to be addressed (Shen, 2015). This thesis explores the potentials of D2D communication in enhancing current network capabilities for future 5G networks. The work focuses on interference management in D2D communication that shares the same resources with conventional cellular networks. The feasibility, performance, and potential gain of D2D communication underlaying 5G cellular networks were investigated.

1.2. Motivation

Mobile communication systems have evolved from networks that provides voice-only services into series of complex, interconnected environment with numerous services integrated into systems that support innumerable applications and provide high-speed data access to an enormous number of users and machines. More applications and services

are continuously being developed to harness the capabilities of these advanced communication devices and machines, and more importantly cater for the need and demand of increasing number of users. 5G research and development projects aim at developing high capacity communication networks with very high capabilities to meet the ever-increasing user's demand for future applications and services. While the introduction of D2D in 5G offers a lot of opportunity for both mobile subscribers and operators, there are several issues and challenges to be addressed before D2D can be fully implemented. One of the challenges is the problem of managing interference between device operating in D2D mode and sharing the same cellular band with devices communicating in cellular mode. Providing a feasible and efficient solution to interference management problem will be a breakthrough for D2D technology, and pave way for its implementation in 5G cellular networks.

1.3. Scope of Thesis

The issue of interference management in *multi-sharing* D2D communication in 5G cellular network is addressed in this thesis. The thesis focuses on sharing or reusing of only *uplink* cellular resource block by D2D communication underlaying cellular 5G cellular networks with the major aim of improving the overall system throughput and power efficiency of the whole network. Key techniques for managing interference in such networks such as mode selection, power control and resource allocation will be analysed. A *centralized* joint *admission control*, *resource allocation* and *power control* algorithm will be implemented as a simulation in a *single cell* environment, and its performance will be evaluated using the percentage gain in system throughput and power efficiency as the major performance metrics. Finally, comparison will also be made between the algorithm and two other similar algorithms using overall system throughput and power efficiency as performance indicators.

1.4. Thesis Outline

The *second* chapter presents an overview of the next generation 5G cellular networks. It starts with a quick examination of the evolution of mobile communication from the first-generation 1G to the future fifth-generation 5G network. It discuses some major research on 5G cellular networks, the requirements as well as the key enabling technologies for 5G networks. The *third* chapter gives a general overview of D2D communication by discussing the different forms of D2D communication, its applications and use cases, as well as technical issues and challenges of implementation. An overview of 3GPP Proximity Service (ProSe) will also be discussed. Direct D2D communication Technology component under the 5G METIS project will be presented with key D2D topic such as device discovery and interference management through mode selection algorithm, resource allocation scheme, SINR target optimization and power control algorithms. The *fourth* chapter presents the analysis and simulations of joint admission control, resource allocation and power control mechanism for multi-sharing D2D communication in uplink frequency reuse mode in a single cell environment. The *fifth* chapter presents the result of simulations conducted in chapter four in three stages. Finally, the *sixth* chapter gives a brief summary of the entire work, draws conclusion to the results presented in the previous chapter, and provides suggestions for future works.

2. FIFTH-GENERATION (5G) CELLULAR NETWORKS

This chapter presents an overview of 5G cellular networks. It starts with a brief examination of the evolution of mobile communication from the first-generation 1G to the future fifth-generation 5G network. It discuses some major research on 5G cellular networks, and the requirements as well as the key enabling technologies for 5G networks.

2.1. Evolution of Mobile Communication

Every evolution or advancement in mobile communication technology over the past few decades have always been driven by the need and demand for communication systems with higher data rate, better coverage and QoS. A new generation of technologies has been released nearly every decade since the first generation (Al-Falahy & Alani, 2017). Since the inception of mobile communication in the late 1970s, it has evolved from being a technology that provides only analogue voice call services, to current digital technology that supports high quality broadband systems providing complex services and applications for subscribers at data rates of several megabits per seconds over a large coverage area, or up to hundreds of megabits per seconds within a short range (Gupta & Jha, 2015). Drastic improvements have been made to architectures and methods employed in each generation, bringing a lot of advancement to communication systems in several ways. A lot of improvement have also been made to communication devices, with the introduction of smart communication devices with very high capabilities and several functionalities.

The generations of mobile communication technology in order of increasing mobility, coverage, data rate and spectral efficiency is shown in Figure 1 below. The mobility, coverage, data rate and spectral efficiency improves as the technology evolves from 1G to 5G. Also, it shows the switching technique used in each generation. Circuit switching was used in both 1G and 2G, 2.5G and 3G made use of both circuit and packet switching, while the later generations from 3.5G use packet switching. The representation further shows the separation between licensed and unlicensed spectrum. All generations from 1G

to 4G are using the available licensed spectrum while other technologies like Wi-Fi, Bluetooth and WiMAX are using from the unlicensed band.

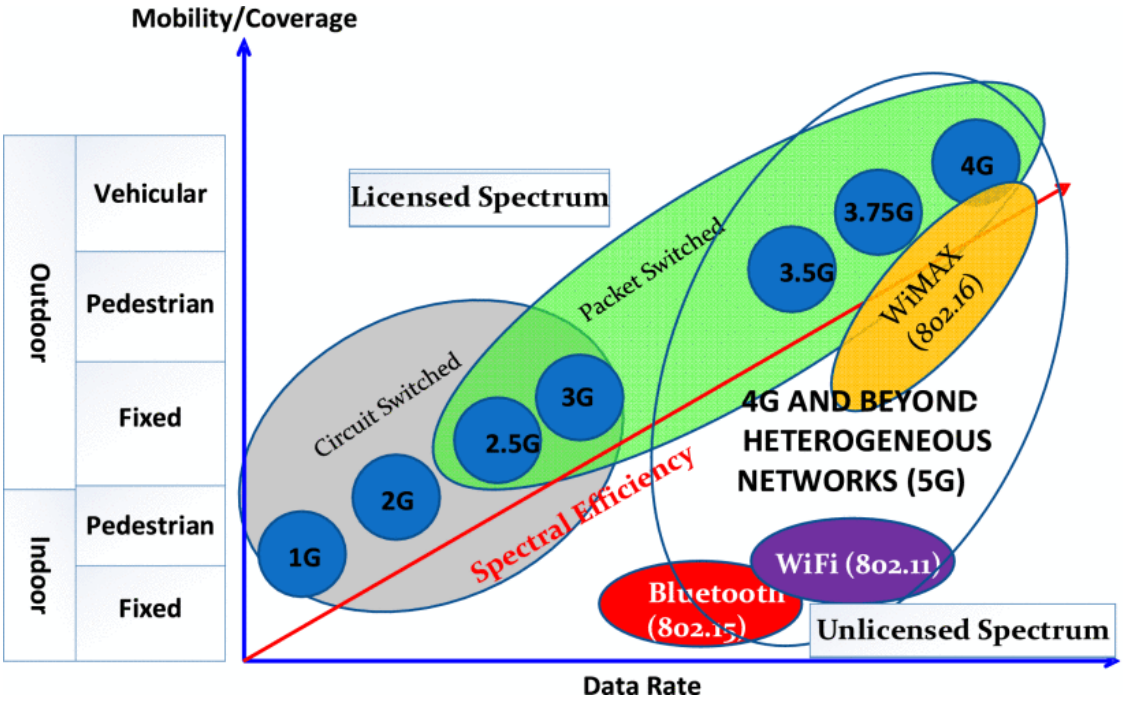

Figure 1. Evolution of Mobile Communication (Gupta & Jha, 2015).

Introduced in the early 1980s, the first-generation telecommunication standards which were analogue systems operated at a data rate of up to 2.4 Kbps providing voice calls only. The prominent first-generation standards were Advanced Mobile Phone System (AMPS) established in the North and Latin America, Nordic Mobile Telephone (NMT) launched in the Nordic Countries of Finland, Sweden, Norway and Denmark, Total Access Communication System (TACS) introduced in the UK (Jaloun & Guennoun, 2010). These systems were known for poor handoff, very low capacity and poor voice quality. Voice calls were stored and played in radio towers. This made the system vulnerable to eavesdropping on calls from unwanted parties (Agrawal, Patel, Mor, Dubey, & Keller, 2015: 1101).

The 2G system was introduced in the late 1980s as an improvement on the 1G technology. Analogue technique was replaced by digital multiple access techniques such as TDMA (Time Division Multiple Access) and CDMA (Code Division Multiple Access), enabling

2G system to have better spectral efficiency, higher data rate for voice and the data services, with the newly introduced roaming service (Tondare, Panchal, & Kushnure, 2014). The first 2G system introduced was Global Systems for Mobile Communications (GSM) primarily used for traditional voice and low rate data services with a data rate of 64 Kbps. Value Added Services (VAS) such as Short Message Service (SMS) and Voice Mail System (VMS) were also provided by GSM. General Packet Radio Service (GPRS) and later Enhanced Data Rate for GSM Evolution (EDGE) were introduced to the 2G system framework, resulting in an intermediate generation between 2G and 3G technology usually referred to as 2.5G. It combined both packet and circuit switching and provided a data rate of up to 144 Kbps (Gupta & Jha, 2015).

The introduction of 3G standards brought a lot of improvement to mobile communication. Great improvement was made in transmission rate, capacity, voice quality and QoS focusing on more complex multimedia applications and value-added services for mobile devices such as video calling, video conferencing, and global roaming. It met the requirements and comply with specifications set by the International Telecommunication Union (ITU) for International Mobile Telecommunications-2000 (IMT-2000) standards to provide wireless access to telecommunication systems globally (Kumar, Liu, Sengupta, & Divya, 2010). The ITU's IMT-2000 standard required a system to have a peak data rate of at least 200 Kbps (Tondare et al., 2014).

The Universal Mobile Telecommunications System (UMTS) developed by 3GPP is the major 3G system. The UMTS generally uses the Wideband Code Division Multiple Access (WCDMA) air interface and provided a data rate of up to 144 Kbps on moving vehicles, 384 Kbps for walking pedestrians, and 2 Mbps for stationary or indoor users (Agrawal et al., 2015). The main components of the UMTS network are the user equipment (UE), UMTS Terrestrial Radio Access Network (UTRAN) and the Core Network (CN). UTRAN usually consists of one or more Radio Network Subsystem (RNS) comprising of one or more Node Bs under the control of a Radio Network Controller (RNC). The CN connects the UMTS network to other services like internet and PSTN. It has the circuit switched domain which is based on MSCs (Mobile Switching Centers) and the packet switched domain built around SGSN (Servicing GPRS Support

Node). The MSC in the CN can also serve GSM-BSS (GSM Base Station Subsystem) in the network (Korhonen, 2003).

Although the introduction of 3G technology effected a lot of remarkable improvements, the technology also came with some disadvantages. The 3G network architecture is more expensive to install than 2G. Also, 3G enabled devices consumes more power and were expensive to acquire. The 3G technology further evolved to 3.5G and 3.75G which are the intermediate generation between 3G and 4G with the creation of High Speed Uplink/Downlink Packet Access (HSUPA/HSDPA), and later $HSPA^{+}$ attaining the highest data rate with UMTS WCDMA (Gupta & Jha, 2015).

The development of the fourth-generation mobile communication system was driven by the unprecedented and ever-increasing growth of users demand for data traffic and the emergence of new technologies, services and applications in mobile communication. The 3GPP developed LTE and later the LTE-Advanced (LTE-A) to further meet ITU's IMT-Advanced requirement for 4G with data rate of 1 Gbps for downlink and 500 Mbps for uplink. LTE, LTE-A and WIMAX are the major standards for the fourth-generation. The major aim of LTE was to create an ALL-IP network with a common platform to integrate all existing technologies created so far from the first-generation (GSM, GPRS/EDGE, UMTS, etc.), and meet up with user's expectations of services being provided (Kumar et al., 2010). LTE system is considered an evolution of the UMTS standard with the use of more efficient modulation techniques and better bandwidth management to obtain higher throughput for both uplink and downlink.

Notable technologies introduced for LTE and LTE-A are Orthogonal Frequency Division Multiplexing (OFDM), Multiple-Input Multiple-Output (MIMO), turbo coding, dynamic link-adaptation techniques, carrier aggregation, and fixed terminal relaying; use of Relay Nodes at cell edges (Zarrinkoub, 2014). Changes were also made to the system architecture from UMTS. The two fundamental components of LTE architecture are Evolved Packet Core (EPC) and the Evolved Universal Terrestrial Radio Access Network (E-UTRAN). These components evolved from the CN and UTRAN of the UMTS system. E-UTRAN consists of eNB(s) (evolved Node B) which combines the functionality of the Node B and RNC of UMTS. EPC consists majorly of servers and gateways with added

functionality. These are the Servicing Gateway (S-GW), Mobility Management Entity (MME), the Packet Data Network Gateway (PDN-GW), and the Policy Charging Rules Function (PCRF) (Salman, Ibrahim, & Fayed, 2014).

The several changes made to the architecture resulted in an extremely flexible, less expensive and more efficient network. LTE also provides better mobility, coverage, efficiency in radio usage, high level of security, better spectral efficiency, reduced latency, and smooth integration with existing mobile communication systems and other non 3GPP systems (Oshin & Atayero, 2015). However, LTE network is hard to implement because of the complexity of the several hardware involved. Also, data prices to be paid by users is very high. Table 1 below summarizes the differences between the mobile communication generations.

As the number of networked device, and demand for applications and services that require very high data and low latency continue to increase at an alarming rate, it has been forecasted that current 4G technologies will soon reach their limits (Shen, 2015). This calls for a set of new mobile communication standard for the future. The fifth-generation 5G is the proposed future mobile communication standards beyond 4G/IMT-Advanced denoted by ITU-R as IMT for 2020 and beyond (IMT-2020). Various research activities are currently being conducted on 5G cellular networks, focusing on providing solutions to challenges and resolving various issues not properly addressed in 4G. These include the need for higher capacity, higher data rate, lower end-to-end latency, massive device and machine connectivity for IoT, reduced cost, more efficient energy consumption, improved QoS and user experience.

Table 1. Evolution of Mobile Communication Technology.

Gen.	Access Technology	Data Rate	Bandwidth	Switching	Services
1G	Advanced Mobile Phone System (AMPS), Nordic Mobile Telephone (NMT), and Total Access Communication System (TACS) – Frequency Division Multiple Access (FDMA)	2.4 Kbps	30 KHz	Circuit	Analog Voice
2G	Global Systems for Mobile Communications (GSM) – Time Division Multiple Access (TDMA)	DL 10 Kbps UP 10 Kbps	200 KHz	Circuit	Digital Voice, Data, Short Message Service (SMS), Voice Mail System (VMS)
	Code Division Multiple Access (CDMA)	10 Kbps	1.25 MHz		
2.5G	General Packet Radio Service (GPRS)	DL 40 Kbps UL 14 Kbps	200 KHz	Circuit / Packet	
	Enhanced Data Rate for GSM Evolution (EDGE)	DL 140 Kbps UL 140 Kbps			
3G	Universal Mobile Telecommunications System (UMTS) – Wideband Code Division Multiple Access (WCDMA)	DL 500 Kbps UL 384 Kbps	5 MHz	Circuit / Packet	High quality audio and video calls, high definition TV, audio and video streaming
	Code Division Multiple Access (CDMA) 2000	384 Kbps	1.25 MHz		
3.5G	High Speed Downlink Packet Access (HSDPA)	DL 14 Mbps UL 384 Kbps	5 MHz	Packet	
	High Speed Uplink Packet Access (HSUPA)	DL 14 Mbps UL 5.7 Mbps			
3.75G	Enhanced High Speed Packet Access HSPA^{+}	DL 42 Mbps UL 22 Mbps	5 MHz	Packet	
4G	Long Term Evolution (LTE) – Orthogonal/Single Carrier Frequency Division Multiple Access (OFDMA/SC-FDMA)	DL 326Mbps UL 86Mbps	1.4 MHz to 20 MHz	Packet	Multiplayer online gaming, high definition TV, mobile broadband, high definition video streaming
	Long Term Evolution Advanced (LTE-A) – Orthogonal/Single Carrier Frequency Division Multiple Access (OFDMA/SC-FDMA)	DL 3Gbps UL 500Mbps			
5G	Beam Division Multiple Access (BDMA) and Non- and Quasi-orthogonal or Filter Bank Multi Carrier (FBMC) Multiple Access	10–50 Gbps (expected)	60 GHz	Packet	UHD video streaming, virtual reality and augmented reality applications, connectivity for IoT

2.2. Fifth-generation 5G Cellular Network

The technology trends in the proposed 5G mobile communication networks suggest a change in pattern from past and existing communication network. Clearly, the main objective of mobile communication has changed from merely enabling users to connect wirelessly to the internet. Research activities are now focused on enabling a seamlessly connected society in 2020 and beyond, bringing together people along with machines, things, data, applications, transport system, healthcare system, traffic control system and other infrastructures in a smart networked communication environment. Although there is no 5G mobile communication standard that has been defined yet, but several innovations have been released and more development are still in progress.

In early 2012, ITU-R initiated IMT-2020 programme, setting a stage for series of 5G research activities being conducted around the world. ITU-R has finalised timeline for IMT-2020 development as shown in Figure 2 through the leading role of the Working Party 5D (WP 5D) (Barreto, et al., 2016). The vision of 5G mobile broadband connected society has been finalized in September 2015 and detailed investigation of the key elements of 5G are already being conducted. Technical performance requirements have been defined and evaluation processes was set between 2016 and 2017. According to the timeframe, IMT-2020 proposals and standardization will be studied in 2018. Between 2018 and 2020, evaluations will be held by external groups and IMT-2020 specifications will be finally defined and released by 2020 (Al-Falahy & Alani, 2017).

The overall goals of 5G cellular networks conforming with the challenges and requirement of future networks are to attain

- 1000 times higher mobile data volume per unit area,
- 10 to 100 times higher typical user data rate and number of connected devices,
- 10 times longer battery life for low power massive machine communication, and
- 5 times reduced end-to-end (E2E) latency compared to 4G networks,

at a similar operating cost and energy consumption level with current communication systems (Aziz, et al., 2015). Although achieving these goals seems like a daunting and impossible task, but current research trends suggests that these goals can potentially be

achieved. Several 5G research activities are being conducted on technologies to enhance the radio interface, support wide range of emerging services, enhance user experience, improve network energy efficiency, and to enhance privacy and security.

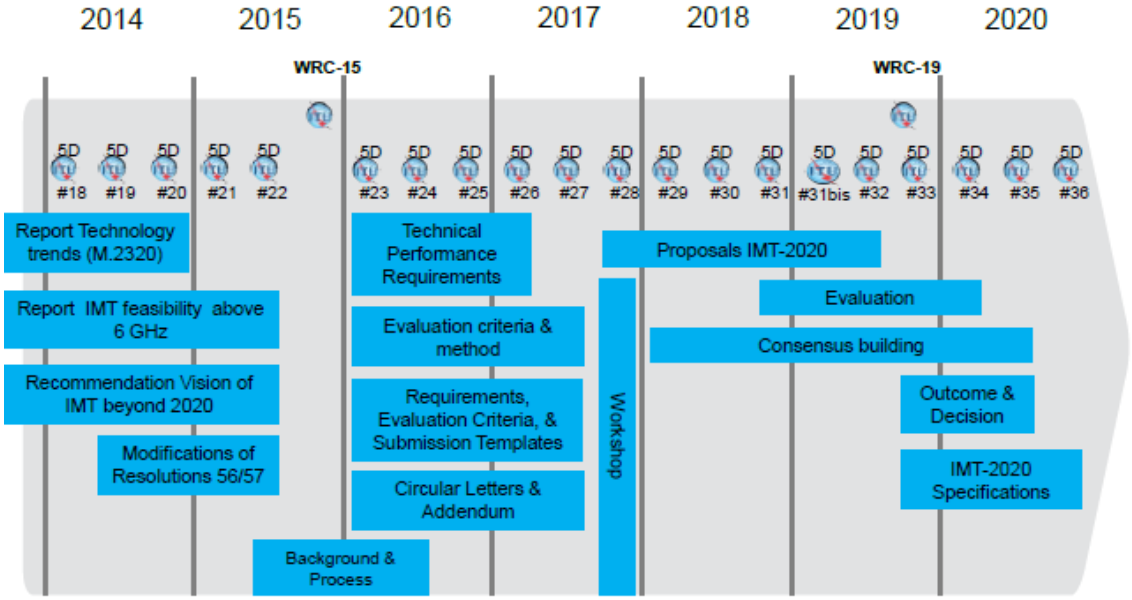

Figure 2. Detailed Timeline and Process for IMT-2020 in ITU-R (Barreto, et al., 2016).

2.2.1. 5G Research and Development Projects by Organizations and Research Groups

Most 5G research activities in Europe are been monitored mainly by the European Union 7th Framework Programme (FP7) Future Networks and Cluster Radio Access and Spectrum projects. Horizon 2020 and 5G Infrastructure Public Private Partnership (5GPPP) coordinate new research programs. The largest and most prominent FP7 5G project is the Mobile and wireless communication Enablers for the Twenty-twenty Information Society (METIS) project consisting of 29 partners including top telecommunication companies and academic institutions (Pirinen, 2014). Five scenarios and twelve test cases were identified by METIS to represent and address the key challenges of 5G networks and the key performance indicators (KPIs) (Osseiran, et al., 2014). The scenarios are summarized below. Figure 3 illustrates the mapping of the scenarios with the test case.

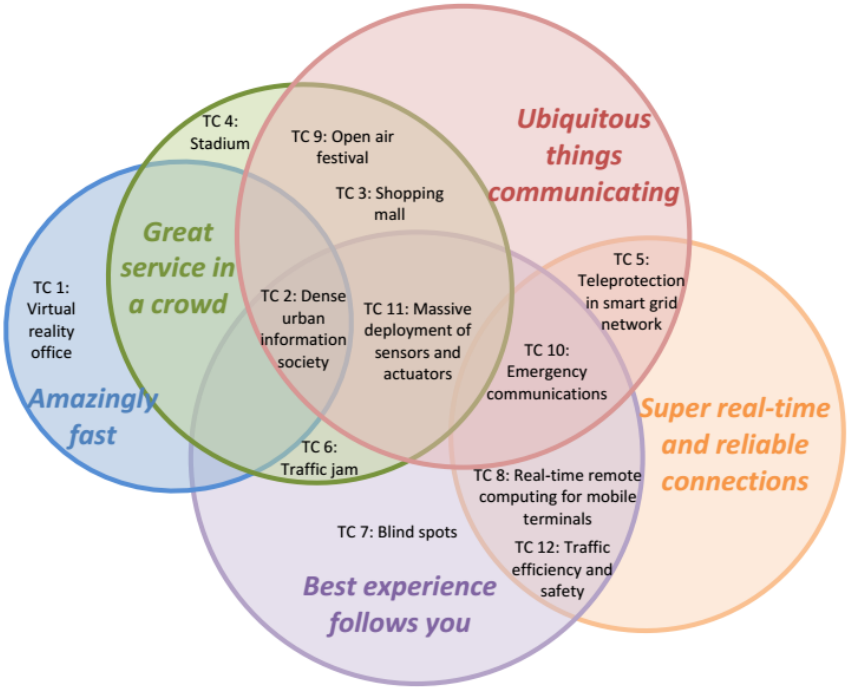

Figure 3. Mapping of METIS Five Scenarios with the Twelve Test Cases (Popovski, et al., 2013).

I. **Amazingly Fast**: This scenario focuses on the provision of a very high data rate for future mobile networks, so end-users of services and applications can experience instantaneous connectivity without any delay. This will have significant impact on the success of emerging cloud-based services and applications such as virtual reality office, real-time online multiplayer games, etc.

II. **Great Service in a Crowd**: This scenario aims at providing end-users with excellent mobile broadband connectivity experience even when they are in very crowded environment such as stadiums, big shopping malls, concerts, campuses, and other event that attract large number of attendants.

III. **Best Experience Follows You**: This scenario focuses on delivering grate mobile broadband connectivity experience to end-users in transit such as in motor vehicle, trains, etc. Users on the move should have reasonable experience on-the-go with high data rate service and applications.

IV. **Super Real-Time and Reliable Connections**: This focuses on improving new applications and services with very strict latency and reliability requirements such

as new functionalities for traffic safety and efficiency, mission-critical real-time control of industrial applications, real-time M2M communication, monitoring and alerting applications for tele-protection in smart grid networks, etc.

V. **Ubiquitous Things Communicating**: This scenario aims at enabling connectivity for enormous number of ubiquitous machine-type devices.

Some horizon topic (HTs) to be integrated with technology components to form an inherent part of the network were also identified by METIS (Osseiran, et al., 2014). These HTs are summarized below. Table 2 further shows the mapping of the HTs to the twelve test cases defined by METIS. Each test case is addressed by at least one horizon topic. The mapping also identifies dependencies between the horizon topics. Figure

I. **Direct Device-to-device (D2D) Communication**: With direct D2D communication, devices can communicate directly without routing the user-plane traffic through any network infrastructure with the goal of increasing coverage, offloading network traffic, providing fall-back connectivity, and increasing spectral efficiency and network capacity. D2D communication will be discussed in detail later in this chapter.

II. **Massive Machine Communication (MMC)**: This provides connectivity for massive deployment of network-enabled machine-type devices which will be the building blocks for future IoT with applications in healthcare services, emergency services, public safety, industrial automation, home automation, transportation, etc.

III. **Moving Networks (MNs)**: This focuses on enhancing and extending network coverage for large number of devices in a group of jointly moving communication devices. This will improve the mobility management and connectivity of moving terminals and nomadic networks.

IV. **Ultra-dense Networks (UDNs)**: This aim at addressing high demand for data traffic through densification which is the denser deployment of small cells with the goal of increasing capacity, energy efficiency of radio links, and better spectrum utilization**.**

V. **Ultra-reliable Communication (URC)**: This will enable high degree of availability for networks hosting application and services with strict reliability and availability requirements.

Table 2. Horizon Topics (HTs) and METIS Test Cases (Popovski, et al., 2013).

Test Cases	D2D	MMC	MN	UDN	URC
TC1: Virtual reality office				✓	
TC2: Dense urban information society	✓	✓		✓	✓
TC3: Shopping mall	✓	✓		✓	
TC4: Stadium	✓			✓	
TC5: Teleprotection in smart grid network		✓			✓
TC6: Traffic jam	✓		✓	✓	✓
TC7: Blind spots			✓		✓
TC8: Real-time remote computing for mobile terminals			✓		✓
TC9: Open air festival	✓	✓		✓	
TC10: Emergency communications	✓		✓		✓
TC11: Massive deployment of sensors and actuators		✓			✓
TC12: Traffic efficiency and safety	✓	✓	✓		✓

According to the final report published by METIS in 2015 containing the result of their simulations and evaluations of the 5G KPIs, their evaluation showed that the work was successful . They achieved a radio access network with approximately 1000 times higher throughput, 50 times higher typical end user data rate, 2000 times higher number of connected devices, 70 times longer battery life for low-power MMC devices and 5 times reduced E2E latency (Aziz, et al., 2015). METIS also presented different RAN architectures and traffic flows for different situations, such as shopping malls, indoor offices, crowded stadiums, and outdoor dense urban environments. METIS II was also launched after the completion of the METIS project, focusing majorly on the overall architecture of 5G radio access network.

Some other notable research groups working on 5G technology are the 5th Generation Non-Orthogonal Waveforms for Asynchronous Signalling (5GNOW), Enhanced Multicarrier Technology for Professional Ad-Hoc and Cell-Based Communications

(EMPhAtiC), Network of Excellence in Wireless Communications (NEWCOM), among others (Pirinen, 2014). 4G America is leading the 5G research in the America. 3GPP have also initialize 5G activities and focus is now set on providing 5G standards in their Release 15 (Barreto, et al., 2016).

2.2.2. Requirements of 5G Networks

Analysing different research initiatives by industries and academia, the next generation 5G radio access network is required to have these major features which are listed as follows (Andrews, et al., 2014; Chen & Zhao, 2014).

I. Enormous number of connected devices: 5G radio access network must be able to provide connectivity for massive number of devices for the full realization of the IoT. About 300,000 connected devices per AP should be realizable.
II. Data rate of 1– 10 Gbps in real networks: 5G will be required to provide more that 10 time the data rate currently provided by LTE networks.
III. End-to-end latency of at most 1 ms: This will be needed to support emerging latency-sensitive applications such as two-way real-time gaming, 3D hologram, cloud-based applications, augmented reality, tactile internet, and machine communications.
IV. Perceived availability and reliability of nearly 99.999 percent: This means that 5G network should practically be available for use every time.
V. Network coverage of almost 100 percent: 5G network should be able to provide network connectivity for users anytime irrespective of their location
VI. Energy usage reduction by almost 90 percent: Energy efficiency with green technology will be crucial for 5G network because of the very high capacity and massive connectivity.
VII. Extended battery life of up to a decade: This will be essential for massive deployment of low power, machine-type devices, sensors and actuators.
VIII. Higher bandwidth per unit area: This is required to provide large number of devices with high bandwidths for as long as possible in certain areas.

2.2.3. Key Technologies for 5G Networks

Research trend have shown that the requirements of 5G networks can be achieved by adopting a *multi-tier* and heterogenous network architecture together with the introduction and implementation of several emerging key technologies such as millimeter-wave, M-MIMO and beamforming, dense small cell deployment, D2D, and M2M. New waveforms, more efficient coding techniques, network virtualization, advanced coordinated multipoint (CoMP), multiple radio access techniques (M-RAT), and cloud radio access networks (C-RAN) will also have significant contribution on the realization of 5G (Boccardi, Heath, Lozano, Marzetta, & Popovski, 2014; Andrews, et al., 2014). Al-Falahy & Alani (2017) classified 5G technologies under four categories arcorging to the impact they have on key 5G network performance. Table 3 shows some challenges of 5G networks and specific technologies that can be used to address them.

I. **Network Capacity and Data Speed Improvement**: These can be achieved through dense small cell deployment, utilization of the millimeter-wave band, and M-MIMO and beamforming.
II. **Latency Reduction**: dense small cell deployment and D2D communication can be implemented to significantly reduce E2E latency.
III. **Spectral Efficiency Improvement**: This can be achieved by increasing modulation order, adopting D2D communication, M-MIMO, and adopting new waveforms for transmission.
IV. **Massive Connectivity for IoT**: This can be enable through dense small cell and M-MIMO, Also, Network function virtualization (NFV) can be use where functions with hardware compatibility issues is deployed from the cloud. CoMP can also be used to take advantage of interference and turn them to useful signals.

Table 3. 5G Network Challenges and Technologies to Provide Solutions (Al-Falahy & Alani, 2017).

Features	Description	Technology
Extreme data rate (Gbps)	Increased data rate to meet services and applications requirements	Millimeter-wave band Massive multiple input, multiple output (M-MIMO)
Number of connected devices (# devices/m^2)	All devices that benefit from wireless connectivity will be connected in 5G such as sensors, actuators, machines, etc.	IoT arising from massive machine-to-machine communications D2D Communication Wider bandwidth (mmWave) Dense small cell deployment
Spectral efficiency (b/s/Hz)	Spectral efficiency will further improve in 5G	New waveform (FBMC, UFMC, GFDM) M-MIMO CoMP
End-to-end latency (ms)	5G networks will support more lower latency than 4G LTE	D2D Communication Dense small cell deployment Smart data caching
Data processing speed (Mbps/m^2)	Data processing will be 100 times faster in 5G compared to 4G networks	Millimeter-wave band Dense small cell deployment NFV D2D communication
Energy efficiency (millijoule/bit)	5G will be able to transfer data with much less power and reduce its carbon footprint	M-MIMO together with millimeter-wave band Millimeter-wave multihop relay stations
Mobility (m/s)	Faster user speeds will be supported by 5G when in transit	Advanced heterogeneous networks (HetNet)

2.2.3.1. Millimetre-wave

Overwhelming majority of current mobile and wireless communication systems operates in the microwave band below 3 GHz (from 300 MHz –3 GHz) band usually referred to as the "*sweet spot*". It is widely used mainly because of its favourable propagation characteristics over several kilometres in different propagation environments (Al-Falahy & Alani, 2017). Moreover, network capacity of any communication system depends on

bandwidth and spectral efficiency. Higher bandwidth and spectral efficiency means higher capacity. However, it is rather impossible for this microwave band to support the bandwidth required to attain a network capacity suitable for 5G networks. Additional spectrum is needed for 5G for higher capacity to support the exploding traffic. Thus, the huge chunk of unused high frequency band from 3–300 GHz called the millimeter-wave band is being exploited for additional spectrum (Boccardi, et al., 2014). Several bands (up to 252 GHz as shown in Figure 4a) within the millimeter band seems promising and can potentially be used for mobile broadband. These include Local Multipoint Distribution Service (LMDS) band from 28–30 GHz shown in Figure 4b, the high oxygen absorption license-free band at 60 GHz suitable for indoor applications which has been exploited for IEEE 802.11ad multi-Gbps Wi-Fi, and additional 12.9 GHz available at 71–76 GHz, 81–86 GHz, and 92–95 GHz from the E-band as shown in Figure 4c (Pi & Khan, 2011; Boccardi, et al., 2014).

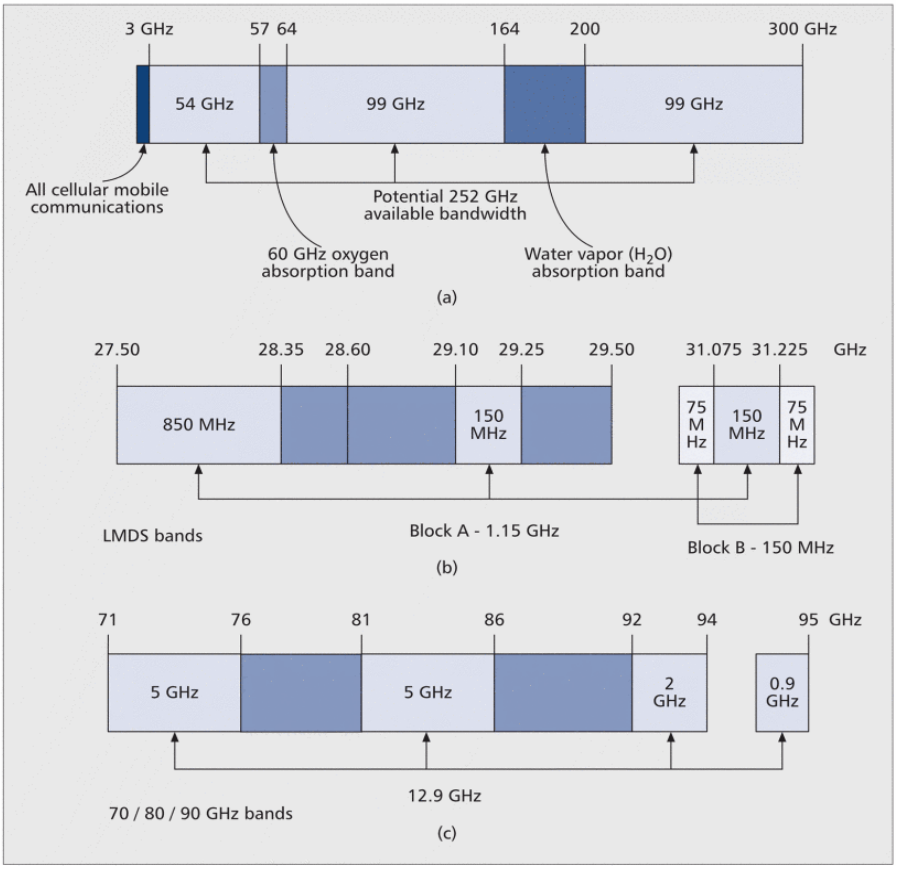

Figure 4. Millimeter-wave Spectrum (Pi & Khan, 2011)

However, utilization of mmWave for mobile and wireless communication possesses some challenges as they have different propagation characteristics, atmospheric absorption behaviour, and hardware constraints when compared to the widely used microwave band.

The *propagation loss* of mmWave is majorly in form of free space loss given in Equation 2.1.

$$L_{FSL} = 32.4 + 20\log_{10} f + 20\log_{10} r \tag{2.1}$$

Where L_{FSL} is the free-space loss in dB, f is the carrier frequency in GHz, and r is the distance between the transmitter and the receiver in meters. A common misconception is to assume that the free space loss depends on frequency, and that higher frequencies such as the mmWave propagates poorly with high losses in free space when compared to lower frequencies. This case is only true if the path loss is calculated at a specific frequency between two isotropic antennas or half-wavelength dipoles (Pi & Khan, 2011; Khan, Pi, & Rajagopal, 2012).

Khan, et al., (2012) Compared transmission gain with the case of omni-directional transmission between two isotropic antennas to the transmission gain in the case of a directional transmission as shown in Figure 5 using the *Friis* transmission equation in Equation 2.2.

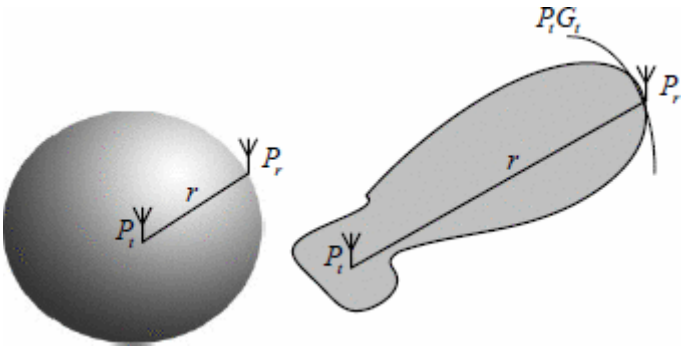

Figure 5. Omnidirectional and Directional Transmission (Khan, et al., 2012).

$$P_r = \frac{P_t G_t G_r \lambda^2}{(4\pi r)^2} \tag{2.2}$$

Where, P_r is the power received at the receiving antenna, P_t is the power input to the transmitting antenna, G_t is the transmitting antenna gain, G_r is the receiving antenna gain, λ is the wavelength and r is the distance between the antennas. In the case of omnidirectional transmission, an isotropic antenna is an ideal or theoretical antenna with directivity of 0 dBi (i.e. G = 1). Therefore, from Equation 2.2, the transmission gain is given by:

$$\frac{P_r}{P_t} = \left(\frac{\lambda}{4\pi r}\right)^2 \tag{2.3}$$

In the case of directional transmission with real antenna, the antenna gain G is related to the maximum effective aperture area A^e of the antenna as shown in Equation 2.4.

$$G = \frac{4\pi A^e}{\lambda^2} \tag{2.4}$$

From Equation 2.4, the larger the aperture of an antenna, the higher the gain of the antenna. Larger antenna will capture more energy from passing radio wave and will also radiate more energy than smaller ones. Substituting Equation 2.4 in equation 2.2 for both G_r and G_t gives:

$$\frac{P_r}{P_t} = \left(\frac{4\pi A_r^e}{\lambda^2}\right)\left(\frac{4\pi A_t^e}{\lambda^2}\right)\frac{\lambda^2}{(4\pi r)^2} = A_r^e A_t^e \left(\frac{1}{\lambda^2}\right)\left(\frac{1}{r^2}\right) \tag{2.5}$$

They concluded that for given transmitter and receiver antenna aperture, shorter wavelengths (i.e. higher frequencies) can propagate longer with more gain compared to

longer wavelengths (i.e. lower frequencies) if the transmission is more directive. If mmWave transmission is directional using *beamforming* with very *large antenna arrays* (such as in M-MIMO), no inherent disadvantage relative to the use of microwave band will be experienced (Khan, et al., 2012).

Another form of loss is the *penetration loss*. Millimeter-wave signals penetrate solid materials with lots of attenuation (Al-Falahy & Alani, 2017). Most of the signals from outdoor cell will remain outside on the street and other outdoor structures, with some reaching indoor through glass windows and wooden doors. Indoor coverage can be provided in this case using *indoor mmWave femtocell or Wi-Fi solutions*. Due the short wavelength, it is difficult for mmWave signals to reflect and diffract around obstacles and this loss depends greatly on the nature of the surface. Typically, except for the oxygen and water absorption band, atmospheric gaseous and precipitation loss of mmWave signal is less than few dB per kilometre. Millimeter-wave propagation can also experience significant loss during *heavy rainfall*. Therefore, *emergency communication* over microwave band when mmWave is disrupted by heavy rain should be integrated as part of the 5G millimeter-wave system as a hybrid mmWave Mobile Broadband (MMB) plus 4G network (Pi & Khan, 2011).

2.2.3.2. M-MIMO and Beamforming

M-MIMO or Large-Scale MIMO is a multiuser MIMO antenna system where the number of antennas at the base station is much larger than the number of devices sharing the same signalling resources from the base station. Beamforming is a form of transmission where the transmitted signal power is concentrated into beam with narrow width which is propagated in a certain direction. Combining M-MIMO with beamforming results in higher transmission gain and consequently improve signal strength significantly. This will increase cell throughput, spectral efficiency and provide better cell-edge performance (Barreto, et al., 2016)

However, implementation of M-MIMO is associated with some challenges. M-MIMO systems experiences *pilot contamination* from nearby cells as the number of antennas

increases (Boccardi, et al., 2014). This can be mitigated by optimizing pilot orthogonality without utilizing network resources. Accurate *channel estimation* is also complicated due to the huge costs and high complexity incurred from to the massive number of antennas used. A more advanced algorithm is needed to accurately estimate the channel characteristics and reduce signalling overhead. Also, due to the large physical size of M-MIMO, a *large-scale architecture* is required for installation. However, a reasonable and suitable array size can be realized if M-MIMO is combined with mmWave band (Young, 2015).

2.2.3.3. New Waveforms for 5G

Advance waveforms have been proposed for 5G systems as an improvement on OFDM which is being used in current high-speed wireless and mobile communication systems such as Wi-Fi, Digital TV, WiMAX, LTE and LTE-A. It is not sure whether OFDM will be the dominant multiple access scheme in future networks as it is not free of drawbacks (Andrews, et al., 2014). Several research papers have suggested that adoption of new efficient transmission waveforms for 5G will further improve spectral efficiency. Alternatively, despite some drawbacks associated with OFDM systems, some researchers have the opinion that it will still be suitable enough to support the requirements of next generation communication systems (Banelli, et al., 2014). In OFDM, the main stream to be transmitted is divided into subframes. The subframes are then modulated separately on different subcarrier frequency before transmitting them simultaneously using multiple carriers. OFDM have been widely adopted for present day high capacity communication systems because of its favourable characteristics and simple implementation. These are efficient implementation through FFT (Fast Fourier Transform) blocks and low-complexity equalization through frequency-domain equalizers which is independent of the number of multipaths. OFDM system also offers great improvement in network capacity when combined with MIMO antenna system since OFDM can deal with spatial interference that arise from transmitting through multiple antenna without the problem of inter-symbol interference (ISI) (Andrews, et al., 2014).

However, OFDM have some drawbacks and some new waveform may be required to meet the requirements of 5G applications and services. In machine-type communication

(MTC) scenario, there may be *loss of subcarrier orthogonality* arising from degradation of synchronization that occurs when devices that may have been idle for a long time wake up to transmit small pieces of information. This can result in loss of packets, and retransmission or resynchronization will produce an increase in latency. In this case, other waveform may be preferred as an alternative to OFDM (Barreto, et al., 2016).

Also, OFDM waveform has a *high peak-to-average power ratio* (PAPR) which is the square of the peak amplitude (i.e. peak power) divided by the square of the RMS value (i.e. average power). The high PAPR can result to degradation of the transmitted signal because of non-linearity of power amplifiers. Use of complex computational techniques or deployment of power amplifiers with large linear dynamic range may provide solution to this problem (Jiang & Wu, 2008). However, this is a trade-off between linearity of transmitted signal and the high energy consumption and cost of power amplifiers. This will be a setback on the road to meet up with 5G requirements of cost and energy efficiency.

OFDM waveform also experience *power leakage outside* of the useful bandwidth. This necessitate the use of guard bands to separate adjacent channels. For example, in LTE system, in a 20 MHz channel, only 18 MHz is used for actual transmission while the remaining 2 MHz (10%) is reserved for as guard band (Barreto, et al., 2016). The *cyclic prefix* (CP) inserted in OFDM subframes to prevent interference between neighbouring blocks also decreases spectral efficiency (Andrews, et al., 2014). Several new approaches have been proposed to address the weaknesses of OFDM. These new approach trades subcarrier orthogonality for increased spectral efficiency and reduced out-of-band emission. Some of these include:

- **Filter Bank Multicarrier (FBMC)**: In this technique, every signal transmitted on each subcarrier are shaped separately by passing them through specifically designed filters. With FBMC, signal power side lobes are suppressed and power leakage outside of useful band is also mitigated. This will eliminate the need to use guard bands.
- **Universal Filtered Multicarrier (UFMC)**: This technique is an extension of FBMC. Instead of filtering signals on each subcarrier separately, filtering is

performed on groups of adjacent subcarriers. Similarly, the aim of UFMC is to reduce signal side lobe levels and interference between adjacent subcarriers that arise because of weak time/frequency synchronization

- **Generalized Frequency Division Multiplexing (GFDM)**: This technique uses a similar approach as the one used in OFDM but transmits in blocks in the time domain as well to reduce transmission overhead. Each time-domain block also has a cyclic prefix as in OFDM, but the duration of the CP is shortened using a tail-biting digital filter.

2.2.3.4. Dense Small Cell Deployment

Deployment of low power small cells or ultra-densification can be used to offload network traffic on macrocells and significantly improve signal transmission power. Small cells can also be used to fill coverage holes such as in rural area where signal quality is poor. Network coverage and capacity issue resulting from the continuous increase in network traffic can be addressed by installing different types of small cells as required, indoors (in house, office, etc.) or outdoors, creating an ultra-dense and *heterogenous network* (HetNet) (Al-Falahy & Alani, 2017).

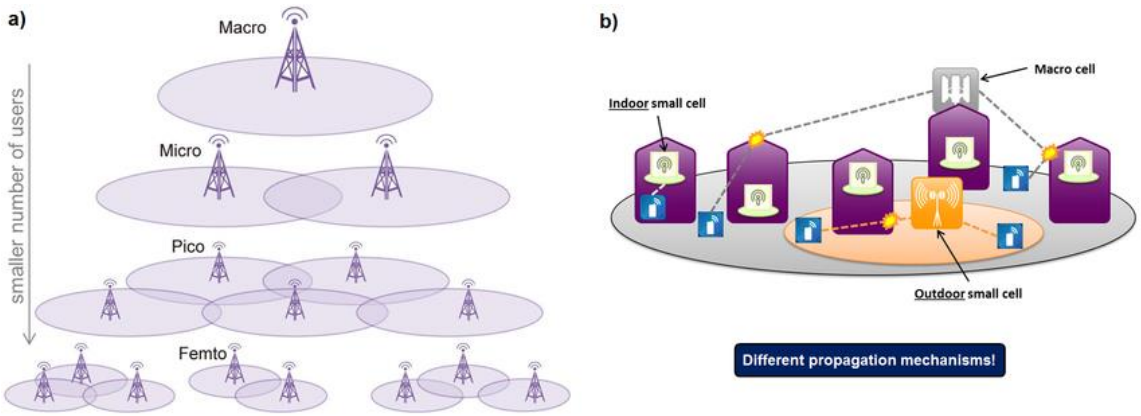

Figure 6. Different Types of Small Cells in Heterogenous Network (Barreto, et al., 2016).

In addition to the traditional macrocells, HetNets can include other types of cells as shown in Figure 6. They can be classified according to the number of users that can be served, coverage area or transmitting power as depicted in Figure 6a. These are Microcells, Picocells and Femtocells. They can also be classified according to location or propagation mechanism as illustrated in Figure 6b. Deploying small cells with reasonable cell radius will increase spectral efficiency through efficient spectrum reuse and increase network capacity. This offers a cost effective and simple solution to network congestion (Barreto, et al., 2016).

However, ultra-densification *increases handoff rate* as too many unnecessary handovers will be established as a mobile terminal moves from one cell coverage area to another due to the small cell radius. Handover failure and call drops may be experienced as too many unnecessary handovers take place. This issue can be addressed by *decoupling user-plane and control-plane*. In 5G heterogenous network, signalling services for a coverage area of a group of small cells can be provided by a specialized base station operation in a licensed microwave band, while the small cells operation in mmWave band provides the resources for high speed data transmission with little control overhead as illustrated in Figure 7b. Another issue is the *intercell interference* that exists between cells. Uncontrolled cell deployment can also lead to *uncontrolled cell shape* where operators will have no control over the cell positions (Al-Falahy & Alani, 2017).

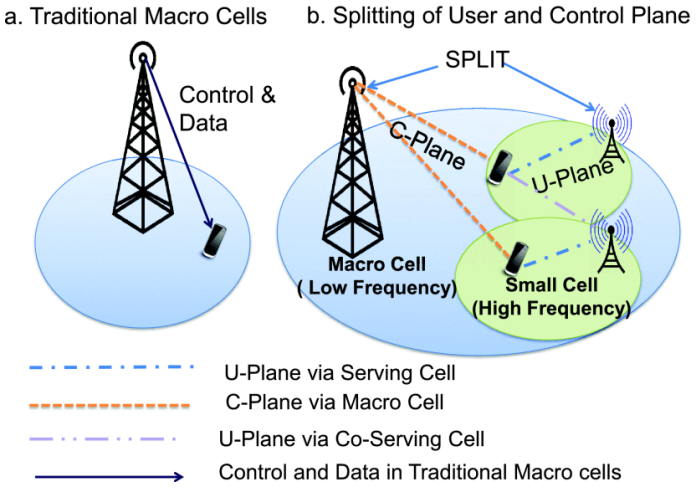

Figure 7. Separation of Control Plane and User Plane (Agrawal, et al., 2015).

2.2.4. 5G Network Architecture

Current wireless and mobile communication network architecture is based on the BS or AP. The BS is a fixed node that provides wireless connectivity for user equipment (UE) located within its coverage area. The demanding requirements of 5G networks has become a motivator for the transition of cellular networks from the traditional base station centric network. Current trends in mobile communication suggests 5G network will be device or user centric rather than base station centric as illustrated in Figure 8. User's device will no longer be a mere end-point of services and applications provided by the network. Devices will be active components of the communication network providing storage, computation, content delivery and relaying functions for other devices within the network (Agrawal, et al., 2015). Moreover, fixed terminal relaying was introduced in 4G using relay nodes at cell edges to strengthen the network link, fill coverage holes, and further extend coverage area. With the incorporation of D2D communication in 5G cellular network, device relaying and user cooperation will be made possible, and the network throughput will further improve (Al-Falahy & Alani, 2017).

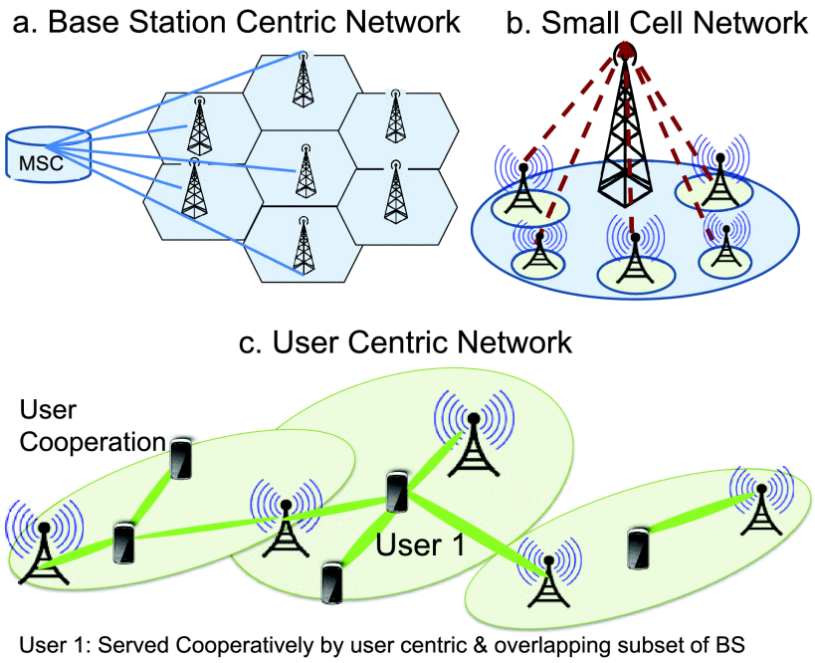

Figure 8. Migration Towards User/Device Centric Architecture (Agrawal, et al., 2015).

There has been a successful densification of cell deployment in the current 4G networks resulting in a network of different kind of cells. This densification approach will continue in 5G networks with a more dense and extreme deployment of small cells with the introduction of the UDN. 5G networks will feature advanced heterogenous networks that integrates different kinds of networks that interoperates, providing diverse services for massive number of users with different varieties of devices. There will be a native support for M2M communication with extremely reliable link for real-time operations on massive number for connected machine-type devices at very low latency. Consequently, the major concern here is the integration of 5G millimeter-wave base stations with the current cellular networks. Since 5G standard has not been released yet, there is no form of standardization or agreements on how 5G network should be. However, some architectural layout approach and techniques have been proposed for 5G and are being investigated in relation to the physical network structure, signalling protocols and network management (Barreto, et al., 2016).

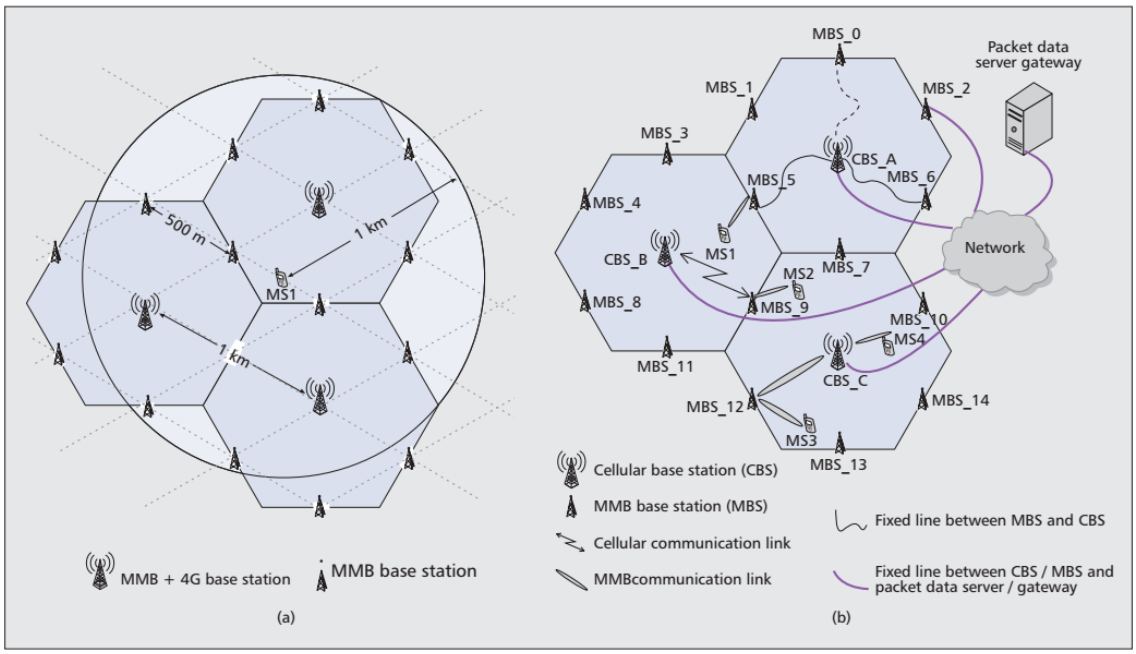

Figure 9. 5G Millimeter-wave Network (a) MMB Architectural Layout (b) Hybrid MMB plus 4G System (Pi & Khan, 2011).

Different configurations were proposed by Pi & Khan (2011) for millimeter-wave mobile broadband (MMB) network. These are the standalone MMB network and the hybrid MMB integrated with 4G network. A grid system layout for MMB base stations (MBS) was also introduced. An MMB network layout example is shown in Figure 9a. Contrary to cellular systems, where geographic areas are partitioned into cells served by one or a few BS, MMB base stations are positioned to form a *grid* with numerous nodes that can serve MMB mobile stations. MMB base stations should be deployed with higher density than macrocells. The use of beamforming for transmission supresses interference from neighbouring BS and extend the range of the MMB link. From the layout in Figure 9a, with site to site distance of 500 m between the MMB base stations, a mobile station can access up to 14 MMB base stations within a range of 1 km. The grid layout eliminates the problem of poor coverage or link quality at cell edges associated with traditional cellular systems. High-quality equal grade of service (EGOS) is ensured irrespective of the mobile station location (Pi & Khan, 2011).

The standalone MMB system can operate exclusively on mmWave spectrum using same spectrum for both wireless access and backhaul without much interference due to large beamforming gain. A hybrid MMB plus 4G system is shown in Figure 9b. With the hybrid MMB plus 4G system, MMB can be used exclusively for high data rate communication, while important system information, signalling information, control channel and feedback can be transmitted over the 4G cellular system operating in the microwave band since they have more favourable propagation characteristics. The 4G system can also cover coverage wholes left by the low density MMB base station deployment in the early stages of 5G deployment (Pi & Khan, 2011). Other techniques envisioned for 5G systems architecture are discussed in the following parts. Some of these are already in existence and have been standardized for current mobile and wireless communication systems.

2.2.4.1. Coordinated Multipoint

CoMP is a technique introduced for the LTE-A network and was standardized by 3GPP in its Release 11 (Lee, et al., 2012). CoMP is a form of cooperation among neighbouring cells that involves the sharing of data and channel state information (CSI) to coordinate

their joint transmission to a specific user in the downlink and joint processing of the received signal from the user in the uplink. The cells simultaneously transmit/receive signal to/from the user while sharing the same resource blocks. CoMP increases network throughput, and increases power and diversity gain by effectively turning inter-cell interference which was supposed to be harmful into useful signals. CoMP is expected to remain a relevant technique for 5G networks. In 5G, synchronization problem among cells arising from propagation delay which is a critical issue for CoMP will become less significant due to the use of smaller cells. However, CoMP requires a complex processing at both the receiver and transmitter. It is also necessary to have a high-speed backhaul network to enable the exchange of data, control information and CSI between the cooperating base stations (Barreto, et al., 2016).

2.2.4.2. Cloud Radio Access Network

Cloud Radio Access Network (CRAN) or Centralized-RAN is a proposed architectural technique for future mobile communication networks. C-RAN is a centralized architecture for radio access networks, based on cloud computing. The whole idea is based on centralization and virtualization. In current mobile communication networks, baseband processes are performed on the BS. In C-RAN, baseband processing units can be moved to a centralized server that operates on the cloud. In this case, the BS will just serve as a RF down/up converter responsible only for the forwarding of uplink and downlink signal to and from the centralized server (Checko, et al., 2015). A typical C-RAN is shown in Figure 10.

Baseband resources are pooled remotely from the cloud via the offsite central baseband unit (BBU). BSs cooperate and dynamically form BS clusters for joint processing on the central server, thereby creating a virtual cell for each cluster that handles all radio resource management tasks. The remote radio heads (RRHs) are connect to the BBU through fiber optic cable. RRHs is made up of transceivers, amplifiers and duplexers responsible for digital processing, digital-analogue conversion, power amplification and filtering. With C-RAN, the network becomes more efficient, affordable, and flexible. Also, network maintenance, upgrade and expansion become much easier. However, raw data

transmission from the base stations to the server requires a backhaul with very high capacity (Barreto, et al., 2016).

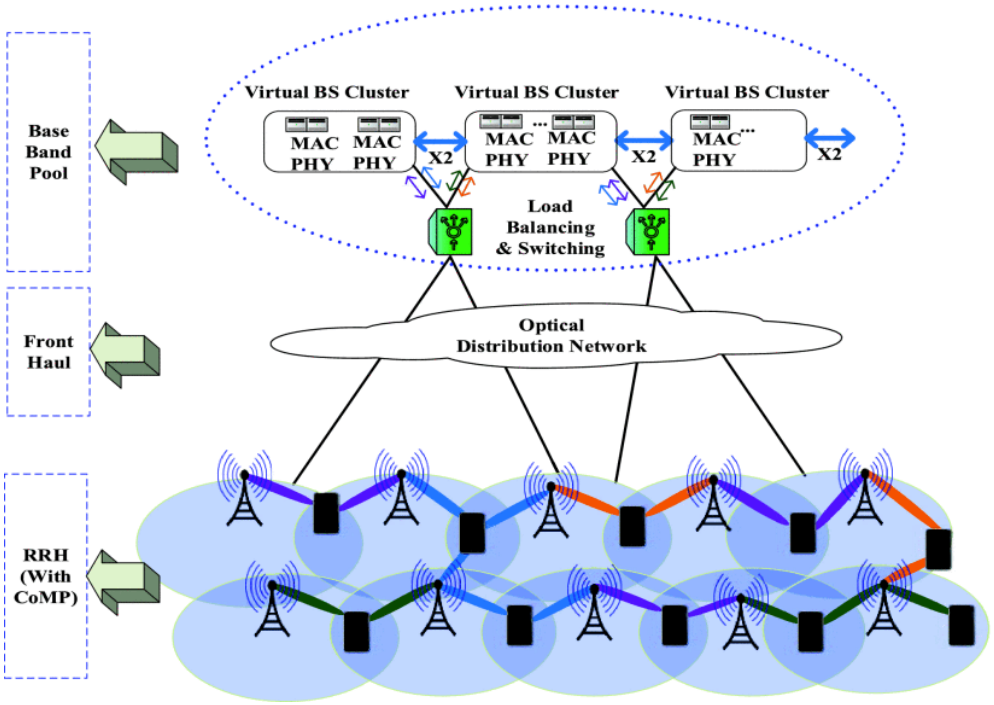

Figure 10. Cloud Radio Access Network Architecture (Agrawal, et al., 2015)

3. DEVICE-TO-DEVICE COMMUNICATION IN 5G NETWORKS

This chapter presents a general overview of D2D communication, discussing the different forms, application and use cases, as well as technical issues and challenges of implementation such as device discovery, security, interference, mobility management. An overview of 3GPP ProSe was also discussed. Direct D2D communication Technology component under the METIS project was presented with key D2D topic such as device discovery and interference management through mode selection algorithm, resource allocation scheme, SINR target setting and power control algorithms.

3.1. General Overview of D2D Communication

Device-to-device communication generally refers to a form of technology that enables nearby devices to communicate directly with each other over the licensed cellular bandwidth with limited or no AP or BS involvement. D2D communication is not a new technology and has been around for some time. *Bluetooth, ZigBee, IrDA* and *Wi-Fi Direct* are the most common low-level techniques that provides short range D2D communication functionality. However, they both operates over the unlicensed industrial, scientific and medical (ISM) band with uncontrolled interference. Therefore, these types of D2D communication are known as *out-band* D2D as they operate outside the cellular spectrum. Moreover, they cannot provide adequate security and the required quality of service usually guaranteed by cellular networks. However, current cellular networks do not provide support for direct over-the-air *in-band* D2D communication between devices (Tehrani, et al., 2014). D2D was proposed as part of 4G LTE-A network and was part of 3GPP LTE-A standard in Release 12 as ProSe. D2D communication has not been widely adopted by operators as part of communication networks in current communication systems. However, with the proliferation of new context-aware services and applications, and new trend in *cooperative communication* paradigm shifting from *fixed terminal relaying* to *device relaying*, D2D communication is expected to continue to evolve and play an important role in future 5G networks (Shen, 2015).

Cooperative communication enables network nodes to assist one another to relay information for spatial diversity realization. This technique offers significant improvement in link reliability, spectral efficiency, system capacity, and network coverage. Fixed terminal relaying as discussed in previous section involves the use of small cells in form of relay nodes to assist communication between source and destination devices. This of course was included in 4G LTE networks and offers a lot of improvement to the network. The benefit of cooperative communication can however be fully realized through device relaying. Device relaying enables user's devices such as cell phones or other portable devices with cellular network connectivity to serve as transmission relays for one another creating a massive ad hoc mesh network of devices. Device relaying can thus be realized through D2D communication (Tehrani, et al., 2014). Several research projects in 5G are exploring the possibilities and potential of the introduction of D2D communication functionality into future cellular networks. As seen from previous section, like 3GPP works on ProSe, D2D communication is also recognized as one of the key research topics under METIS 5G project as a component of the evolving 5G architecture for 2020 and beyond (Aziz, et al., 2015).

3.1.1. Forms of D2D Communication

With the integration of D2D communication into 5G systems, the whole cellular network can be considered as a two-tier network which is made up of the *macrocell tier* and *device tier*. Here, the macrocell tier represents the conventional cellular system with BS-to-device (B2D) communication, while the device tier represents the D2D communication aspect of the network. When a device connects to the cellular network via the BS or macrocell, such device is said to be operating in the macrocell tier. On the other hand, when a device communicates directly with another device, or a source device communicates with the destination device by routing the transmitting information through relaying devices, the devices are said to be operating in the device tier (Tehrani, et al., 2014). In the implementation of D2D, the communication can be direct communication or in form of device relaying. The direct D2D communication scenario can also be inform of unicast (one-to-one) or multicast (one-to many). Also, the operator can have different levels of control ranging from zero to full control over the allocation of network resources

among the source, destination, and relaying devices. This means that D2D communication can be *stand-alone* with no control link from the BS or *network-assisted* with control link created from the BS (Alkurd, Shubair, & Abualhaol, 2014). Tehrani et al. (2014), classified D2D communication generally into four different categories depending on the degree of involvement of the BS as discussed below.

I. **Device relaying with operator-controlled link establishment (DR-OC)**

In this mode of D2D communication, a device at the cell edge or in an area with poor network coverage and signal quality can reach the BS station by relaying the information to be transmitted through other devices as shown in Figure 11. By relaying information through other devices, users experience higher quality of service and increased battery life. A control link is created for the BS to have partial or full control over the allocation of resources.

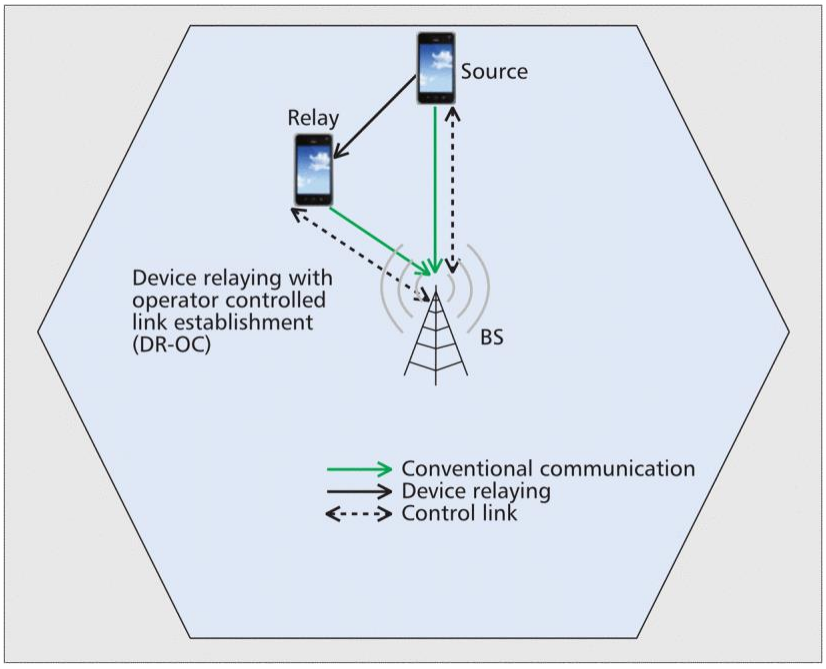

Figure 11. Network-controlled D2D Relaying (Tehrani, et al., 2014).

II. Direct D2D communication with operator-controlled link establishment (DC-OC)

In form of D2D communication, the source and destination devices communicate directly and transmit data without going through the BS as illustrated in Figure 12. However, the BS is still required to create control links for managing radio resources.

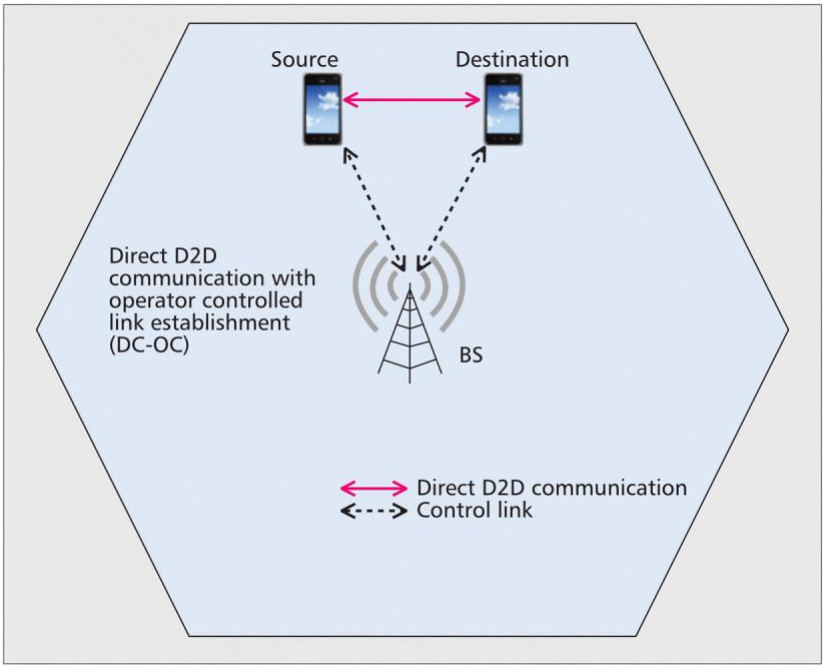

Figure 12. Network-controlled Direct D2D Communication (Tehrani, et al., 2014).

III. Device relaying with device-controlled link establishment (DR-DC)

This mode is like the DR-OC. But unlike DR-OC, the BS is not needed to establish and manage a control link. The source and destination devices coordinate the communication between them and use relaying devices to realize the transmission of data as shown in Figure 13.

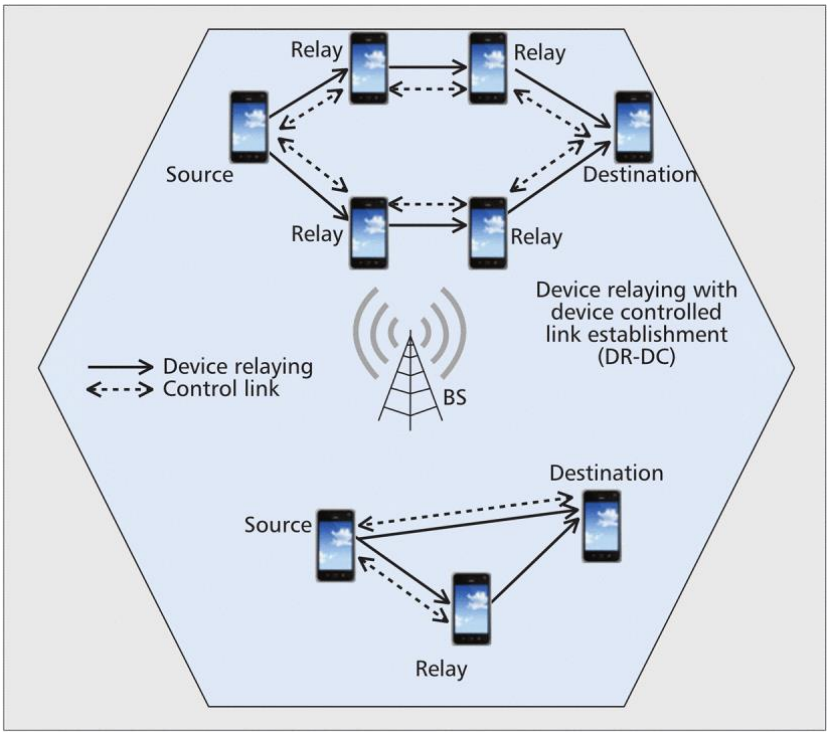

Figure 13. Device-controlled (Stand-alone) D2D Relaying (Tehrani, et al., 2014).

IV. Direct D2D communication with device-controlled link establishment (DC-DC)

In this D2D communication mode, the source and destination devices communicate directly with each other without requiring the BS to establish control link as illustrated in Figure 14. Thus, the two communicating devices are responsible for managing the available radio resources to minimize the interference with other devices operating in either the macrocell or the device tier.

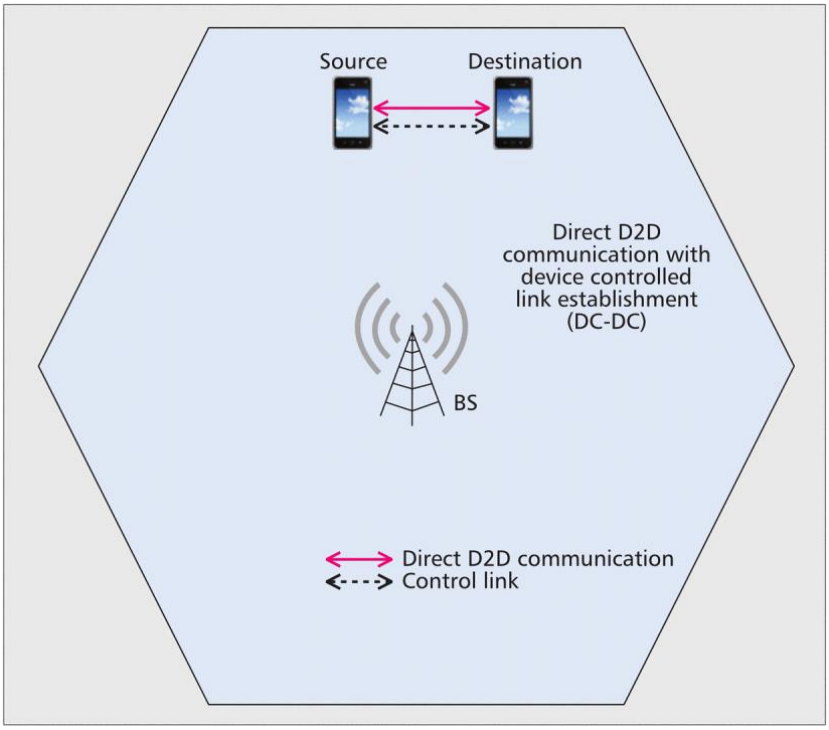

Figure 14. Device-controlled Direct D2D Communication (Tehrani, et al., 2014).

3.1.2. Application and Use Cases of D2D Communication

D2D communication can play important role in the implementation and improvement of *context-aware services and applications*. Context-aware services is an emerging computing technology that utilizes information about the current location of a mobile device to provide useful services to the user of the device. This technology requires the discovery of the device location, other proximate devices, and of course communication among these proximate devices. In these proximity-based services scenarios, mobile devices detect their proximity and relevant services are subsequently triggered (Tehrani, et al., 2014). Such services include social applications, online gaming, advertisement, local exchange of information, real-time traffic update, V2X communication i.e. vehicle-to-vehicle (V2V), vehicle-to-infrastructure (V2I), vehicle-to-pedestrian (V2P) communication, etc.

Public safety support is another scenario where D2D communication can be applicable. The inclusion of D2D communication in 3GPP LTE Release 12 was motivated by *public safety* (PS) applications for emergency authorities like police, firefighters and emergency medical services. D2D communication network can provide local connectivity at least in cases where the radio infrastructure is damaged. D2D communication can also be used in times of natural disaster such as earthquake to create an emergency communication network that temporarily replaces the damaged communication network and internet infrastructure for critical communication (Lien, Chien, Tseng, & Ho, 2016).

D2D Communication can also be used in *mobile cloud computing* and content delivery. D2D communication functionality can also facilitate *local content distribution* and effective sharing of data and resource among spatially close devices (Tehrani, et al., 2014). Network operators can also use D2D functionally to for *network traffic offloading* in crowded areas and peak periods. Deployment of small cells have been used in the past to offload hot-spot traffic, and cover network coverage holes. D2D on the other hand can be utilized to offload proximity services. Coverage holes can also be minimized through device relaying functionality of D2D communication (Shen, 2015).

3.1.3. Technical Challenges in Implementing D2D Communication

Enabling D2D communication functionality over cellular network offers a lot of potential benefits such as increase in network capacity and coverage, reduced latency, power consumption and operating cost. However, there are several challenges and design issues that must be addressed to fully exploit the potential benefits of implementing D2D communication. Some of the key technical challenges are discusses below.

3.1.3.1. Interference in D2D

Interference management is a major concern in D2D communication integrated in to a dense heterogenous 5G network. Devices operating in the device tier can be allowed to reuse macrocell tier spectrum to optimize resource utilization and improve spectral efficiency. When D2D users and cellular users share the same frequencies, interference occur between D2D connections and cellular connections. The D2D connection may

reuse cellular frequencies either in the *uplink* or *downlink* mode (Alkurd, et al., 2014). This is illustrated in Figure 15 with a D2D pair i.e. D2D transmitting device Tx UE and D2D receiving device Rx UE, a BS each in two neighbouring cells and two cellular devices, one in the home cell and the other in the neighbouring cell. When a D2D connection reuses the uplink frequencies in a cell, the two BS, eNB-1 and eNB-2, will receive interference signals from the transmitting D2D device, and the receiving D2D device will also receive interference signals from the transmitting cellular users UE1 and UE2. Conversely, when a D2D connection reuses downlink frequencies, the cellular users UE1 and UE2 will receive interference signals from the transmitting D2D device, and the receiving D2D device will receive an interference signal from the two BS.

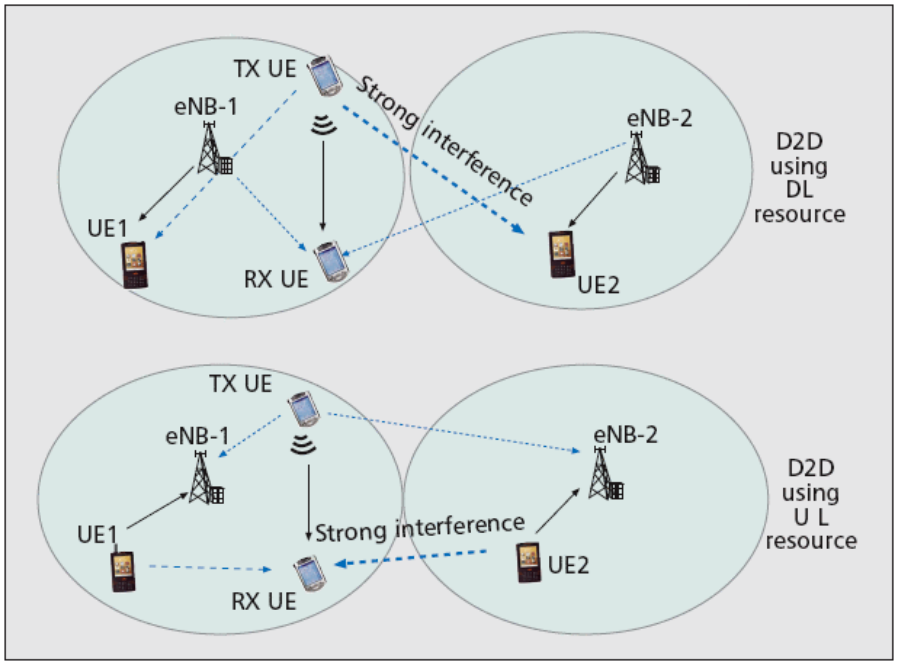

Figure 15. Cellular Frequency Reuse by D2D Communication (Fodor, et al., 2012).

In network-assisted or network-controlled D2D communication, i.e. DR-OC and DC-OC, resource allocation, power control and other signalling functions are handled by the BS or macrocell. Since a central entity exists in the form of the BS, interference management can be easily implemented using *centralized algorithms* which is a well-known research area in wireless communication that has been proven to be effective in managing radio

resources. Through the BS, resources can be assigned to each D2D connection dynamically just like what we have in conventional cellular communication. Likewise, the network can semi-statically assign dedicated resource pool D2D connections. However, with a stand-alone D2D network i.e. DR-DC and DC-DC, a centralized unit such as the BS does not exist to control communication and manage the allocation of resources among D2D devices. Therefore, implementing an interference management scheme to mitigate the impact of the D2D devices on the cellular network connections in the macrocell tier is more challenging. Moreover, interference also exists between the D2D devices in the device tire, i.e., interference can exist between D2D pairs. A *distributed approach* must be employed to implement an effective resource allocation scheme to mitigate interference (Tehrani, et al., 2014). Interference management for D2D communication in cellular networks primarily centres around three major function blocks. These are *mode selection*, *resource allocation* and *power control* (Alkurd, et al., 2014).

3.1.3.2. Security Challenges in D2D

Like all wireless communication technology, D2D is vulnerable to all forms of attack in wireless communication. Moreover, device relaying functionality of D2D communication routes data to be transmitted by a user equipment through other users' devices. In this situation, threats to *user privacy*, *location privacy* and *data integrity* must be addressed. To properly address this issue, all possible forms of risks and potential threats on user's identity and location, as well as information integrity must be identified. These threats to user, location and data privacy may be in form of eavesdropping, data fabrication or manipulation, identity impersonation, or privacy violation (Haus, et al., 2017). Based on these threats, D2D communication applications should provide data confidentiality and integrity, data authentication, entity authentication and privacy preservation.

As identified by Tehrani et al. (2014), one common way to establish security in D2D communication is to have groups of devices that trust each other in a *closed access* such as in a workplace environment or close neighbourhood. These devices can communicate with each other over the device tier while satisfying some level of privacy. There will be a proper encryption in place to prevent access to information by untrusted devices. A device will have a list of all trusted devices and devices not on its trusted list must

communicate with it over the macrocell tier or cellular network. However, this *trust-based* approach to security is not flexible and only suitable for direct D2D communication. In *open access* D2D communication, where devices act as communication relay for other devices without constraints making security solutions challenging.

Software based cryptography techniques such as public key cryptography and symmetric key cryptography can be implemented at the *application layer* to ensure data confidentiality and integrity, and authentication in D2D communication. Public key cryptography can be certificate-based, identity-based, or certificateless. With the certificate-based public key cryptography, certificates that bind users to their public key are issued by a trusted authority. The BS can function as a trusted authority in this case. However, certificate management creates additional load for the BS. This is against the goals of introducing D2D. Identity-based public key cryptography does not require BS for certificate management but experiences key escrow problem. On the other hand, certificateless public key cryptography does not require certificate management, and neither does it suffer from key escrow problem. Encryption keys are generated by collaboration of both the user and a semi-trusted authority. Therefore, *certificateless public key cryptography* can be used effectively in D2D communication. Also, *symmetric key cryptography* can also be implemented with symmetric key agreement between the communicating parties, to ensure data confidentiality and integrity (Zhang & Lin, Security-Aware and Privacy-Preserving D2D Communications in 5G, 2017).

Another security solution is to implement secrecy-based access control at the *physical layer* by exploring the physical characteristics of the wireless channel. Physical layer security solutions in wireless communication can be implemented using secrecy capacity, channel-based key agreement, and physical layer authentication (Zhang, Zhou, & Wang, 2016). Channel *secrecy capacity* can be adopted in D2D communication with further improvement by exploring the interference nature of the channel due to frequency reuse by D2D devices (Zhang & Lin, 2017). A simple D2D setup with a cellular user in uplink, an eavesdropper, and a D2D-pair that reuses the cellular link spectrum is illustrated in Figure 16. The capacity of the D2D link from the illustration can be expressed as;

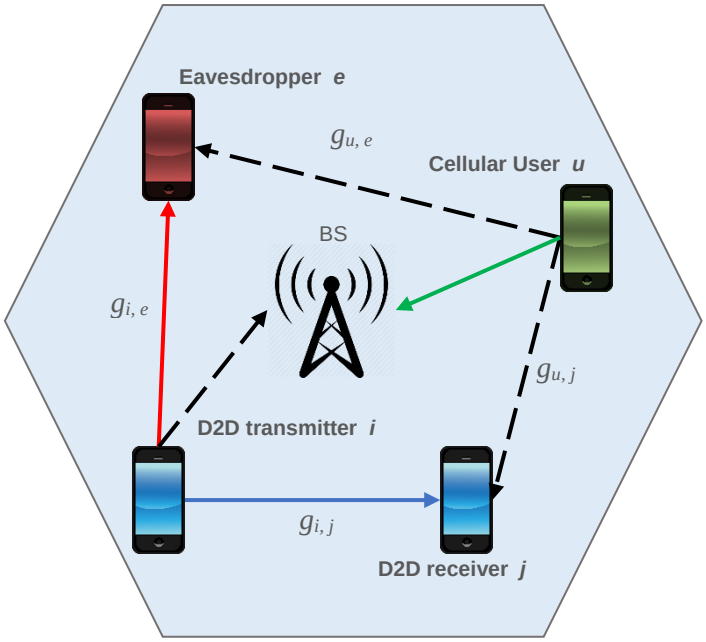

Figure 16. Illustration of a D2D Setup with an Eavesdropper.

$$C_1(i,j) = W\log_2\left(1+\frac{P_i g_{i,j}}{P_u g_{u,j}+\sigma_a^2}\right) \tag{3.1}$$

where P_i and P_u are the power transmitted by the D2D transmitter i and the cellular user u respectively, $g_{i,j}$ is the channel gain of the D2D link, $g_{u,j}$ is the gain of the interference channel from cellular user to D2D receiver, W is the bandwidth, and σ_a^2 is the additive white Gaussian noise at the D2D receiver. Similarly, the capacity of the interception channel from eavesdropper can be deduced as;

$$C_2(i,e) = W\log_2\left(1+\frac{P_i g_{i,e}}{P_u g_{u,e}+\sigma_e^2}\right) \tag{3.2}$$

where $g_{i,e}$ is the channel gain of the eavesdropping channel, $g_{u,e}$ is the channel gain of the interference channel from the cellular user to the D2D eavesdropper, and σ_e^2 is the additive noise at the eavesdropper's end. Therefore, the secrecy capacity of the D2D link with interference can be obtained from Equation 2.8.

$$C_a(i,j)=[C_1(i,j) - C_2(i,e)]^+ \tag{3.3}$$

where $[x]^+ = \max[x, 0]$. If the interference from the cellular user is not considered, the secrecy capacity of the D2D channel becomes;

$$C_b(i,j)=W\left[\log_2\left(1+\frac{P_i g_{i,j}}{\sigma_a^2}\right) - \log_2\left(1+\frac{P_i g_{i,e}}{\sigma_e^2}\right)\right]^+ \tag{3.4}$$

Secrecy capacity when interference is considered and when interference form cellular user is ignored are compared in Figure 17. Normally, $g_{i,j}$ is usually greater than $g_{i,e}$. The comparison from the representation shows that when $g_{u,e} > g_{u,j}$, $C_a(i,j) > C_b(i,j)$. This demonstrates that the secrecy capacity improves when interference from the cellular user on eavesdropper is greater than the interference on the D2D receiver.

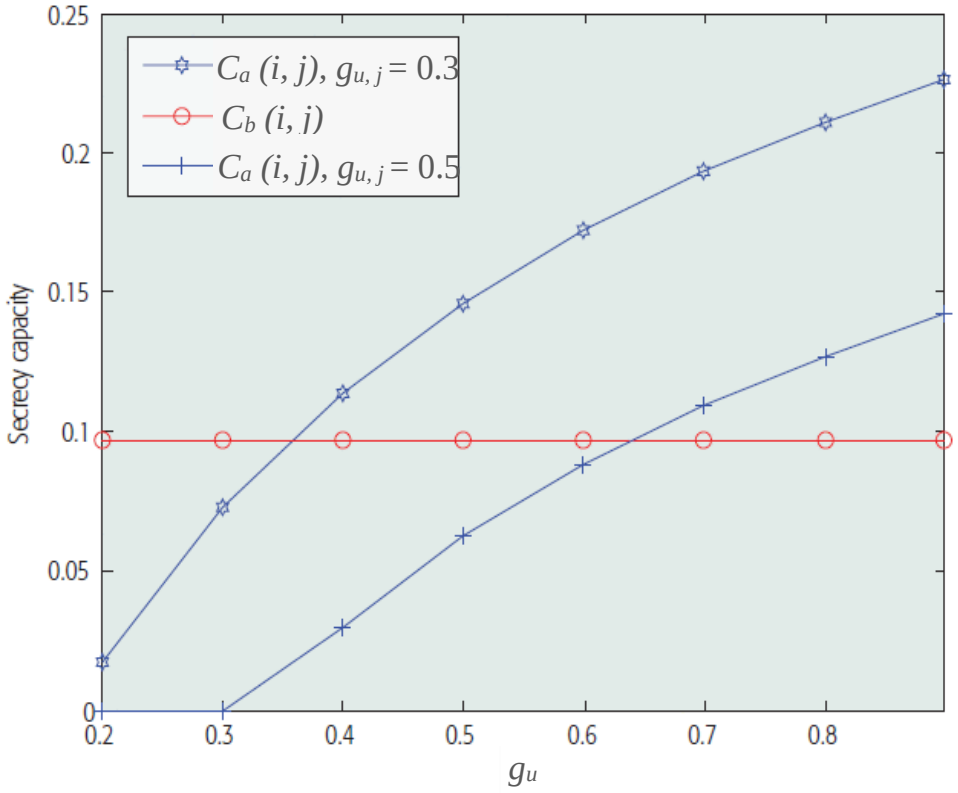

Figure 17. Comparison of the Secrecy Capacity with and without Interference (Zhang & Lin, 2017).

Both *channel-based key agreement* and *physical-layer entity authentication* techniques are based on channel characteristics measurement such as the CSI, channel phase, and received signal strength (RSS). In these techniques, the communicating parties can acquire the same channel measurements during the coherence time. On the other hand, the measurements obtained by the eavesdropper will be different if the distance between the eavesdropper and the transmitter is longer than the channels coherence distance (Premnath , et al., 2013). According to Zhang & Lin (2017), security solutions in wireless systems currently consider application-layer and physical-layer techniques separately. They identified that they can both be combined to obtain more desirable security solutions.

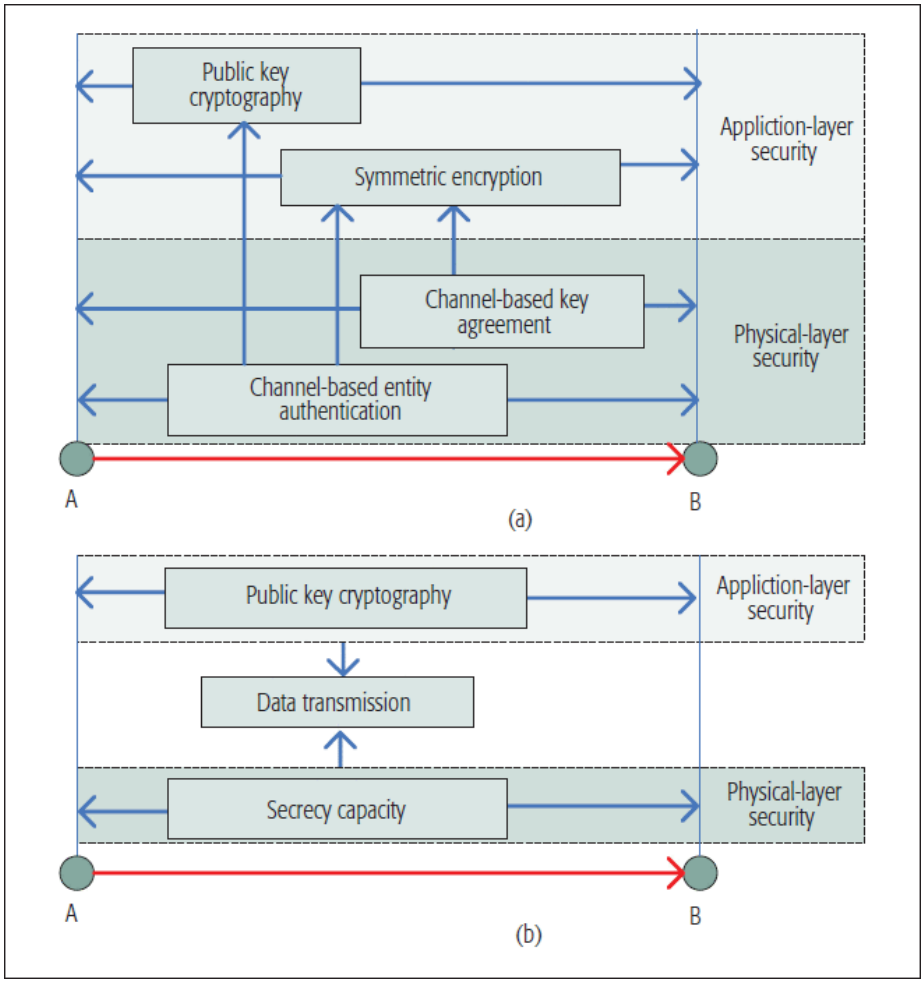

Figure 18. Two Joint Physical-Application Layer Security Frameworks (Zhang & Lin, 2017).

A cross-physical-application-layer security was proposed consisting of two different frameworks to choose from. Figure 18a illustrates the first framework. The D2D user obtains symmetric key from channel characteristic measurement as discussed to execute either channel-based entity authentication or channel-based key agreement. The result of authentication and the symmetric key are then transferred to the application layer for cryptography through symmetric encryption. This framework avoids key management at the application layer but requires the knowledge of random channel characteristics. In the second framework shown in Figure 18b, The D2D transmitter obtains the secrecy capacity and transmits data at this rate ensuring that data can only be intercepted only by the legal D2D receivers. Public key cryptography is then employed at the application layer. This framework also eliminates the need for key management but requires the knowledge of the eavesdropper's channel characteristics to obtain the secrecy capacity.

3.1.3.3. Device Discovery and Mobility Management

In addition to the issue of security and interference management for coexistence of the different tiers involved, efficient device discovery mechanism is necessary for detecting the proximity of D2D communication-enabled devices. Devices must be able to detect other devices near them to potentially establish a D2D communication session. Device discovery can be managed by the network in network-controlled D2D communication, or devices can perform discovery on their own using the information local to them especially in cases when network infrastructure is not available and D2D communication is independent of the network. Moreover, D2D communication devices can be mobile, in case of cell phones, smartphone tablets, etc., or stationary such as in machine-type communication. A D2D handover mechanism is also necessary in addition to the existing cellular handover to efficiently manage the movement of D2D devices between cells.

3.2. Overview of 3GPP Proximity-based Services in Release 12

The need for a D2D communication technology that will serve as an underlay to the widely deployed LTE and LTE-A networks is the main motivation behind the

development of ProSe by 3GPP. Integrating D2D technology into cellular networks will greatly improve the capabilities of the technology and open doors for other technologies with advanced services and application. D2D communication for cellular networks did not attract much attention in terms of research and standardization until ProSe which was defined in 3GPP Release 12 was endorsed by the Federal Communications Commission (FCC) of the United States for Public Safety (PS) networks replacing old systems such as Terrestrial Trunked Radio (TETRA) system developed in the 1990s. D2D communication underlaying LTE/LTE-A networks was approved as the first network (FirstNet) responsible for providing communication services in the occurrence of events that requires public safety (Lien, et al., 2016). Public Safety Networks requires high data rate and low latency communication with very high reliability and availability. Moreover, for Public Safety, D2D must be able to provide urgent communication when BSs and other communication infrastructures are damaged by natural disaster or malicious attacks (Lin, Andrews, Ghosh, & Ratasuk, 2014).

3.2.1. ProSe D2D Communication Scenarios

Apart from public safety purposes, 3GPP also identified other potential use cases for D2D communication in future applications. These includes commercial and social proximity-based services and application, network traffic offloading as well as the integration of existing network infrastructures and services. Although 3GPP Release 12 focused primarily on public safety applications, but a general approach of ProSe was followed to develop the system architecture of D2D communications to support all potential applications (Lien, et al., 2016). 3GPP ProSe must support urgent communications in several cases when:

I. all BSs are available,
II. some BSs are available, while some are out of operation, and when
III. all BSs are unavailable.

To provide support for these three D2D communication cases, 3GPP defined three different scenarios depicted in Figure 19.

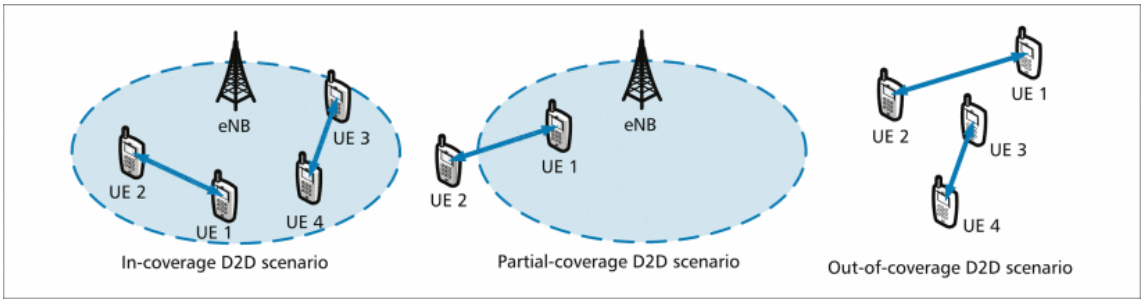

Figure 19. 3GPP Release 12 (ProSe) Communication Scenarios (Lien, et al., 2016).

I. **In-coverage D2D Scenario**: In this scenario, the user equipment (UE) in question is within the coverage area of the eNB(s).
II. **Out-of-coverage D2D Scenario**: This scenario indicates that the UE being considered is out of the coverage area of the eNB(s).
III. **Partial-coverage D2D Scenario**: This scenario represents the event when some UEs are within the coverage area of the eNB(s) while some UEs are outside the coverage area of the eNB(s).

As *uplink* and *downlink* denotes data transmission from UE to eNB and eNB to UE respectively, direct D2D transmission between two UEs (i.e., UE – UE) in 3GPP ProSe is referred to as *sidelink*. Considering the ProSe direct communication path, network coverage status (in-coverage or out-of-coverage), and the Public Land Mobile Network (PLMN) on which two UEs are registered, different direct D2D communication scenarios were identifies and defined by 3GPP (2014) in Release 12 as shown in Table 4. These scenarios are further illustrated in Figure 20.

Table 4. E-UTRAN ProSe Direct Communication Scenarios *(3GPP, 2014)*.

	UE1	UE2	Serving PLMN/Cell	Data Path
1A	Out	Out	–	Direct
1B	In	Out	–	Direct
1C	In	In	same PLMN, Same cell	Direct
1D	In	In	same PLMN, Different cell	Direct
1E	In	In	different PLMN, different cell (both UEs are in both cells' coverage)	Direct
1F	In	In	different PLMN, different cell (one UE is in both cells' coverage and the other UE is in serving cell's coverage)	Direct
1G	In	In	different PLMN, different cell (both UE are in its own serving cell's coverage)	Direct
NOTE: In = in coverage, Out = out of coverage				

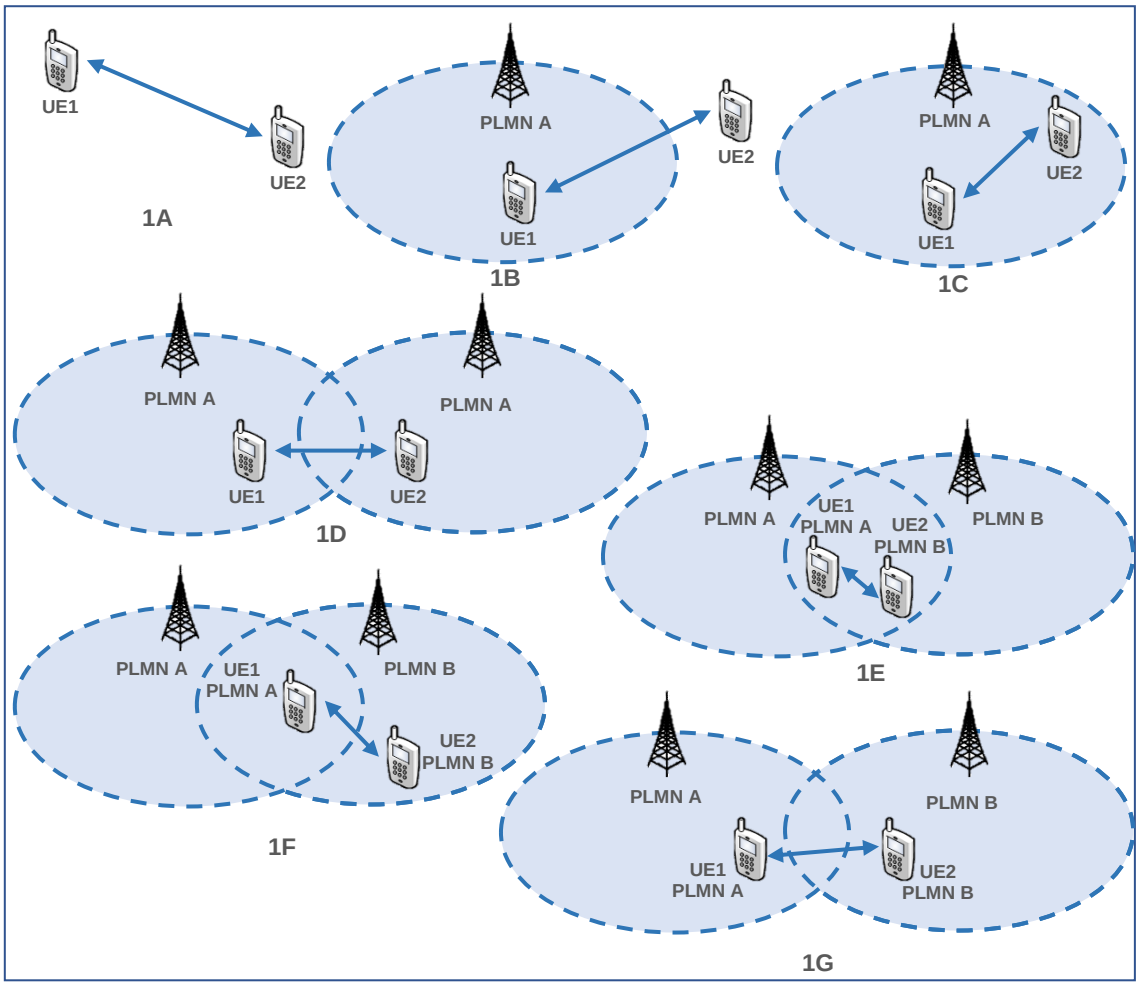

Figure 20. E-UTRAN ProSe Direct Communication Scenarios (3GPP, 2014).

These supported direct communication scenarios can be in form of;

I. **Network-independent direct communication** which does not require assistance from the network to authorize D2D connection. This mode can be used when UEs have been pre-authorized for ProSe public safety, and when UEs operate in in-coverage or out-of-coverage scenario for either ProSe one-to-one or one-to-many direct communication.

II. **Network-authorized direct communication** which requires the assistance of the network for connection authorization. This mode can only be used only in in-coverage scenario and one-to-one ProSe direct communication mode.

Apart from direct communication, 3GPP ProSe also support two types of D2D relay communication. These are:

I. **UE-to-Network Relay**: An in-coverage UE-Relay (UE-R) being served by the eNB can relay one-to-one or one-to-many ProSe communication from the eNB to UEs out of the eNB coverage, or from a UE out of coverage to the eNB as shown in Figure 21a.

II. **UE-to-UE Relay**: An in-coverage or out-of-coverage UE-R can relay one-to-many or one-to-one ProSe communications between Public Safety-enabled UEs within its coverage as shown in Figure 21b and Figure 21c.

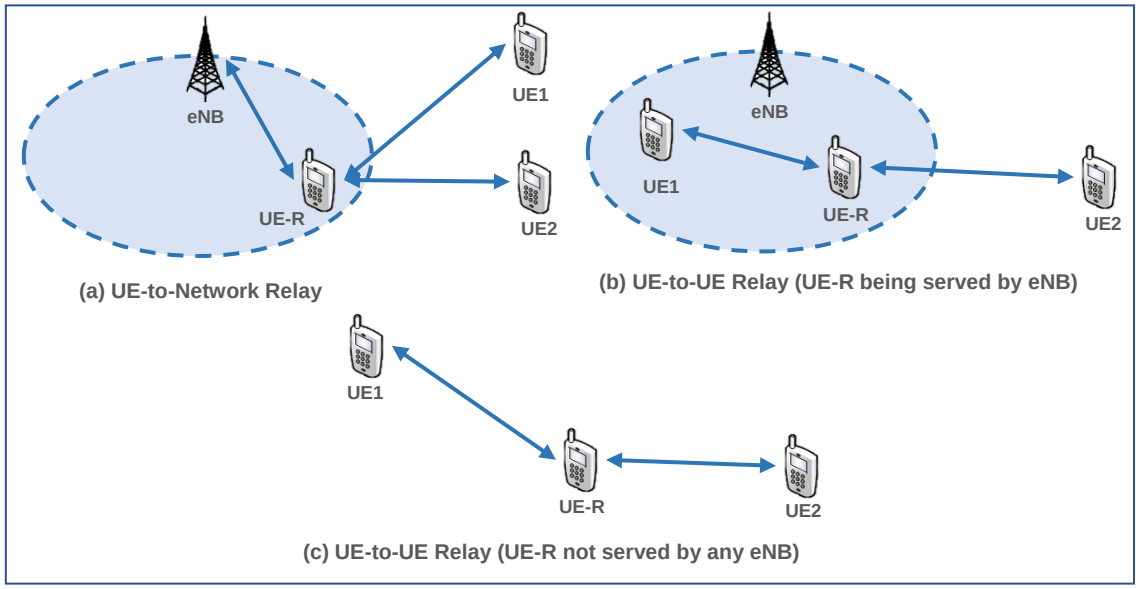

Figure 21. Types of UE-Relay in ProSe (3GPP, 2014).

3.2.2. ProSe Reference Architecture and Interfaces

The 3GPP ProSe reference architecture for D2D communication designed to support the three scenarios is shown in Figure 22. The architecture defined more reference points and interfaces PC1 through PC8 and SGi in addition to the Uu interface between a UE and an eNB in the E-UTRAN, and the S1 interface between the EPC and an eNB. The additional reference points are described as follows.

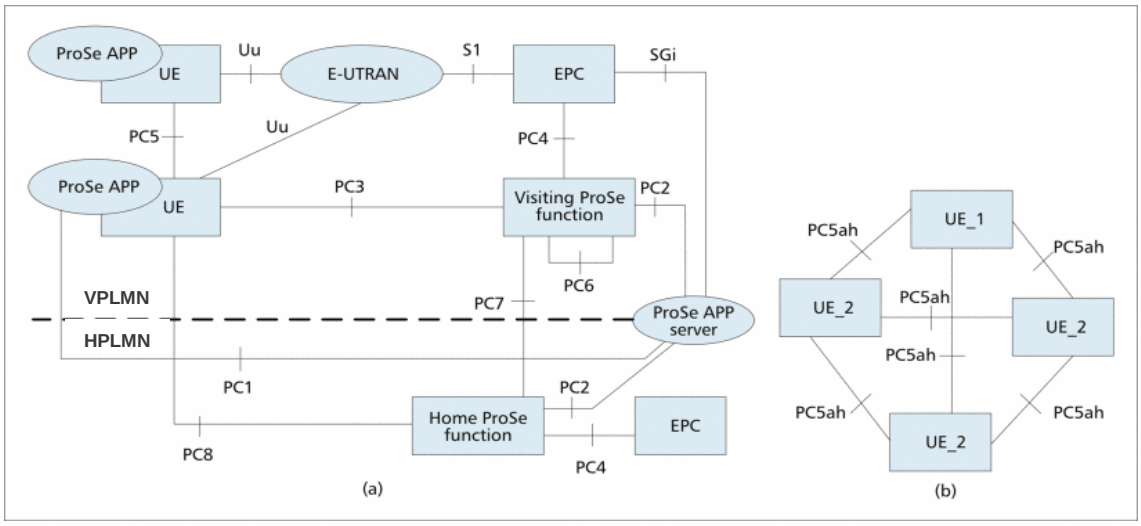

Figure 22. ProSe Reference Architecture (a) Roaming (b) One-to-many Communication (Lien, et al., 2016).

PC1: This is the reference point between the UE and the ProSe App Server. It defines application level signalling requirements. ProSe App installed on the UE exchanges data with ProSe APP Server through the interface.

PC2: This interface defines the interaction between the ProSe App Server and the ProSe Function. ProSe Function defines the ProSe functionalities provided by 3GPP Evolved Packet System (EPS). An example of these ProSe functionalities is the update of application data for a ProSe database.

PC3: A UE requires D2D discovery to locate other UEs in its proximity. PC3 is the reference point between a roaming UE and the Visiting PLMN (VPLMN) ProSe

Function. It defines the interaction between the UE and Visiting ProSe Function for configurating ProSe discovery and communication when roaming.

PC4: The EPC interacts with the supported ProSe functionalities via PC4. It defines the interaction between the ProSe function and the EPC. An example is the validation and authorization of ProSe services for real-time session and mobility management. Also, this is needed when setting up one-to-one communication path between UEs.

PC5: This is the interface between two UEs used for control and user plan interaction for discovery and communication such as one-to-one and relay communication i.e. direct communication between UEs and between UEs through LTE-Uu.

PC6: This is the reference point between ProSe Functions in different PLMNs. It is used for functions such as ProSe discovery between UEs subscribed to different PLMNs.

PC7: This is the interface between the ProSe Function within the VPLMN and the ProSe Function within the Home PLMN (HPLMN). It is used for HPLMN control of the validation of ProSe service.

PC8: This is the reference point between a roaming UE and the ProSe Function of the HPLMN. It can be used for by the ProSe Function in the HPLMN for configuring the UE for ProSe application.

SGi: The reference point facilitates the exchange of application data and application level control information between the EPC and the ProSe App Server.

3.2.3. Device Discovery in ProSe

A UE must locate other UEs within its proximity to make use of D2D for public safety, or commercial and social applications. Device discovery under 3GPP specification is classified into two broad groups. These are *direct discovery* and *EPC-level discovery*. With direct discovery, a UE equipment autonomously searches for nearby UEs by periodically transmitting or receiving discovery messages (Lin, et al., 2014). Two different discovery models were defined by 3GPP (2014) for direct discovery mode. These are:

Model A ("I am here"): Two different roles were defined for UEs taking part in the direct discovery process.

a. *Announcing UE*: This UE announces its presence by broadcasting useful information that can be used by nearby UEs that have permission to discover it.
b. *Monitoring UE*: This UE receives useful information by listening for announcement.

The announcing UE broadcast a discovery message about itself containing for example, its ProSe UE Identities or ProSe Application Identities, at predefined intervals for interested UEs to receive and process them accordingly.

Model B ("who is there"/ "are you there"): This model also defined two roles for UEs taking part in the discovery process.

a. *Discoverer UE*: This UE transmits a discovery message directed to a particular UE.
b. *Discoveree UE*: This UE responds to the request message with information about requesting UE message.

The discoverer sends request message about UE(s) that it is interested in discovering e.g. ProSe Application Identity of a group or a UE's ProSe Identity.

The signalling sequence diagram in Figure 23 and Figure 24 illustrates the D2D discovery procedures for Model A and Model B respectively. When a UE needs to perform device discovery to use D2D communication, its ProSe App sends a message to the ProSe App Server to request for the UE's friends list. The friend list in the UE's application layer maps each friend to their corresponding friend identity (Friend-ID). On obtaining the friend list from the server, the ProSe App of the UE requests for the *expression code* of each Friend-ID on the list from the ProSe Server through the 3GPP layers. The server then responds with the expression code. After obtaining the expression code, the UE ProSe App can then proceed to use either Model A or Model B for other UE discovery.

For instance, if UE-A chooses to announce its existence as in Model A, its expression code is sent to the 3GPP layers as shown in Figure 23. The 3GPP layers then broadcast a Model A discovery message containing the expression code of UE-A. When a friend of

UE-A e.g., UE-B receives a Model A discovery message, it becomes aware of the presence of UE-A. The 3GPP layers of UE-B then acknowledge the discovery to its ProSe App. Alternatively, if the ProSe App of UE-A chooses to discover a friend e.g., UE-B, its ProSe App sends the corresponding expression code of UE-B to the 3GPP layers, as shown in Figure 24. The 3GPP layers of UE-A then broadcast a Model B discovery message containing the expression code of UE-B. When UE-B receives the Model B discovery message, it responds with a Model A discovery message to UE-A to inform it of its presence.

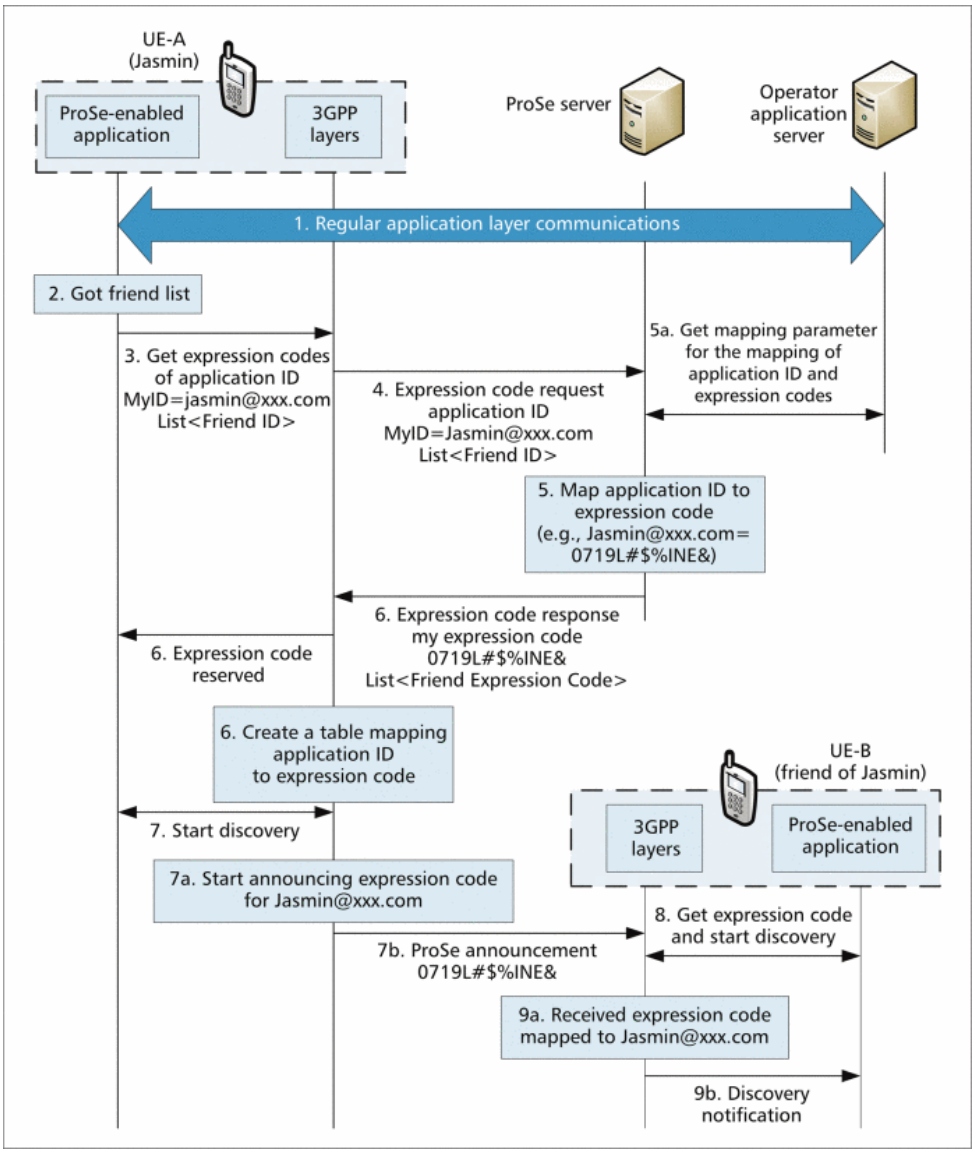

Figure 23. Signalling Procedures for Model A Direct Discovery (Lien, et al., 2016).

EPC-level discovery determines the proximity of UEs, and a UE device starts the device discovery process upon receiving its target information from the network. This discovery mode requires the network to keep track of the UEs in the network, reducing the discovery burden on the UE devices. However, this mode does not work under out-of-coverage D2D scenario (Lin, et al., 2014).

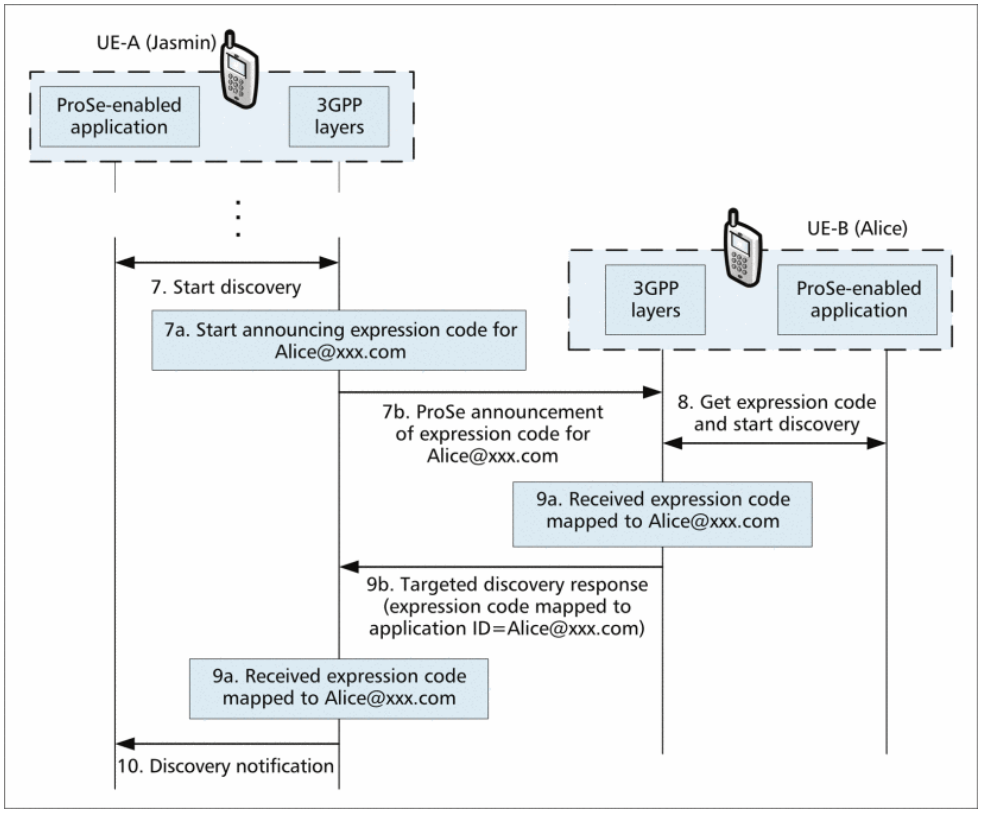

Figure 24. Signalling Procedures for Model B Direct Discovery (Lien, et al., 2016).

3.2.4. Mobility and Radio Resource Management in ProSe

3GPP ProSe specified in Release 12 does not provide support for paging procedure, especially for UE out of the coverage area of the eNB. Therefore, mobility management for D2D communication is very limited (Lien, et al., 2016). However, 3GPP air interface define two modes of resource allocation for D2D communications.

Mode 1: In this mode, radio resources are scheduled by the eNB for D2D transmission of data and control information by a UE.

Mode 2: In this resource allocation mode, a UE autonomously acquire radio resource randomly from a pool of pre-defined resources for D2D transmission of data and control information.

The Mode 2 resource allocation can be used by a UE operating in either in-coverage or out-of-coverage D2D scenario. On the other hand, Mode 1 can only be used by UE in the in-coverage scenario. A transmitting UE must inform the receiving UE about the radio resources (either scheduled by the eNB or randomly selected by the transmitting device) being used for the transmission. This information about the radio resources is known as the Sidelink Control Information (SCI). SCI transmission is done twice, and it contains the Time domain Resource Pattern of Transmission (T-RPT), which is the number of resources available for the transmission repetition of a data packet. The SCI also specifies the group ID of the receiving UE, and the modulation and coding scheme (MCS) being used for each data transmission (Lien, et al., 2016).

3.2.5. Physical Signals and D2D Channels

D2D communication under 3GPP definition reuses the Physical Uplink Shared Channel (PUSCH) of the Uu i.e., eNB-UE interface for D2D broadcast communications. Since the UEs are the transmitter while the eNB is the receiver in uplink, when the PUSCH is reused for D2D communication, several D2D pair can communicate simultaneously if interference from D2D link on eNB is minimal. Alternatively, in downlink, the UEs are the receiver while the eNB is the common transmitter. Therefore, reusing Physical Downlink Shared Channel (PDSCH) will produce interference from eNB that significantly impedes simultaneous communication between D2D pairs. Thus, reusing PUSCH produces higher spectral efficiency. Moreover, in LTE/LTE-A, SC-FDMA is used for PUSCH while OFDMA is used for PDSCH. Since SC-FDMA have a smaller PAPR than OFDMA, reusing PUSCH also produces higher energy efficiency (Lien, et al., 2016). Addition physical channels and signals were defined by 3GPP (2014) to support D2D communication.

- **Physical Sidelink Broadcast Channel (PSBCH)** – In D2D communication, physical layer synchronization is important. This can be achieved via a UE or the eNB which derives and transmits a *timing reference* for other UEs. The timing reference is conveyed in the *Sidelink Synchronization Signal.* The transmitter of the timing reference is the *synchronization source*. The synchronization source also transmits the PSBCH which contains the synchronization source ID and other information such as the frame number of the D2D communication, the type of synchronization source, system bandwidth, configuration of the time division duplex (TDD) or frequency division duplex (FDD) and the stratum level.
- **Physical Sidelink Discovery Channel (PSDCH)** – The *discovery signal* containing the *discovery message* for D2D device discovery is transmitted via the PSDCH
- **Physical Sidelink Shared Channel (PSSCH)** – Just like PUSCH used for data communication in LTE uplink, PSSCH is used for Layer 1 data transmission in D2D communication.
- **Physical Sidelink Control Channel (PSCCH)** – Just like Physical Uplink Control Channel (PUCCH) used for transmitting control information in LTE uplink, PSCCH is used for Layer 1 transmission of control information in D2D communication.

Energy efficiency in UE and interference mitigation can also be achieved through appropriate power control scheme. Since uplink transmit power is controlled by eNB, with increased complexity of the network due to the inclusion of D2D communication which reuses the uplink channel, there will be an increase in eNB signalling overhead. To avoid this setback, the UE can be given some control over the computation of the transmit power by making the eNB responsible for open loop power control to set a suitable transmit power range while the UE can be responsible for closed loop power control (Lin, et al., 2014).

3.3. Overview of D2D Communication Technology Component in METIS Project

D2D communication in METIS project focuses on *direct D2D communication* (one of its HTs) as an underlay to cellular network where UE can communicate either directly with each other in the D2D mode or through the BS in the cellular mode. Direct D2D communication that reuses cellular spectrum concurrently with other active cellular connection promises three major categories of potential gains namely; *proximity gain* (high bit rates, low latency, and low power consumption, *reuse gain* (better spectrum usage due to reuse of cellular frequency) and *hop gain* (downlink/uplink resources freed due to direct D2D communication (Aydin, et al., 2013; Fodor, et al., 2016). Just like 3GPP ProSe, METIS project addressed issues in designing D2D communication that reuses cellular frequency in both device discovery and D2D communication stages. D2D communication can reuse both uplink and downlink resource block. However, it is worthy to note that downlink frequencies are more congested compared to uplink especially for high data rate communication. Thus, D2D communication in cellular network are more likely to be set up with uplink resource reuse rather than downlink (Alkurd, et al., 2014). When a D2D pair (Tx UE – Rx UE) and a cellular user equipment (CUE) (UE1) use the same uplink physical resource block (PRB), this coexistence causes intra-cell interference as well inter-cell interference between D2D and cellular links as illustrated in Figure 25.

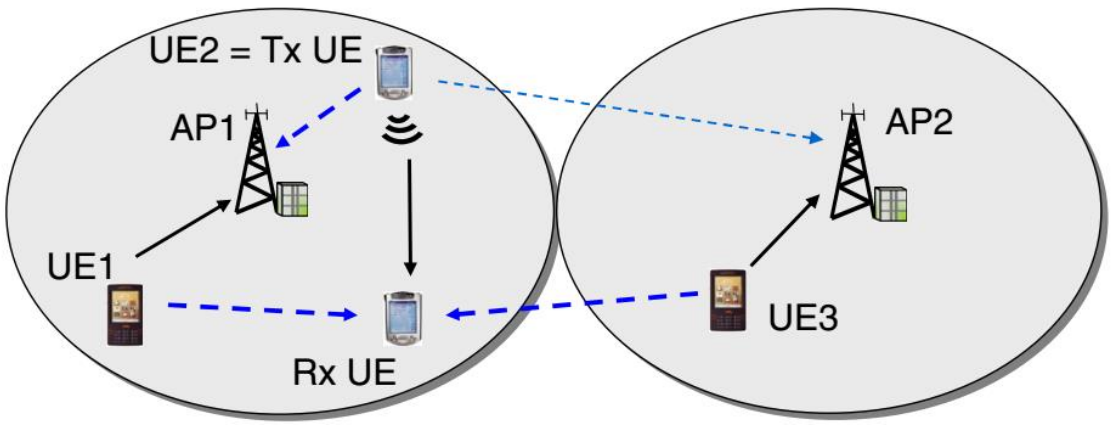

Figure 25. Illustration of Cellular Uplink Frequency Reuse by D2D Link in Multicell Environment (Reider & Fodor, 2012).

The D2D aspect of METIS project aimed at creating autonomous power-efficient, and scalable device discovery mechanism with efficient resource utilization. Moreover, to enable the coexistence of D2D and cellular communication, METIS D2D technology components aimed to achieve interference mitigation through *mode selection*, *resource allocation, power control*, and *SINR target setting*. The mode selection mechanism selects between direct D2D or network routed D2D. The resource allocation part will ensure dynamic allocation of time-frequency resources among D2D and cellular links (Aydin, et al., 2013). The following subsections generally discusses new practical, low complexity algorithms needed for device discovery, mode selection, power control, and resource allocation introduced by several authors in METIS research for cellular network-underlaying direct D2D communication

3.3.1. Device Discovery in METIS Direct D2D Communication

Here, the focus was set on optimizing the use of resources by UE for the transmission of discovery signals for device discovery. Resource allocation for D2D discovery considers scenarios when UEs are in coverage, partial or out of coverage of the network. UE should use resources in such a way to avoid selecting resources being used by other devices to increase the chances of discovery. This can be achieved through either Network-(NW) based or UE-based approach. In *UE-based discovery*, each UE selects discovery resources (DR) from all available resources based on local observations and common set of rules. This approach is scalable, ensures spatial reuse of resources, independent of the network, and can therefore be used when UE is out of network coverage. However, there is risk of collision with other UEs. On the other hand, in *NW-based discovery*, the BS allocates DR to each UE maintaining intra-cell orthogonality, thereby avoiding discovery delay and collision among UEs. Nevertheless, this NW-based approach applies to only UEs with network coverage. Also, it results in low resource utilization and high signalling overhead (Aydin, et al., 2013). Conclusively, these two approaches both have their advantages and disadvantages as well.

A *unified device discovery* solution, which can function in both network coverage and out of coverage situations, was however proposed in METIS. The DR allocation procedure is made up of two steps. The BS allocates one resource group (RG) containing at least one DR to each UE. The UE then choose one DR from the RG allocated to it. Different RG pattern exists for different scenarios varying the degree of network involvement. In full NW-based discovery, one RG is allotted one DR. On the other hand, in full UE-based discovery, all RG are available for selection as DR by the UE. In partial UE-based discovery, the DRs are divided among RGs which are assigned to each UE. A UE can then select a DR autonomously from the RG. This scheme benefits from both NW-based and UE-based device discovery. However, only one RG pattern can be used at a time (Aydin, et al., 2013).

3.3.2. Mode Selection in METIS Direct D2D Communication

Two novel mode selection (MS) algorithms were introduced for D2D communication in multi-cell cellular systems. These are distributed CSI-based mode selection and location-based mode selection. CSI-based MS uses the signal-to-noise ratio (SNR) instead of SINR to eliminate the complexity of acquiring and using the information about the transmit power of the interferer (Cellular UEs and other D2D pairs). Location-based MS relies on the usage of user's geographical location information by the BS for transmission mode selection (Li, et al., 2014).

3.3.2.1. Distributed CSI-based Mode Selection Algorithm

This mode selection algorithm was proposed by Reider & Fodor (2012) adopted in the D2D aspect of METIS project. The system model is considered with a single cell environment for simplicity as shown in Figure 26, with the assumption that each CUE is allocated its own PRB and intra-cell orthogonality is maintained without D2D. Also, at most one D2D link is allocated to one uplink PRB being used by a CUE, resulting in at most two links for each PRB (i.e. one cellular link and one D2D link). As mentioned earlier, with the use of SNR, the algorithm only depends on the information from the D2D pair i.e., Rx device (RxD) and Tx device (TxD) in question. The hypothetical SNR values

of each link, both useful and interfering, is first calculated using the channel gains g_1, g_2, g_3, and g_4 as shown in Equations 3.5, 3.6, 3.7 and 3.8.

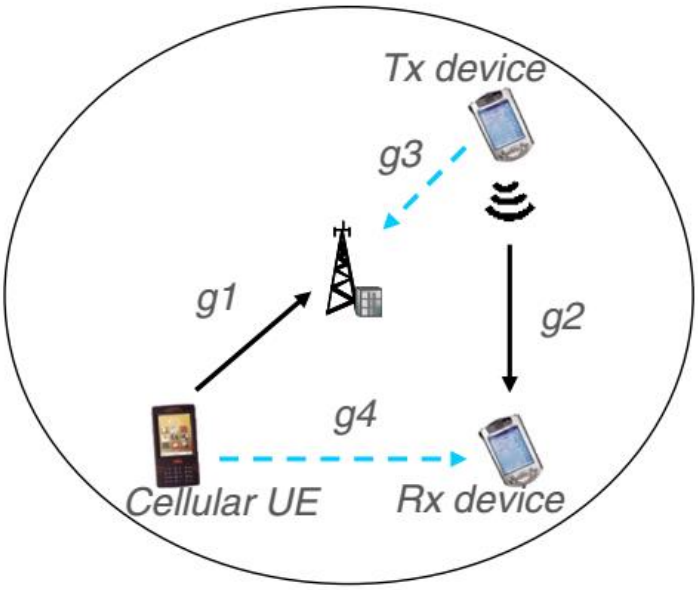

Figure 26. System Model for the Distributed CSI-based Mode Selection Algorithm (Reider & Fodor, 2012).

$$\gamma_l^{u,\,C} = \gamma_l^{g_1} = \frac{Pg_1}{\sigma_n^2} = \frac{Pg_{BS_l,\,CUE_l}}{\sigma_n^2},\ g_1 = g_{BS_l,CUE_l} = d_{BS_l,CUE_l}^{-\rho}\chi_{BS_l,CUE_l} \qquad 3.5$$

$$\gamma_l^{u,\,D2D} = \gamma_l^{g_2} = \frac{Pg_2}{\sigma_n^2} = \frac{Pg_{RxD_l,TxD_l}}{\sigma_n^2},\ g_2 = g_{RxD_l,TxD_l} = d_{RxD_l,TxD_l}^{-\rho}\chi_{RxD_l,TxD_l} \qquad 3.6$$

$$\gamma_l^{i,\,C} = \gamma_l^{g_3} = \frac{Pg_3}{\sigma_n^2} = \frac{Pg_{BS_l,TxD_l}}{\sigma_n^2},\ g_3 = g_{BS_l,TxD_l} = d_{BS_l,TxD_l}^{-\rho}\chi_{BS_l,TxD_l} \qquad 3.7$$

$$\gamma_l^{i,\,D2D} = \gamma_l^{g_4} = \frac{Pg_4}{\sigma_n^2} = \frac{Pg_{RxD_l,CUE_l}}{\sigma_n^2},\ g_4 = g_{RxD_l,CUE_l} = d_{RxD_l,CUE_l}^{-\rho}\chi_{RxD_l,CUE_l} \qquad 3.8$$

where g_1, g_2, g_3, and g_4 are the channel gain of useful cellular link, useful D2D link, interfering cellular link and interfering D2D link respectively. $\gamma_l^{u,\,C}$, $\gamma_l^{u,\,D2D}$, $\gamma_l^{i,\,C}$, and

$\gamma_l^{i,\,D2D}$ are the hypothetical SNR values of the *useful cellular link*, *useful D2D link*, *interference on cellular link* and *interference on D2D link* of Cell-*l* respectively. *P* is the transmitted power =P_{max}, $d_{i,j}$ is the distance between receiver *i* and transmitter *j*, ρ is the path loss exponent, while σ_n^2 is the additive noise. D2D mode is selected if the hypothetical channel capacity values of the useful links are higher than the hypothetical channel capacity values of the interfering links plus an additional tuneable system parameter Δ measured in bit/s/Hz. This means that if Equation 3.9 or Equation 3.10 is true, D2D mode is selected, otherwise, cellular mode is selected.

$$\log_2(1+\gamma^{u,\,C}) + \log_2(1+\gamma^{u,\,D2D}) - \log_2(1+\gamma^{i,\,C}) - \log_2(1+\gamma^{i,\,D2D}) > \Delta \qquad 3.9$$

$$\log_2(1+\gamma^{u,\,D2D}) - \log_2(1+\gamma^{i,\,D2D}) > \Delta \qquad 3.10$$

When Δ is increased, the algorithm becomes stricter and selects D2D mode less often. Alternatively, if Δ is set to a negative value, the algorithm becomes more conservative and D2D mode will be selected more frequently. The CSI-based mode selection mitigates the complexity of joint power control and mode selection by using SNR metric instead of SINR. However, the algorithm requires the Channel Quality Information (CQI) (distance path loss and shadowing) of the D2D transmitter – D2D receiver link and the D2D transmitter – BS link (Aydin, et al., 2013).

3.3.2.1. Location-based Mode Selection

The location-based mode selection algorithm uses the user's location to determine the suitable mode. The BS acquires the distance between the two potential D2D pair and the distance between each of the D2D UE and the BS. The distances are used by the BS to estimate received signal power using appropriate propagation model (Li, et al., 2014). The communication mode is selected based on the distance and received signal power estimation as shown in Figure 27. As shown in Equation 3.11, if the distance d_1 between the potential D2D pair is less than the distance d_2 or d_3 between either one of the D2D UEs and the BS, and less than a predefined limit $d_{D2D_{max}}$, direct D2D link is selected for

communication between the D2D UEs. Otherwise, the cellular mode is selected and communication between the pair is routed through the BS. Location-based mode selection ensures smooth transition between D2D mode and cellular mode. Moreover, the CSI from the D2D UEs are not required. However, the algorithm requires the geographical location of UEs and path loss model of the channels (Aydin, et al., 2013).

$$(d_1 < d_2 \text{ OR } d_1 < d_3) \text{ AND } d_1 < d_{D2D_{\max}} \qquad 3.11$$

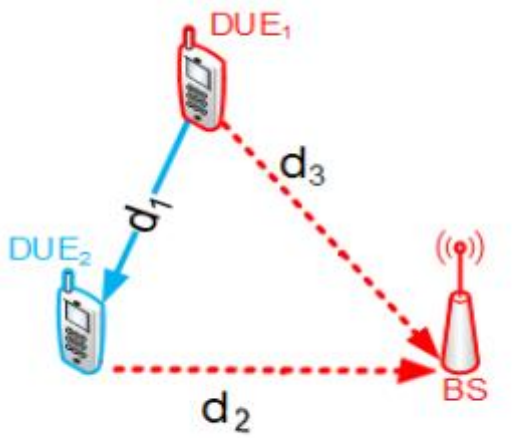

Figure 27. Location-based Mode Selection.

3.3.3. Resource Allocation in METIS Direct D2D Communication

Resource allocation can avoid interference between CUEs and D2D links by assigning only dedicated resources not used by CUEs to D2D links. A resource allocation scheme can also mitigate interference by selecting the best CUE to share resources with a D2D pair. METIS technology component proposed four different approaches to ensure efficient allocation of resources in multi-tier network with cellular and D2D links (Aydin, et al., 2013). The first approach is an extended Inter-Cell Interference coordination (ICIC) technique that enables the use of muted resources of macrocell for D2D transmission in heterogenous network. The second technique focus on a flexible joint coordinated

resource allocation among multiple cells, especially for indoor dense deployments. The third approach utilizes the signal-to-interference ratio (SIR) estimation to detect the best pattern for sharing resources between D2D UEs and CUEs. The fourth technique focus on resource allocation for high mobility applications such as D2D communication devices in vehicles or vehicle UEs.

3.3.3.1. Enhanced ICIC for enabling D2D in Heterogeneous Networks

This focus on an heterogenous network environment consisting of two layers (i.e., macro layer and small cell layer), in which D2D links reuses the downlink resources. Some resources of the macro later are muted either in the time or frequency domain. Interference measurements is used to allocate the muted resources to D2D transmission with two rules. First, if no strong small cell transmission using some macrocell muted resources is discovered, these muted resources can be used by D2D pairs in the same macro layer as shown in Figure 28, otherwise D2D pairs in the layer use unmuted resources. Second, if the D2D pair are in different layers, the muted resources can be used if the allocation of resources is controlled by the small or the usage is specified at the small cell. With this scheme, network capacity can be improved without causing uncontrollable interference (Aydin, et al., 2013). However, measurements such as the Received Signal Strength Indicator (RSSI) from small cells are required.

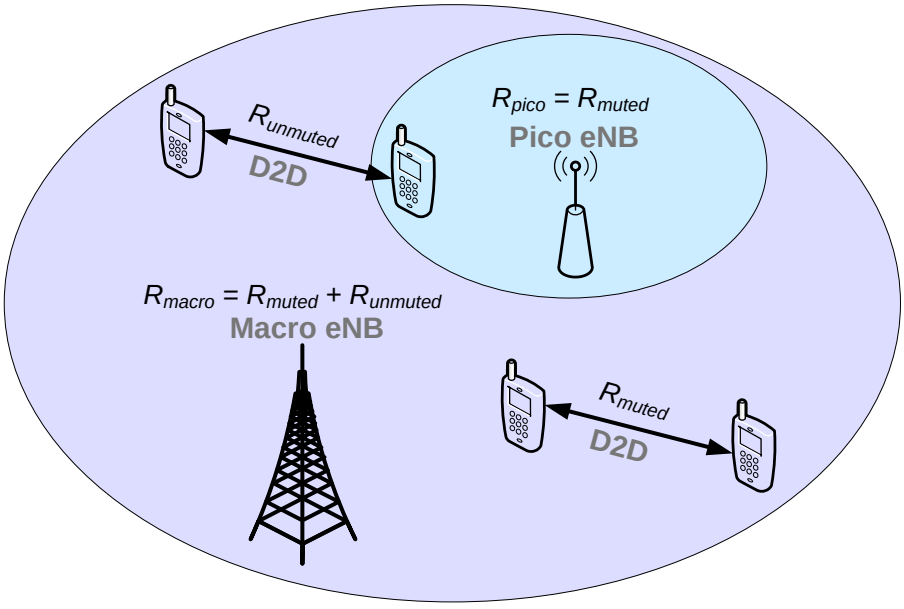

Figure 28. Enhanced ICIC for D2D Communication in HetNet (Aydin, et al., 2013).

3.3.3.2. Location-based D2D Resource Allocation

This approach assumed that D2D links can reuse either uplink or downlink PRBs. It is assumed that intra-cell orthogonality exists between CUEs, and same PRBs being used by CUEs can be allocated to D2D transmissions. The BS estimates the path loss and the SIR for D2D UE and CUEs sharing the same resources, using the distance between the D2D UEs and CUE involved as well as the distance between those UEs and the BS as shown in Figure 29. The information is used to determine the best candidate CUE to share resource with a D2D link. Since increasing the distance improves SIR, selection is done based on distance maximization (Aydin, et al., 2013). For instance, in the downlink, for a CUE to be able to share resources with a D2D link, the distance between the CUE and the BS (d_2) must be greater than the distance between the D2D receiver and the BS (d_4), and the distance between the D2D pair (d_1) must be less than the distance between the D2D transmitter and the CUE (d_3). If more than one CUE meets these criteria, the one with the longest distance to the D2D transmitter (d_3) is selected to share resource with the D2D link. Similarly, in the uplink, for a CUE to enter resources sharing with a D2D link, the distance between the BS and the CUE (d_2) must be less than the distance between the D2D receiver and the CUE (d_4) as well as the distance between the BS and the D2D transmitter (d_3). Here, if multiple CUEs meet the condition, the CUE with the longest distance to the D2D receiver (d_4) is selected.

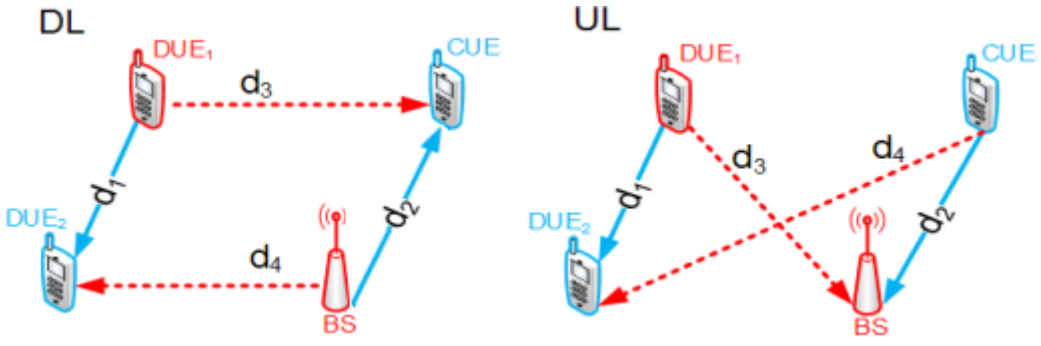

Figure 29. Location-based Resource Allocation (Aydin, et al., 2013).

For downlink, $d_2 > d_4$ AND $d_3 > d_1$, $\max(d_3)$ 3.12

For uplink, $d_4 > d_2$ AND $d_3 > d_2$, $\max(d_4)$ 3.13

This technique is simple as no CSI is required for D2D UEs. This approach also enables multiple D2D pairs to share the same resources with a single CUE if the distance between the transmitters and receivers of different D2D pairs is greater than the length of any D2D link. Therefore, the network capacity is increased since multiple D2D pairs can share same PRB.

3.3.4. Power Control and SINR Target Setting in METIS Direct D2D Communication

After selecting the radio resource sharing pattern, SINR targeting and power control techniques can be implemented to control interference. Power control mechanism can be combined with SINR target setting algorithms which allows minimization of the overall power corresponding to a sum target rate. One SINR target setting algorithm and two power control schemes for D2D transmission was introduced (Aydin, et al., 2013).

3.3.4.1. Adaptive Distributed SINR Targets Setting for D2D Communication

This algorithm proposed by Reider & Fodor (2012) in the METIS project assumes a mixed D2D and cellular communication scenario where each CUE is allotted its own PRB, and intra-cell orthogonality is maintained without active D2D links. A minimum link quality value is set, and transmitters whose transmit power rise results in high increase in capacity are compensated with higher link quality. A minimum SINR target is set and the value is adjusted iteratively for all links to reach an optimal power allocation, subject to capacity limit. The SINR target is increased continuously until a predefined capacity target C^{sum} for all links is reached. Assume there are K receivers and J transmitters, the channel gain g between *kth* receiver and *jth* transmitter of the D2D link is modelled as in Equation 3.14 where ρ is the path loss exponent, and $d_{k,j}$ is the distance between *kth* receiver and *jth* transmitter. The inputs are the predefined sum capacity target C^{sum}, and $SINR_{\min} > 0$.

$$g_{k,j} = d_{k,j}^{-\rho} \chi_{k,j} \quad 3.14$$

The algorithm starts by estimating the power increase ΔP_k that is needed to increase the SINR by a value $\Delta > 1$ for link k as in Equation 3.15. The capacity increase corresponding to the increase in SINR is also calculated as in Equation 3.16. A benefit value b_k is computed indicating the gain of increasing the power for link k as in Equation 3.17, i.e., the ratio of the capacity increase and the power increase in *bits/s/Hz/mW*. These steps are executed for all links. The transmitter then populates a vector **b** of benefit values for all links. The link with the highest benefit value is chosen, and its corresponding SINR target is increased. The sum capacity of all links is then calculated as in Equation 3.19, and the whole procedure is repeated until the predefined sum capacity C^{sum} is reached provided the target capacity is achievable.

$$\Delta P_k^{(t)} = \frac{\gamma_k^{(t)}(\Delta - 1)\left(\sum_{j \neq k}^{J} P_j^{(t-1)} g_{k,j} + \sigma_n^2\right)}{g_{k,k}} \qquad 3.15$$

Where $t = 1, 2, 3, \ldots T$ such that $C^{\text{sum}} \leq C^{(T)}$

$k = 1, ..., K$

$j = 1, ……, J$

$\gamma_k^{(0)} = SINR_{\min} > 0$, and

$P_k^{(0)} = \gamma_k^{(0)} . \sigma_n^2 / g_{k,k}$.

$$\Delta C_k^{(t)} = \log_2\left(1+\gamma_k^{(t)} \, . \, \Delta\right) - \log_2\left(1+\gamma_k^{(t)}\right) \qquad 3.16$$

$$b_k^{(t)} = \frac{\Delta C_k^{(t)}}{\Delta P_k^{(t)}} \qquad 3.17$$

$$\mathbf{b}^t = \left[b_1^{(t)}, b_2^{(t)}, b_3^{(t)}, ..., b_k^{(t)}\right], \text{ where } \mathbf{b}^0 = \left[b_1^{(0)}, b_2^{(0)}, b_3^{(0)}, ..., b_k^{(0)}\right] \qquad 3.18$$

$$C^{(t+1)} = \sum_{s=1}^{N_t} \log_2\left(1+\gamma_k^{(t+1)}\right) \qquad 3.19$$

The output of this algorithm will be a $K \times K$ diagonal matrix $\boldsymbol{\gamma}$ with the resulting SINR value of each link as the diagonal elements, i.e., $\boldsymbol{\gamma} = \text{diag}(\gamma_1, \gamma_2, \gamma_3, \ldots, \gamma_K)$ where γ_k is the resulting SINR of link k. Since a minimum link quality i.e., $SINR_{\min}$ is set for all link at the beginning, this algorithm ensures that all UEs experience at least a reasonable minimum quality of service. Moreover, this distributed approach does not require a central entity such as the BS since the algorithm can be implemented on each transmitter. However, the CSI (path loss and shadowing) for all links is required at all transmitters (Aydin, et al., 2013).

$$\boldsymbol{\gamma} = \text{diag}(\gamma_1, \gamma_2, \gamma_3, \ldots, \gamma_K) = \begin{bmatrix} \gamma_1 & 0 & 0 & \cdots & 0 \\ 0 & \gamma_2 & 0 & 0 & 0 \\ 0 & 0 & \gamma_3 & 0 & 0 \\ \vdots & 0 & 0 & \ddots & \vdots \\ 0 & 0 & 0 & \cdots & \gamma_K \end{bmatrix} \qquad 3.20$$

3.3.4.2. Distributed Iterative Power Control Algorithm for D2D Communication

The algorithm also proposed by Reider & Fodor (2012) for the METIS project assumes a MIMO Minimum Mean Square Error receiver for both D2D receiver and BS, D2D pair communicates over a bidirectional channel with D2D link operation in a TDD mode. The target SINR of a transmitter is set to all the MIMO stream from the transmitter. It assumes a feedback channel between the receiver and transmitter. The covariance measurements (RSSI measurements) is continuously performed by the D2D receiver and is fed back to the corresponding transmitter for the transmitter to iteratively adjust its transmit power accordingly in such a way that the predefined SINR targets are achieved.

The algorithm starts with the estimation of the covariance matrix of the received total interference-plus-noise Φ_k by each receiver as in Equation 3.21. $\boldsymbol{\Phi}_k$ is to the covariance matrix corresponding to receiver k. This is feed back to the corresponding transmitter k.

The transmitter then calculates the reduced covariance matrix $\mathbf{\Phi}_k^{\text{red}}$ by subtracting its own interference contribution from the total interference-plus-noise as in Equation 3.22.

$$\mathbf{\Phi}_k^{(t)} = \sum_{j=1}^{K} P_j^{(t-1)} d_{k,j}^{-\rho} \chi_{k,j} \mathbf{H}_{k,j} \mathbf{T}_j^{(t-1)} \mathbf{T}_j^{(t-1)\dagger} \mathbf{H}_{k,j}^{\dagger} + N_t \sigma_n^2 \mathbf{I}_{N_r \times N_r} \tag{3.21}$$

$$\mathbf{\Phi}_k^{\text{red},(t)} = \mathbf{\Phi}_k^{(t)} - P_k^{(t-1)} d_{k,k}^{-\rho} \chi_{k,k} \mathbf{H}_{k,k} \mathbf{T}_k^{(t-1)} \mathbf{T}_k^{(t-1)\dagger} \mathbf{H}_{k,k}^{\dagger}$$

$$= \sum_{j \neq k}^{K} P_j^{(t-1)} d_{k,j}^{-\rho} \chi_{k,j} \mathbf{H}_{k,j} \mathbf{T}_j^{(t-1)} \mathbf{T}_j^{(t-1)\dagger} \mathbf{H}_{k,j}^{\dagger} + N_t \sigma_n^2 \mathbf{I}_{N_r \times N_r} \tag{3.21}$$

Where $\mathbf{H}_{k,k}$ is the channel matrix of the link between transmitter k and receiver k assume to be known and estimated by transmitter k since bidirectional D2D link exists between the two D2D pair (i.e., transmitter k and receiver k). $\mathbf{H}_{k,j}$ is the cross-channel matrix between receiver k and transmitter j normally expected to be known by the receiver k. N_t and N_r are the number of MIMO transmitter and receiver antenna respectively. $\mathbf{T}_k$ is the N_t x N_t power loading matrix of transmitter k, while $\mathbf{I}_{N_t \times N_t}$ is an identity matrix with dimension N_t x N_t. The initial inputs are $\mathbf{T}_k^0 = \mathbf{I}_{N_t \times N_t}$ $\forall k$, and $\boldsymbol{\gamma}_k^{(0)} = \text{diag}\left(\gamma_k^{\text{tgt}}\right)$ where γ_k^{tgt} is the SINR target at receiver k, and initial transmit powers $\mathbf{p}^0$.

The transmitter also calculates the effective interference ζ_k and then adjust the power loading matrix $\mathbf{T}_k$ and the transmit power P_k accordingly. The power loading matrix is adjusted in such a way that the MIMO streams s affected by higher effective interference are compensated with higher transmit power. The unequal power loading is to ensure that transmit power is not wasted on stronger streams. The transmit power P_k of transmitter k is determined by its MIMO stream s that requires the highest transmit power as in

Equation 3.24, where P_k is proportional to ζ_k and γ_k^{tgt}, i.e., the higher the effective interference and the SINR target, the higher the transmit power. This means that if the power loading is equal, increasing the SINR of the weakest stream to the target will cause the SINR of the stronger stream to go above the target, thus, wasting transmit power.

$$\zeta_{k,\,s}^{(t)} = \left\{ \left(d_{k,\,k}^{-\rho} \chi_{k,\,k} \mathbf{H}_{k,\,k}^{\dagger} \left(\mathbf{\Phi}_k^{\text{red},\,(t)} \right)^{-1} \mathbf{H}_{k,\,k} + \frac{1}{P_k^{(t-1)}} \mathbf{I}_{N_t \times N_t} \right)^{-1} \right\}^{(s,\,s)} \tag{3.22}$$

$$\left\{ \mathbf{T}_k^{(t)} \right\}^{(s,\,s)} = \sqrt{\frac{\zeta_{k,\,s}^{(t)} N_t}{\sum_{w=1}^{N_t} \zeta_{k,\,w}^{(t)}}} \quad , \quad \forall s \in [1,\, N_t] \tag{3.23}$$

$$P_k^{(t)} = \max_s \left\{ \frac{\zeta_{k,\,s}^{(t)}}{\left| \left\{ \mathbf{T}_k^{(t)} \right\}^{(s,\,s)} \right|^2} \left(\gamma_k^{\text{tgt}} + 1 \right) \right\} \tag{3.24}$$

Where $\{\mathbf{A}\}^{(i,\,j)}$ denotes the $(i,\,j)^{(th)}$ element of matrix **A**, i.e., the i^{th} row of j^{th} column. $|x|$ represents the absolute value of real or complex number x. The steps are repeated until the difference between the current transmit power and the previous one is less than a predefined value ε_{gap}, i.e., $\left| P_k^{(t)} - P_k^{(t-1)} \right| \leq \varepsilon_{\text{gap}}$, $\forall k$. Just like the distributed algorithm for setting SINR target discussed in the previous subsection, this algorithm executes on a fast time scale compensate for the variation in SINR of the D2D and cellular connections. The algorithm does not require channel quality information. It only requires each D2D transmitter to estimate the channel matrix of its link to its corresponding receiver (Aydin, et al., 2013).

3.3.4.3. Location-based Power Control Algorithm for D2D

This approach aims to achieve power control by setting a *minimum* and *maximum* boundary for the transmit power of the D2D transmitters sharing same resources with

cellular UEs either in the uplink or downlink. The estimated distance between transmitter and receiver and the path loss model are exploited to set the transmit power boundary as shown below. The D2D transmit power boundary is prevent severe disruption of the cellular link by D2D transmission. The maximum boundary is also limited by the maximum allowed transmit power.

$$P_d^{\min} = \begin{cases} S_{Rx} + PL_{Tx,\,Rx} & \text{if } I_{\text{rec}} < S_{Rx} \\ \delta_{Tx,\,Rx} + PL_{Tx,\,Rx} + I_{\text{rec}} & \text{if } I_{\text{rec}} > S_{Rx} \end{cases} \quad 3.25$$

$$P_d^{\max} = S_{sh} - \delta_{sh} + PL_{sh,\,Tx} \quad 3.26$$

Where S_j is the sensitivity of receiver j, δ_j is the SIR of receiver j in dB, I_{rec} is the received interference power and $PL_{i,\,j}$ is the path loss between transmitter i and receiver j. The lower bound of the transmit power can be used as a starting point for setting D2D transmit power. The transmitter can then adjust the transmit power based on the channel condition while maintaining the transmit power below the upper bound. This is a simple approach that requires no CSI. However, the geographical location of cellular and D2D users is required (Aydin, et al., 2013).

4. SYSTEM MODEL AND SIMULATIONS

The previous chapter discussed the three-major potential gain of D2D communication that reuses cellular spectrum simultaneously with other active cellular connection. However, as previously discussed, reusing cellular resources for D2D links can cause serious interference problems. Some METIS approach, in form of mode selection, efficient resource allocation, power control and SINR target setting, aimed at controlling interference were also analyzed. Resource sharing between cellular and D2D links can be inform of multi-sharing (RB for a cellular connection is shared with multiple D2D connections at a time) and single-sharing (RB for a cellular connection is shared with at most one D2D connection at a time). As mentioned in the previous chapter, D2D communication can share either downlink or uplink resources. However, majority of research work in D2D communication concentrates on uplink reuse. Several works have been done on both single-sharing and multi-sharing D2D communication.

An Optimal Resource Allocation (ORA) algorithm consisting of resource allocation, admission control and power control scheme was developed by Feng, et al. (2013) to maximizing the overall system throughput of single-sharing D2D communication. Likewise, a Greedy Resource Allocation (GRA) algorithm was proposed by Sun, et al. (2013) to maximimize the number of admitted D2D links for cellular spectrum reuse at a specific transmit power in a multi-sharing system. GRA utilizes the conflict graph (CG) of D2D links and select reuse candidates in order of smallest interference degree i.e. smallest degree first. Similarly, Ciou, Kao, Lee, & Chen (2015) studied multi-sharing D2D communication and developed a Greedy Throughput Maximization (GTM+) algorithm. GTM+ utilizes both CG and the maximum weighted independent set of the conflict graph to maximize overall system throughput.

However, both GRA and GTM+ as multi-sharing schemes does not include power control. Lin, Chen, Kao, & Hsiao (2017) studied joint RB reuse and power control for multi-sharing D2D communication in order to develop a technique that maximizes both system throughput and power efficiency, and also capable of supporting large number of D2D communication users in 5G mobile networks. They developed the Maximum Independent Set-based and Stackelberg Game-based Power Control (MiSo) algorithm.

MiSo is similar to GTM+ as it also utilizes the maximum independent set of the CG of the network. Apart from the RB allocation component, MiSo algorithm also include power control that uses the derived Stackelberg power which is based on the Stackelberg Strategic Game.

This chapter presents the analysis and simulation of joint admission control, resource allocation and power control mechanism for multi-sharing D2D communication in uplink frequency reuse mode in a single cell environment. All simulations in this work will be implemented in MATLAB, and they are in three parts. The first part is a link-level simulation that analyses and evaluates the proximity gain of a single D2D communication link. The other two parts is based on the System-level implementation of the MiSo algorithm. The algorithm was implemented, and its performance was evaluated and compared with the GRA and GTM+ algorithm.

4.1. System Model and Assumptions

For simplicity of discussion, a single cell scenario is considered in this work as shown in the illustration of the system model in Figure 30. The cell is composed of N DUE pairs and M CUEs. DUE pairs and CUEs will be denoted as d or D_d and c or C_c respectively where $d = 1, 2, 3, \ldots, N$ and $c = 1, 2, 3, \ldots, M$. A DUE pair d is made up of the *transmitting* DUE represented as D_dTx or Tx and the *receiving* DUE represented as D_dRx or Rx. It is assumed that there are also M orthogonal uplink RBs and each CUE c is allocated one uplink RB. This means that orthogonality exists among CUEs in the cell. Also, it is assumed that the serving BS represented as B have adequate knowledge of the CSI of all communication links.

A CUE can share its allotted RB with multiple DUEs. Δ_c denotes the set of DUE pairs that CUE c shares its RB with. Interference exists between CUE c and the member DUE pairs of Δ_c. Also, there is mutual interference among these member DUE pairs. For example, in the illustration in Figure 30, C_1 shares its RB with D_2 and D_3, RB of C_2 is shared with D_1, RB of C_3 is not shared with any DUE pair, and D_4 is not granted reuse of any CUE's RB. Therefore, D_1 interferes with the transmission of C_2 and vice versa.

Likewise, D_2 and D_3 interferes with the transmission of C_1 and vice versa. In addition, D_2 and D_3 interferes with each other's transmission.

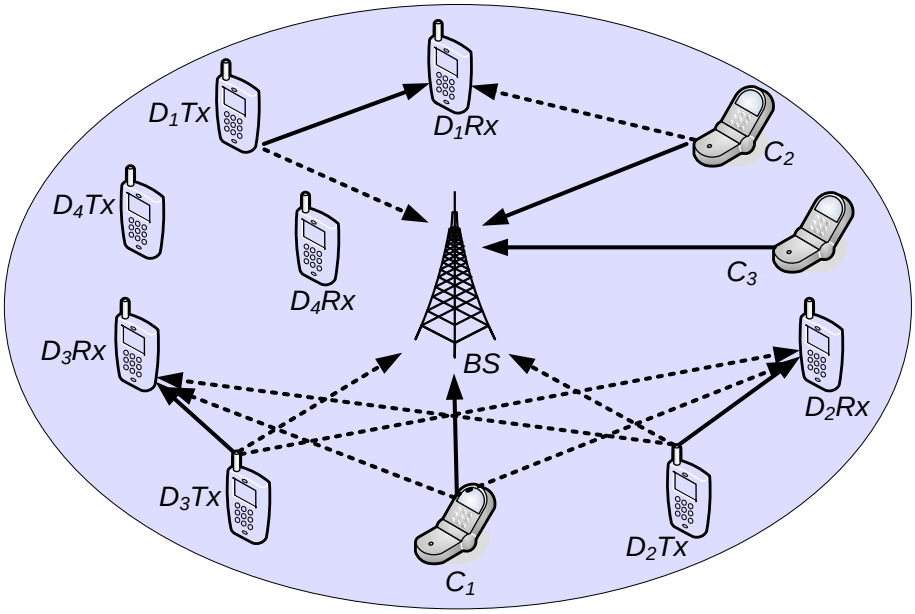

Figure 30. System Model - DUE Pairs Reuse Uplink RB of CUEs.

4.1.1. Channel Model

Different approaches have been used by different authors to model the D2D communication channel in different scenarios between the transmitter and the receiver. For instance, Reider & Fodor (2012) considered only distance dependent path loss and slow fading due to shadowing for the distributed SINR target optimization and mode selection as shown in Equation 4.1. Whereas, in addition to the distance dependent path loss and slow fading due to shadowing, fast fading due to multipath propagation was also considered in their centralized approach for setting the optimum SINR target of D2D links as shown in Equation 4.2.

$$g_{i,j} = \chi_{i,j} d_{i,j}^{-\rho} \qquad 4.1$$

$$g_{i,j} = K\xi_{i,j}\,\chi_{i,j}d_{i,j}^{-\rho} \qquad 4.2$$

where K is the path loss constant, ρ is the path loss exponent, $\xi_{i,j}$ is the fast fading gain which is exponentially distributed, $\chi_{i,j}$ is the slow fading gain with log-normal distribution, $g_{i,j}$ and $d_{i,j}$ denote the channel gain and the distance in meters between the transmitter i and the receiver j respectively. Similarly, Sun, et al. (2013), Ciou, et al. (2015), and Lin, et al. (2013) also considered the fast fading gain as in Equation 4.2 for their resource allocation schemes with or without power control. The model in Equation 4.2 will be used for all links in this work. Because reuse is considered only in the uplink phase, *i* can represent a transmitting DUE *Tx* or a CUE *c*, while *j* can be a receiving DUE *Rx* or the BS *B*.

4.1.2. Problem Statement

The joint resource allocation and power control deals with the appropriate allocation of resources among the CUEs and DUE pairs for RB reuse. The first problem here is the appropriate selection of DUE pair that can reuse RB of a certain CUE in a way that the system throughput will be optimized and not deteriorated. The second problem focuses on controlling the transmit power (power consumption) of D2D links to optimize the systems power efficiency. These two objectives are optimization problems aimed at overall *system throughput* and *power efficiency* optimization. As shown in Equation 4.3, a CUE *c* can share its RB with a set of DUE pairs Δ_c if its SINR does not fall below the required or target SINR γ_c^{tgt}. Likewise, as depicted in Equation 4.4, a DUE pair *d* is permitted to reuse RB of CUE c if the SINR of *d* does not fall below the SINR target of the link γ_d^{tgt}. RB will not be allocated to CUEs and DUEs that does not meet their SINR target.

$$\gamma_c = \frac{P_c g_{c,B}}{\sum_{d\in\Delta_c} P_d g_{d,B} + \sigma_c^2} \geq \gamma_c^{\text{tgt}} \qquad 4.3$$

$$\gamma_d = \frac{P_d g_{d,d}}{P_c g_{c,d} + \sum_{d' \in \Delta_c - \{d\}} P_{d'} g_{d',d} + \sigma_d^2} \geq \gamma_d^{\text{tgt}}, \ \forall c: d \in \Delta_c \quad 4.4$$

where P_c and σ_c^2 are the transmit power of the CUE c and the additive noise at the BS respectively. Similarly, P_d and σ_d^2 are the transmit power of the transmitting DUE d and the additive noise at the receiving DUE d respectively. d' represents other DUE pair(s) in the same set Δ_c as d. P_d is usually within a limit i.e. $P^{\min} \leq P_d \leq P^{\max}$. The sets $\Delta_1, \Delta_2, \Delta_3, \ldots, \Delta_M$ and DUE transmit power values $P_1, P_2, P_3, \ldots, P_N$ will be determined by joint resource allocation and power control. The overall system throughput is the summation of the Shannon capacity of all CUEs and DUE pairs that meet their respective SINR target. The power efficiency η of the system is the overall system throughput T divided by the total power consumed P_T.

$$\eta = \frac{\text{Overall System Throughput}}{\text{Total Power Consumed}} = \frac{T}{P_T} \quad 4.5$$

$$\text{where } T = \sum_{c \in \{1,2,\ldots,M\}} \log_2(1+\gamma_c) + \sum_{d \in \Delta_c,\, c \in \{1,2,\ldots,M\}} \log_2(1+\gamma_d) \quad 4.6$$

$$\text{and } P_T = \sum_{c \in \{1,2,\ldots,M\}} P_c + \sum_{d \in \Delta_c,\, c \in \{1,2,\ldots,M\}} P_d \quad 4.7$$

$$\forall c: \gamma_c \geq \gamma_c^{\text{tgt}} \ \& \ \forall d: \gamma_d \geq \gamma_d^{\text{tgt}}$$

4.2. Maximum Independent Set-based and Stackelberg Game-based Power Control and Resource Allocation (MiSo) Algorithm

As seen in the pseudocode given in Appendix 1, the MiSo algorithm consists of both resource allocation for RB reuse and a power control scheme. It involves three stages; initialization and candidate selection, tier-1 and tier-2 allocation. In the initialization and candidate selection phase, all DUE pairs are grouped under the CUE with which they

have the maximum *share rate*. When DUE *d* joins c's group, this means that *d* is a reuse *candidate* for *c*'s RB. Γ_c represents the *candidate set* of *c* and it is the set of DUE pairs that eventually joins group *c*. The share rate as shown in Equation 4.8 is simply determined by adding throughputs of both *c* and *d* when only *d* reuses RB of *c*.

$$r_{(c,\,d)} = \log_2\left(1+\frac{P_c g_{c,B}}{P_d^{\text{init}} g_{d,B}+\sigma_c^2}\right)+\log_2\left(1+\frac{P_d^{\text{init}} g_{d,d}}{P_c g_{c,d}+\sigma_d^2}\right) \tag{4.8}$$

$$\text{where}\quad P_d^{\text{init}} = \min\left(P^{\max},\ \min_{c\in\{1,2,\ldots,M\}}\frac{1}{g_{d,B}}\left(\frac{P_c g_{c,B}}{\gamma_c^{\text{tgt}}}-\sigma_c^2\right)\right) \tag{4.9}$$

The initial transmission power value P_d^{init} is calculated for all $d\in\{1,2,\ldots,N\}$ at the beginning of the algorithm. Using this value ensures that any DUE *d* can alone reuse RB of any CUE *c* without causing the condition $\gamma_c \geq \gamma_c^{\text{tgt}}$ to be violated. All groups are then set as unmarked. After this initialization and candidate selection, the algorithm iterates and selects the largest unmarked group, marks the selected group, select *nominees* from the corresponding candidate sets Γ_c of the group, and elect *tier-1* and *tier-2 electees* at every iteration. Tier-1 electees transmit at their respective initial transmission power. Tier-2 electees on the other hand, transmits at their calculated Stackelberg power. Candidates in Γ_c that are not selected for tier-1 or tier-2 reuse join another unmarked group with which they have the maximum share rate. The iteration terminates when all groups have been marked.

The *nominees*, denoted by Λ_c, to be elected for tier-1 and tier-2 reuse in the currently selected largest group *c* with *candidate set* Γ_c is determined by computing the *maximum independent set* of the of the *conflict graph* $CG_c=(V_c, E_c)$ of group *c*. The DUEs in Γ_c constitutes the vertices V_c in CG_c, i.e. a vertex in CG_c represents a DUE in Γ_c. Two vertices *x* and *y* are connected by an edge if conflict exists between them, meaning they cannot both reuse same CUE's RB simultaneously (i.e. cannot exist *c*'s network at the same time). E_c represents the set of edges connecting conflicting nodes or vertices. A conflict exists between *x* and *y* if the condition in Equation 4.10 or 4.11 is true, i.e. *x*

reusing the same RB with *y* causes *x*'s SINR requirement to be violated or vice versa. This means that they inflict too much interference on one another. Conflict can also be said to exist if the distance between the two pair is smaller than a predefined threshold.

$$\gamma_{x(y)} = \frac{P_x g_{x,x}}{P_c g_{c,x} + P_y g_{y,x} + \sigma_x^2} \leq \gamma_x^{\text{tgt}}, \quad x,y \in \Gamma_c \tag{4.10}$$

$$\gamma_{y(x)} = \frac{P_y g_{y,y}}{P_c g_{c,y} + P_x g_{x,y} + \sigma_y^2} \leq \gamma_y^{\text{tgt}}, \quad x,y \in \Gamma_c \tag{4.11}$$

The set of DUEs for tier-1 reuse denoted by Δ_c^1 is determined from Λ_c. Δ_c^1 is initialized to contain elements in Λ_c arranged in descending order of interference on CUE *c*. DUEs in Δ_c^1 are removed one at a time until SINR requirements of CUE *c* and all DUEs in Δ_c^1 are met. The resulting member DUEs of set Δ_c^1 are the tier-1 electees and are granted RB reuse at their respective initial transmission power.

The nominees that did not qualify for tier-1 reuse compete for re-election in tier-2. Δ_c^2 denotes the set of DUEs that will eventually get selected for tier-2 reuse. The final set of DUEs for tier-1 and tier-2 reuse is denoted as $\Delta_c = \Delta_c^1 + \Delta_c^2$. The nominees that will not be selected for either tier-1 or tier-2 reuse, i.e. *undetermined nominees* is denoted as $\Lambda_c^{'}$. At the beginning of tier-2 allocation, since Δ_c^2 is empty, Δ_c is initialized to Δ_c^1 and $\Lambda_c^{'}$ is initialized to $\Lambda_c - \Delta_c^1$. Tier-2 allocation is conducted with the transmit power condition $P_d^{\min} \leq P_d \leq P_d^{\max}, \forall d \in \Lambda_c^{'}$. The lower power bound $P_d^{\min}$ ensures that *d* can meet its SINR target while the upper power bound $P_d^{\max}$ ensures that *d* will not cause the SINR of CUE *c* and the DUEs already in Δ_c to fall below their respective target when *d* is added to Δ_c. $P_d^{\min}$ and $P_d^{\max}$ is given in Equation 4.12 and 4.13.

$$P_d^{\min} = \frac{\gamma_d^{\text{tgt}}}{g_{d,d}} \left(\sigma_d^2 + P_c g_{c,d} + \sum\nolimits_{d' \in \Delta_c} P_{d'} g_{d',d} \right) \tag{4.12}$$

$$P_d^{\max} = \min\left(\frac{M_c}{g_{d,B}},\ \min_{d' \in \Delta_c} \frac{M_{d'}}{g_{d,d'}},\ P^{\max}\right) \quad 4.13$$

where M_c and M_d are the interference margin of CUE c and DUE d respectively. M_c is computed for the CUE c and M_d is computed for all $d \in \Delta_c$ as shown in Equations 4.14 and 4.15.

$$M_c = \frac{P_c g_{c,B}}{\gamma_c^{\text{tgt}}} - \left(\sigma_c^2 + \sum_{d \in \Delta_c} P_d g_{d,B}\right) \quad 4.14$$

$$M_d = \frac{P_d g_{d,d}}{\gamma_d^{\text{tgt}}} - \left(\sigma_d^2 + P_c g_{c,d} + \sum_{d' \in \Delta_c - \{d\}} P_{d'} g_{d',d}\right) \quad 4.15$$

On every selection round of s tier-2 electee, one element denoted by d^*, which is the winner, with the highest *pairwise throughput* $\lambda_{c,\Delta_c}(d)$ among the elements in Λ_c' is selected as shown in Equation 4.17. The winner d^* is added to the set Δ_c and removed from Λ_c'. As shown in Equation 4.16, the pairwise throughput of any DUE $d \in \Lambda_c'$ is the sum of its throughput and the CUE's throughput if both their SINR requirements are satisfied. If the requirements are not satisfied, d's pairwise throughput is set to zero.

$$\lambda_{c,\Delta_c}(d) = \begin{cases} \log_2\left(1 + \dfrac{P_c g_{c,B}}{P_d^* g_{d,B} + \Omega}\right) + \log_2\left(1 + \dfrac{P_d^* g_{d,d}}{P_c g_{c,d} + \Phi}\right) \\ \text{if } \dfrac{P_c g_{c,B}}{P_d^* g_{d,B} + \Omega} \geq \gamma_c^{\text{tgt}} \text{ and } \dfrac{P_d^* g_{d,d}}{P_c g_{c,d} + \Phi} \geq \gamma_d^{\text{tgt}} \\ 0, \text{otherwise} \end{cases} \quad 4.16$$

$$d^* = \arg\max_{d \in \Lambda_c'} \lambda_{c,\Delta_c}(d) \quad 4.17$$

where $\Omega = \sigma_c^2 + \sum_{d' \in \Delta_c} P_{d'} g_{d',B}$, $\Phi = \sigma_d^2 + \sum_{d' \in \Delta_c} P_{d'} g_{d',d}$ and P_d^* is the selected Stackelberg power. The six Stackelberg power values corresponding to the six possible values of the Stackelberg variable α_c^* are computed as given in Equation 4.18.

$$P_d^* = \begin{cases} \widehat{P}_d & \text{if } P_d^{\min} \le \widehat{P}_d \le P_d^{\max} \\ P_d^{\min} & \text{if } \widehat{P}_d < P_d^{\min} \\ P_d^{\max} & \text{if } \widehat{P}_d > P_d^{\max} \end{cases} \quad 4.18$$

where $\widehat{P}_d = \frac{1}{\alpha_c^* g_{d,B} \ln 2} - \frac{P_c g_{c,d} + \Phi}{g_{d,d}}$, $P_d^{\min}$ and $P_d^{\max}$ are the upper and lower bound transmission power values defined in Equations 4.12 and 4.13, while the six possible values of α_c^* are given in Equation 4.19.

$$\begin{aligned} \alpha_{c,1} &= \frac{B}{\beta\Omega} - \frac{B}{A} \\ \alpha_{c,2} &= \frac{B}{A} - \frac{B}{\beta(A+\Omega)} \\ \alpha_{c,3} &= \frac{-B(A+2C) - \sqrt{D}}{2C(A+C)} \\ \alpha_{c,4} &= \frac{-B(A+2C) + \sqrt{D}}{2C(A+C)} \\ \alpha_{c,\min} &= \frac{B}{P_d^{\max} g_{d,B} + \Omega - C} \\ \alpha_{c,\max} &= \frac{B}{P_d^{\min} g_{d,B} + \Omega - C} \end{aligned} \quad 4.19$$

where $A = P_c g_{c,B}$, $B = \frac{1}{\ln 2}$, $C = -\frac{g_{d,B}}{g_{d,d}}(P_c g_{c,d} + \Phi) + \Omega$, $D = AB^2\left(A + 4C(A+C)\frac{1}{\beta(\Omega - C)}\right)$ and β is constant ratio of what c earns out of the price d pays.

Among the six possible values (α_c, P_d), the one that maximizes the utility of the CUE as given in Equation 4.20 is selected as the best Stackelberg power. If the pairwise throughput of the winner d^* is not zero, d^* is added to the set Δ_c and removed from Λ_c', and its transmission power is set to its Stackelberg power. This tier-2 selection round continues until Λ_c' becomes empty or the pairwise throughput of the winning DUE is zero.

At the end of tier-2 allocation, Δ_c now contains both tier-1 and tier-2 electees, the rest of the candidate not granted RB reuse in both tier-1 and tier-2 allocation (i.e. $\Gamma_c - \Delta_c$) can then join another unmark group with which they have the maximum share rate.

$$U_c(\alpha_c, P_d) = \log_2\left(1 + \frac{P_c g_{c,B}}{P_d g_{d,B} + \Omega}\right) + \alpha_c \beta P_d g_{d,B} \quad 4.20$$

4.3. Greedy Throughput Maximization Plus (GTM+) Algorithm

The GTM+ algorithm is similar in some extent to MiSo algorithm with the exclusion of a power control scheme. The pseudocode is shown in Appendix 2. It exploits the SINR information of CUEs and DUEs for efficient resource allocation. It also exploits the principle of taking the maximum independent set of the conflict graph of the network. The main idea here is that the total interference suffered by a link, either CUE or DUE, does not exceed the maximum tolerable interference of the link. Expressed in Equations 4.21 and 4.22, I_c and I_d represents the *maximum tolerable interference* of a given CUE *c* and DUE *d* respectively.

$$I_c = \frac{P_c g_{c,B}}{\gamma_c^{\text{tgt}}} - \sigma_c^2 \quad 4.21$$

$$I_d = \frac{P_d g_{d,d}}{\gamma_d^{\text{tgt}}} - \sigma_d^2 \quad 4.22$$

After obtaining the set of reuse *nominees* Λ_c from the candidate set Γ_c by determining the maximum independent set of the conflict graph group *c*, the algorithm initializes the final set of DUEs admitted for reuse i.e. Δ_c to Λ_c, and perform two basic steps. All DUEs whose SINR requirement is not satisfied are removed from the set, i.e. a DUE *d* will be removed from the reuse set if total interference suffered by *d* is greater than its maximum tolerable interference as shown in Equation 4.23. The resulting DUEs in Δ_c are then

reordered in descending order of interference inflicted on CUE *c*. One element is removed at a time from Δ_c until SINR requirement of *c* is satisfied, i.e. DUEs will be removed from the group as long as the total interference suffered by *c* is greater that *c*'s maximum tolerable interference as expressed in Equation 4.24. After this, similar to the case of MiSo, the rest of the candidate not granted RB reuse (i.e. $\Gamma_c - \Delta_c$) can then join another unmark group that maximizes their share rate.

$$P_c g_{c,d} + \sum_{d' \in \Delta_c - \{d\}} P_{d'} g_{d',d} > I_d \qquad 4.23$$

$$\sum_{d \in \Delta_c} P_d g_{d,B} > I_c \qquad 4.24$$

4.4. Greedy Resource Allocation Algorithm (GRA) Algorithm

The GRA algorithm uses a Smallest degree first approach where DUE with the smallest degree of interference on the CUE is considered first. The pseudocode is given in Appendix 3. As in both MiSo and GTM+, the conflict graph of the network corresponding to say a group *c* is constructed, and selection is done on the conflict graph $CG_c=(V_c, E_c)$ of the group. The GRA algorithm consist of two steps executed sequentially. First, a DUE pair $d^* \in V_c$ which has the smallest interference degree on CUE *c* is selected and moved to set Δ_c (i.e. set of DUE pairs admitted for RB reuse). DUE pairs conflicting with d^* are removed from V_c and the total interference of elements in $V_c$is updated. Second, a second DUE pair $d^{**} \in V_c$ with the smallest degree of interference on *c* is selected. If the SINR requirements of all DUE pairs in set $\Delta_c \cup \{d^{**}\}$ are satisfied, d^{**} is added to Δ_c and removed from V_c. All DUE pairs conflicting with d^{**} are removed from V_c. If SINR requirements are not satisfied, d^{**} is removed from V_c but not added to Δ_c. Then the total interference of elements in V_c is updated. The second step is repeated if the total interference of elements in V_c is greater than zero.

4.5. Simulation Parameters

For the joint resource allocation and power control simulations, CUEs and DUEs were randomly placed in the cell with the BS at the cell center. The positioning of the nodes (i.e. DUEs and CUEs) in the cell was achieved by using the *x* and *y* coordinates of the nodes from the BS at the cell center. Therefore, distance between a specific node and the BS is determined as expressed in Equation 4.25. However, the distance between two nodes is calculated using the BS as reference as given in Equation 4.26. The simulation parameters and their corresponding values are shown in Table 5.

Table 5. Simulation Parameters and their Corresponding Values.

Parameters	**Values**
Cell Radius R	500 m
Distance between DUE Transmitter and Receiver $d_{Tx,Rx}$	30 m – 100m
Path Loss Exponent ρ	4
Slow Fading χ	Log-normal Distributed, St. Dev. of 5 dB
Noise Power of each CUE and DUE σ^2	-120 dBm
Transmit Power of each CUE P_c	23 dBm
Maximum Transmit Power of DUE $P^{\max}$	23 dBm
Transmit Power of each DUE for algorithms with no power control P_d	10 dBm
SINR Target of each CUE γ_c^{tgt}	5 dB – 35 dB
SINR Target of each DUE γ_d^{tgt}	5 dB – 35 dB
Bandwidth W	5 MHz
Number of CUEs M	10
Number of DUE Pairs N	20 – 200

$$d_{z,B}=\sqrt{\left(x_{z,B}\right)^2+\left(y_{z,B}\right)^2} \qquad 4.25$$

where $d_{z,B}$ is the distance between node z and the BS, $x_{z,B}$ and $y_{z,B}$ are the corresponding x and y coordinate distances between node z and the BS.

$$d_{a,b}=\sqrt{\left(\left|x_{a,B}-x_{b,B}\right|\right)^2+\left(\left|y_{a,B}-y_{b,B}\right|\right)^2} \quad 4.26$$

where $d_{a,b}$ is the distance between node a and node b, $x_{a,B}$ and $y_{a,B}$ are the respective x and y coordinate distances between node a and the BS respectively, while $x_{b,B}$ and $y_{b,B}$ are the respective x and y coordinate distances between node b and the BS.

5. SIMULATION RESULTS AND DISCUSSION

The previous chapters presented an in-depth overview of 5G cellular networks. D2D communication was identified as one of the major enabling technology for the next generation network, and the potential benefits of implementing D2D communication as an underlay to the 5G network were recognized. These benefits as mentioned include *proximity*, *reuse* and *hop* gain. Interference imposed on CUEs by DUEs and mutual interference among DUEs were identified as the major challenges in a D2D network underlaying 5G cellular network. Some *mode selection, resource allocation*, and *power control* schemes were also discussed as solutions to the challenges of interference in D2D communication. These interference management techniques can be implemented together as a joint scheme or separately. Three resource allocation algorithms for multi-sharing D2D communication were also discussed in detail one of which was jointly implemented with a power control scheme. The simulation results are presented in this chapter. The simulations were conducted in three stages. The first stage analyzes the proximity gain of D2D mode over cellular mode for a D2D pair in four different scenarios. It demonstrates how the position of the D2D transmitter and the CUE affects the communication link. The second stage implements the MiSo joint resource allocation and power control algorithm to validates the gain of reusing resources allocated for cellular transmission for D2D communication, and also demonstrate the effect of some parameters on the performance of the system. The third stage compares the MiSo algorithm with GTM+ and GRA algorithms and evaluates their performance.

5.1. Proximity Gain of D2D Mode over Cellular Mode

A single DUE Pair (i.e. a *DUE Tx* and *Rx*) was considered in this case. The DUE Pair reuses the uplink RB of the *CUE* being served by a *BS* located at the center of the cell. To ascertain the proximity gain of D2D transmission and show how the distance between the *DUE Tx* and *Rx*, as well as the distance between the *CUE* and the *DUE Rx* affect the D2D transmission quality, D2D *channel capacity* and *received signal SINR* of the DUE pair when communicating in D2D mode and cellular mode were compared in four

different scenarios described as follows. In all cases, the *DUE Rx* was positioned at the cell edge. When communicating in *D2D mode*, the *DUE Tx* transmits data directly to the *Rx*. Whereas, in *cellular mode*, transmission is routed via the serving *BS*. However, in both cases, the *DUE* transmitter is considered to share the same uplink RB with the *CUE*.

I. **Scenario 1**

In this scenario, the *CUE* and the *DUE Rx* were considered to be stationary at a fixed position with Rx at the cell edge and the *CUE* is at a reasonable distance from the serving *BS*, while the *DUE Tx* is in transit. The movement of the *Tx* is in such a way that as it travels a distance of length *r* away from the *Rx*, it has moved a distance *Tx*, *BS r* closer to the *BS* This means that the distance between *Tx* and the *BS* is *R* minus the distance between the *DUE* pair, where *R* is the radius of the cell.

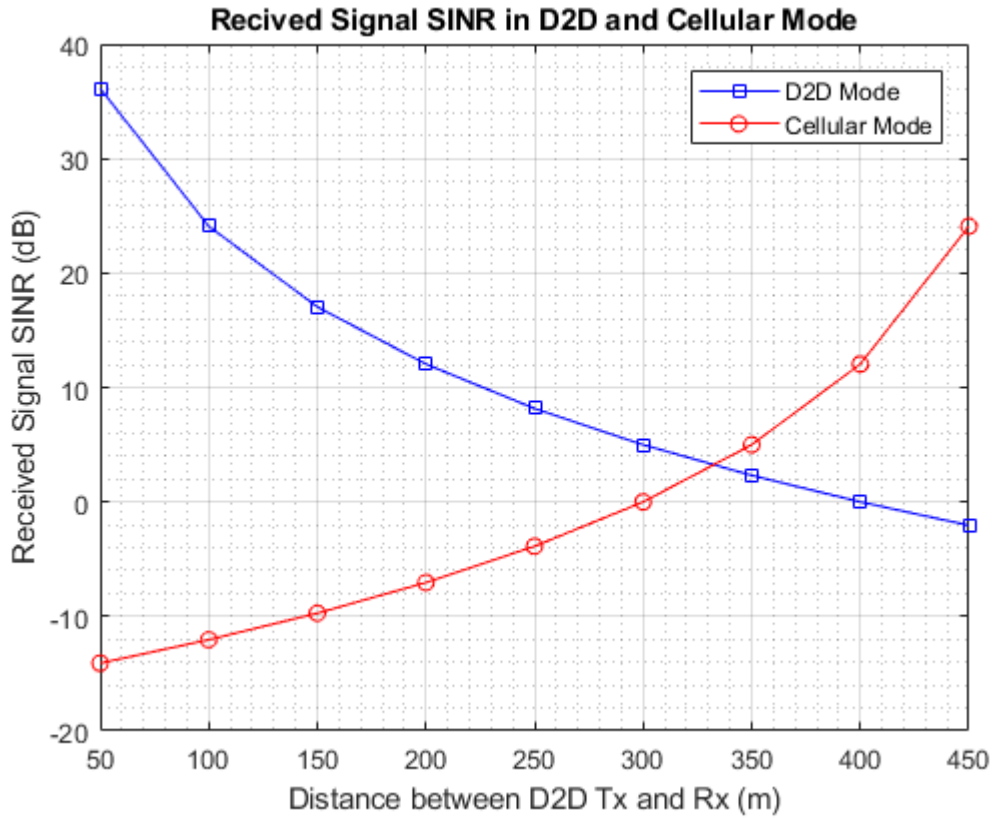

Figure 31. Scenario 1 - Received Signal SINR in D2D and Cellular Mode ($d_{CUE,Rx}$= 400 m, $d_{CUE,BS}$ = 200 m and $d_{Tx,BS} = R - d_{Tx,Rx}$).

Since the *Rx* is at the cell edge and the *CUE* is reasonable close to the BS, the distance between the *CUE* and the *Rx* will be very long, and interference imposed on D2D transmission by the *CUE* will be minimal. The received signal SINR and channel capacity in D2D and cellular modes are shown in Figures 31 and 32 respectively. As seen in the plot, the SINR and capacity in D2D mode decreases while that of cellular mode increases as the *Tx* moves away from the *Rx* and towards the *BS*. However, at all points, the SINR and capacity values in D2D mode are higher than that of cellular mode for a reasonably long distance up to a point where they both intersect. At this intersection point and forward, it will be reasonable to transmit using cellular mode.

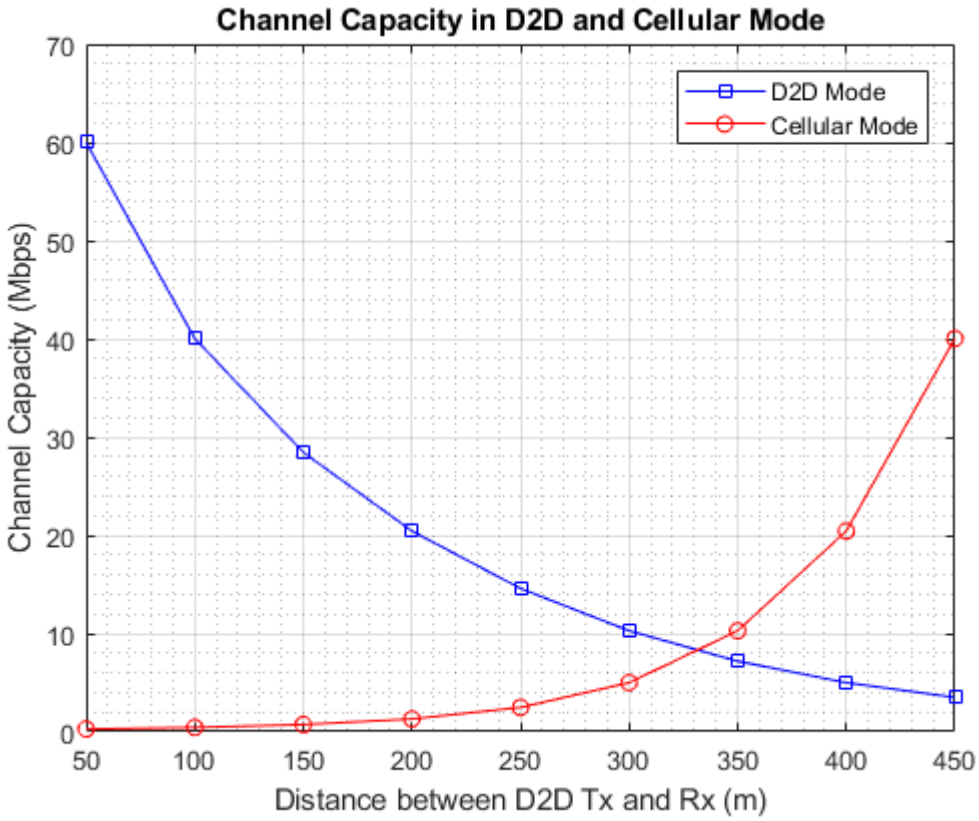

Figure 32. Scenario 1 - Channel Capacity in D2D and Cellular Mode ($d_{CUE,Rx}$= 400 m, $d_{CUE,BS}$ = 200 m and $d_{Tx,BS} = R - d_{Tx,Rx}$).

II. Scenario 2

All conditions and values in Scenario 1 remained the same except for the direction of travel of the *DUE Tx*. The *Tx* was considered to be moving away from both the *Rx* and the *BS*. Figures 33 and 34 shows the corresponding plot of the received signal SINR and channel capacity respectively in both D2D and cellular modes for this scenario. Due to signal attenuation, in both D2D and cellular modes, the quality of the transmission decreases as the distance increases. However, at any point, the SINR and capacity values in D2D mode is always higher than in cellular mode. The location of the *CUE* with respect to the *DUE Rx* also affect the D2D transmission. The closer the *CUE* is to the *Rx*, the higher the amount of interference it will impose on the D2D link. This condition is confirmed in scenarios 3 and 4.

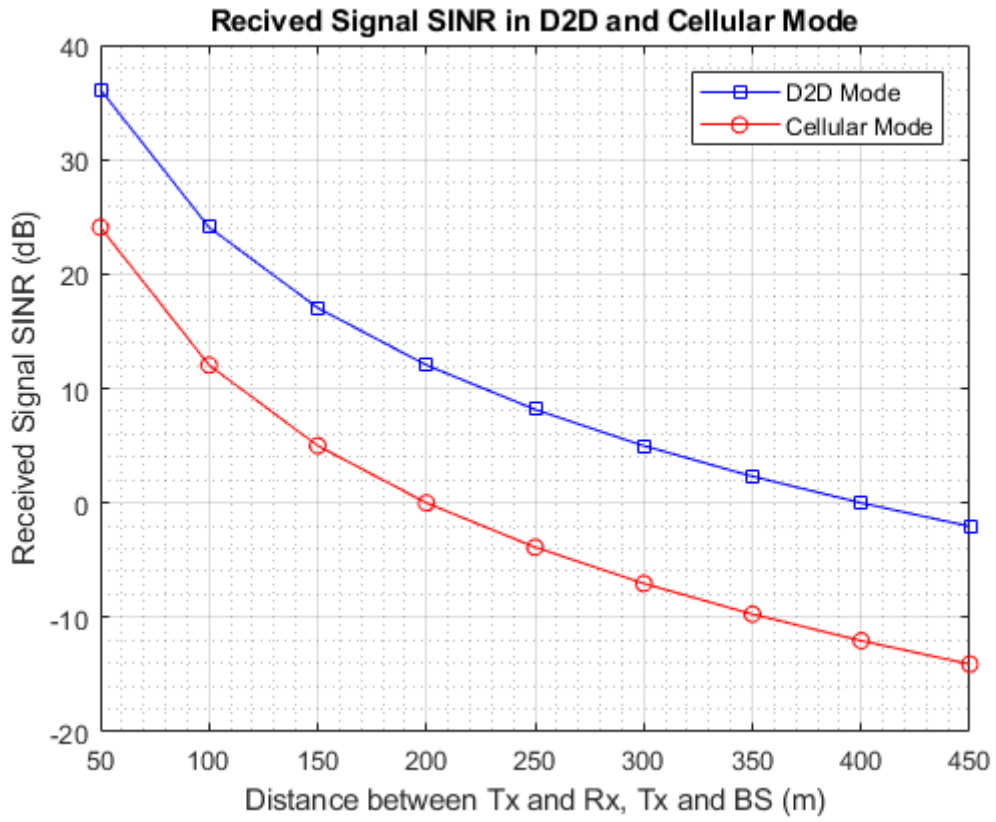

Figure 33. Scenario 2 - Received Signal SINR in D2D and Cellular Mode ($d_{CUE,Rx}$= 400 m and $d_{CUE,BS}$ = 200 m).

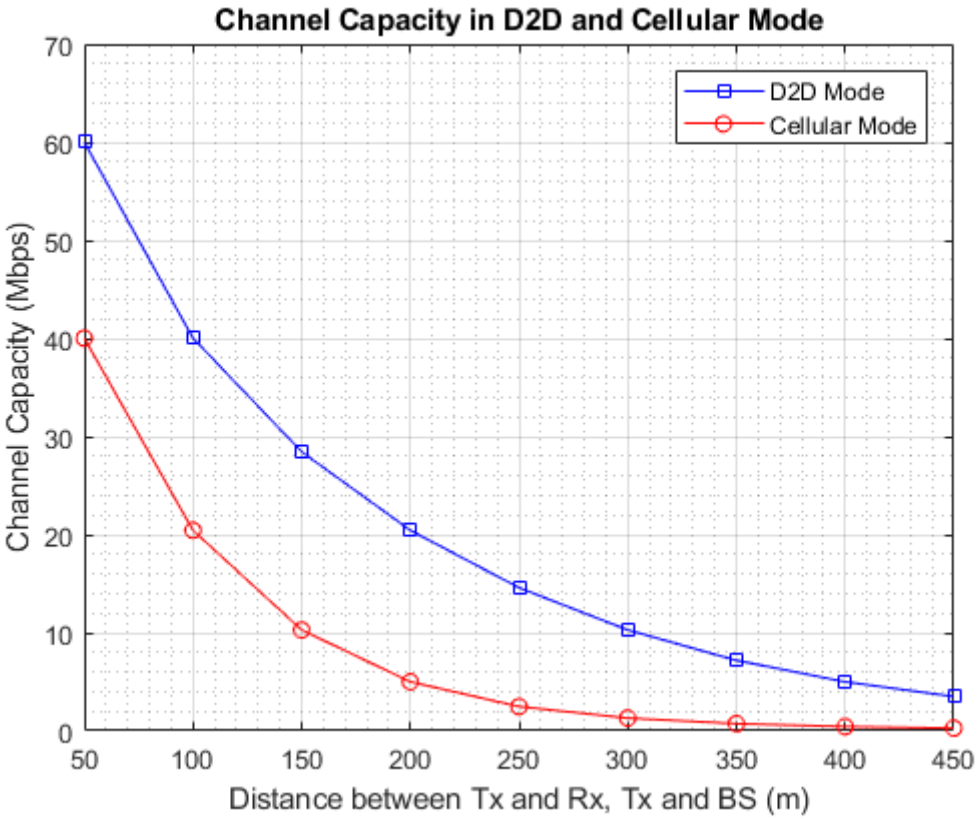

Figure 34. Scenario 2 - Channel Capacity in D2D and Cellular Mode ($d_{CUE,Rx}$= 400 m and $d_{CUE,BS}$ = 200 m).

III. **Scenario 3**

In this scenario, the position of the *DUE Tx* and *Rx* were fixed, while the *CUE* was considered to be on the move. The movement of the *CUE* is exactly the same as that of the *Tx* in scenario 1, i.e. as it moves away from the *Rx*, it moves towards the *BS*. As seen in the corresponding plot of the received SINR and channel capacity in Figures 35 and 36 respectively, as the *CUE* moves away from the *Rx*, the amount of interference it inflicts upon the D2D link reduces, consequently increasing the quality of the D2D transmission significantly.

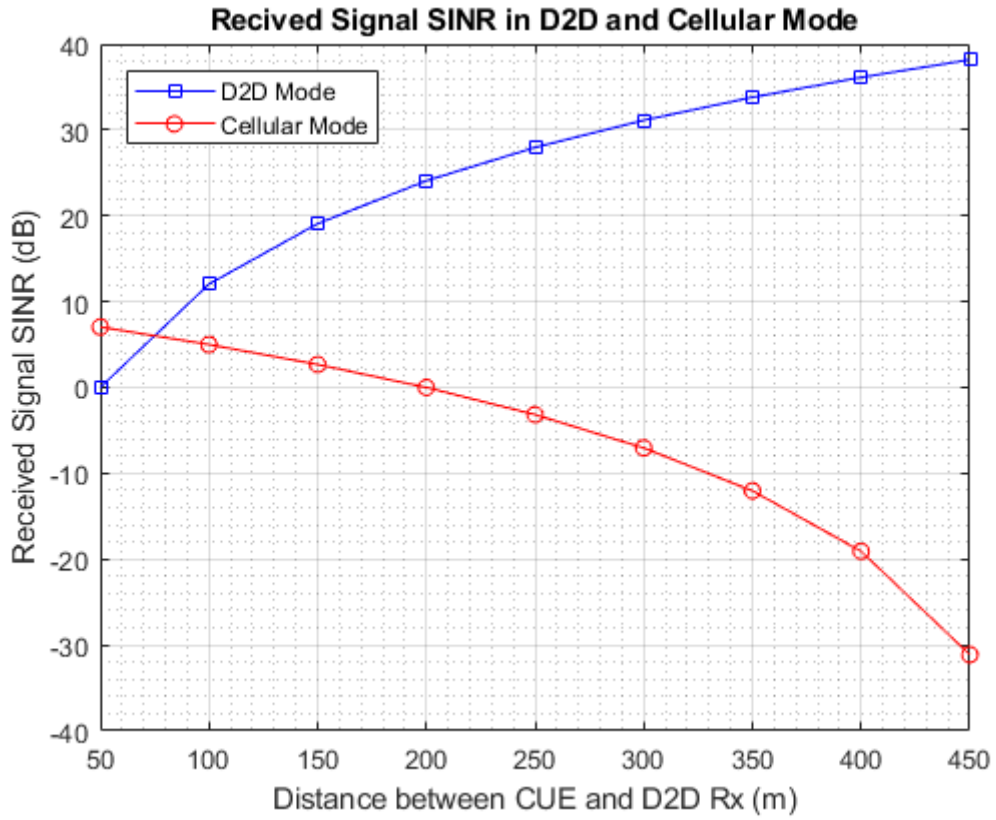

Figure 35. Scenario 3 - Received Signal SINR in D2D and Cellular Mode ($d_{Tx,Rx}$= 50 m, $d_{Tx,BS}$ = 300 m and $d_{CUE,BS} = R - d_{CUE,Rx}$).

IV. **Scenario 4**

All conditions and values from scenario 3 were kept the same for scenario 4 except for the movement of the *CUE*. The *CUE* was considered to be moving away from both the *BS* and the *Rx*. It is clear from the corresponding plot of the received signal SINR and channel capacity in Figures 37 and 38 that there is significantly large gain in the quality of transmission between D2D and cellular mode at all points.

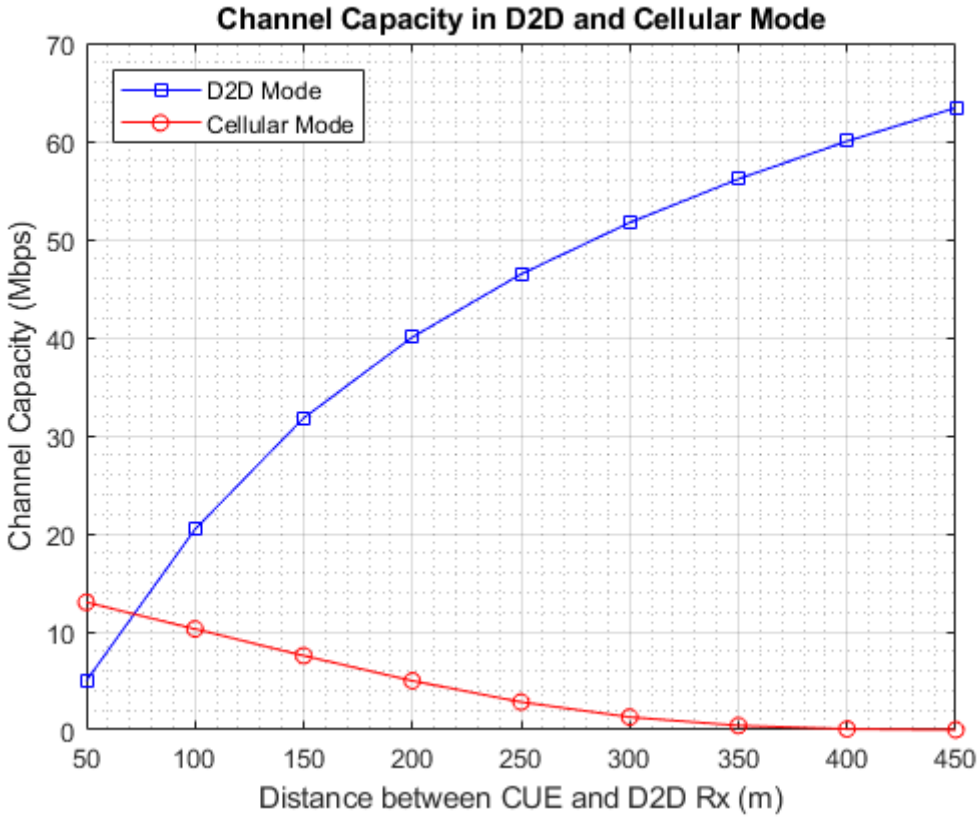

Figure 36. Scenario 3 - Channel Capacity in D2D and Cellular Mode ($d_{Tx,Rx}$= 50 m, $d_{Tx,BS}$ = 300 m and $d_{CUE,BS} = R - d_{CUE,Rx}$).

It is clear that the position of the host CUE with respect to the *DUE Rx* reusing its RB is an important factor to be considered. It is important to consider this when selecting the host *CUE* for a D2D transmission in resource allocation. For instance, in scenario 1, shorter $d_{CUE,Rx}$ means cellular mode becomes more favorable. Thus, the location of the host CUE affects *mode selection*. This is evident from the *location-based resource allocation* which tends to select the CUE farthest from the D2D Rx for RB reuse. Moreover, the distance between the pair also affect the transmission quality. The shorter the distance between the pair, the higher the quality of transmission. A maximum limit $d_{\max}$ should be set for the distance between the pair that qualifies for D2D mode, beyond this point, cellular mode should be used. For example, in scenario 1, $d_{\max}$ can be set to the value of $d_{Tx,Rx}$ where the values of D2D and cellular modes intersect on the plot. When D2D pair are close to some extent, the pair can communicate in D2D mode to take

advantage of the proximity gain. In addition, if cellular mode is used, the transmission between the *Tx* and *Rx* requires two phases; uplink (*Tx* to *BS*) and downlink (*BS* to *Rx*). Despite all the gain achieved in the four scenarios, only uplink part of the cellular mode was accounted for in the simulation. Using cellular mode when D2D mode can be used results in unnecessary power consumption resource utilization. Also, since the direct D2D link only reused uplink resources, the downlink resource is freed up resulting in *hop gain*.

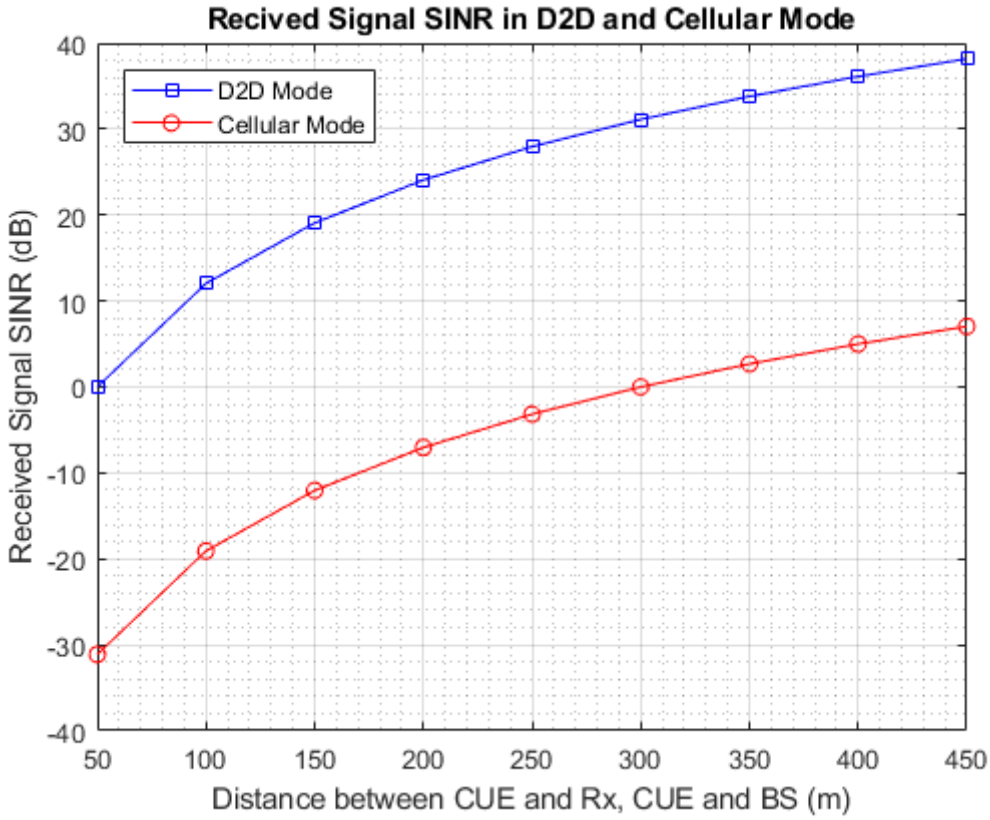

Figure 37. Scenario 4 - Received Signal SINR in D2D and Cellular Mode ($d_{Tx,Rx}$= 50 m and $d_{Tx,BS}$ = 300 m).

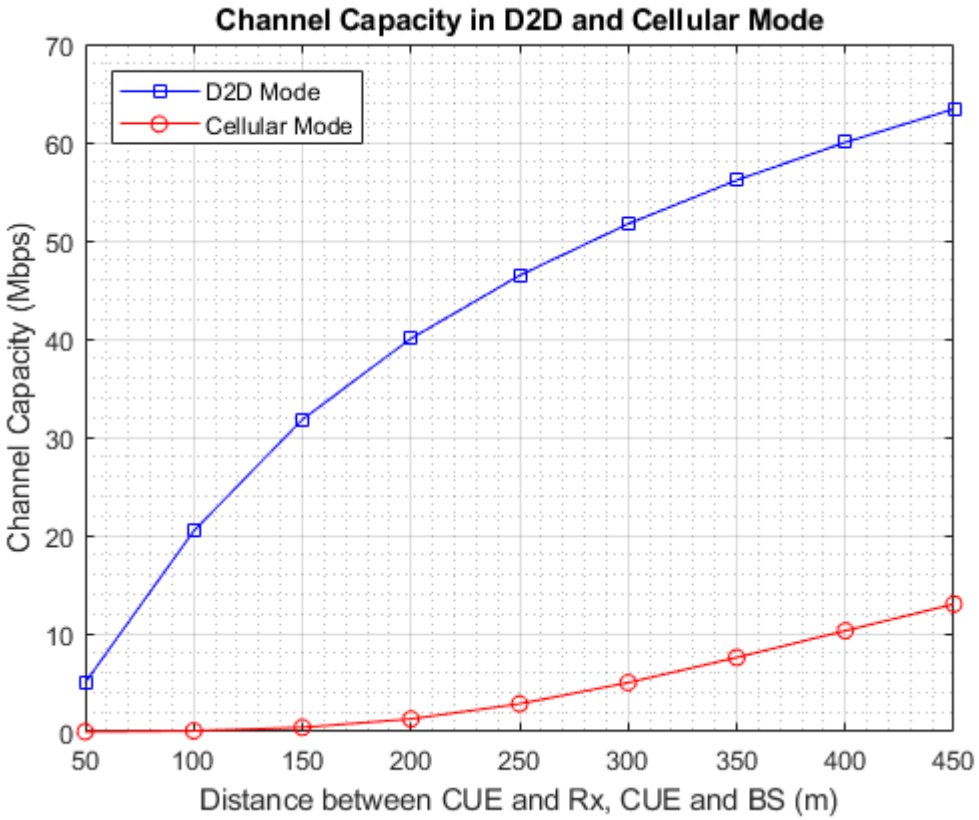

Figure 38. Scenario 4 - Channel Capacity in D2D and Cellular Mode ($d_{Tx,Rx}$= 50 m and $d_{Tx,BS}$ = 300 m).

5.2. Numerical Result and Performance Evaluation of MiSo Algorithm

This section presents the numerical result and detailed analysis of the MiSo Algorithm. Three *performance metrics* were used to evaluate the performance and feasibility of the joint power control and resource allocation algorithm for implementing D2D infrastructure underlaying cellular network. The first metrics is the *total number of DUE pair admitted* for reuse of RBs allocated to CUEs, i.e. the DUE pairs that can share their host CUE's RB without violating their SINR requirements or the SINR requirements of their host CUE and other DUE pairs under the same host. The second metrics considers the *percentage gain in the overall system throughput*. This is simply the percentage throughput gain realized by increasing the system throughput from the throughput value attained when there were only CUEs to the throughput value attained after the

introduction of the DUE pairs to the network. Similarly, the third metrics, which is the *percentage gain in power efficiency*, is the percentage gain achieved by increasing the power efficiency of the system from the power efficiency value attained when only CUEs exist in the network to the power efficiency value attained after the DUE pairs were introduced to the network.

The parameters were set as shown in Table 5, with 10 CUEs and the DUE count set to 20 and increased with a step of 20 to up to as high as 200 DUE pairs. With respect to these values, DUEs and CUEs were randomly positioned within the cell. The effect of SINR target of both DUEs and CUEs (γ_d^{tgt} and γ_c^{tgt}), as well as the distance between the DUE transmitter and receiver $d_{Tx,Rx}$ on the overall performance of the system were investigated using the aforementioned metrics and varying the values of γ_d^{tgt}, γ_c^{tgt}, and $d_{Tx,Rx}$ as necessary.

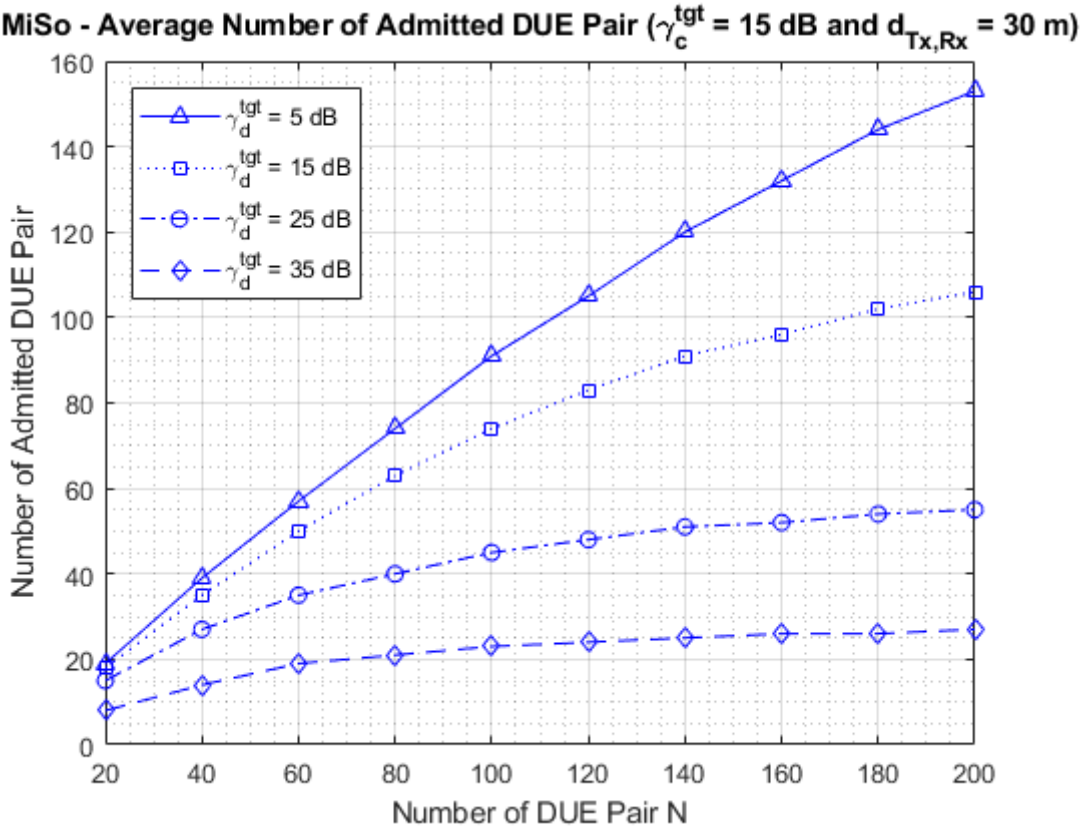

Figure 39. Average Number of Admitted DUE Pairs with Different Values of γ_d^{tgt}.

Although, DUEs and CUEs can have different SINR targets, in this simulation stage, at any point, all DUEs were set to have the same SINR target. Likewise, all CUEs were also set to have the same SINR target. The transmit power of each CUE is set to 23 dBm while each DUE can transmit between 0 dBm and 23 dBm (i.e. $P^{\max}$ = 23 dBm), since the actual transmit power will be determined by power control. To reveal true overall performance and feasibility, the simulation was repeated 500 times and the respective average values were plotted.

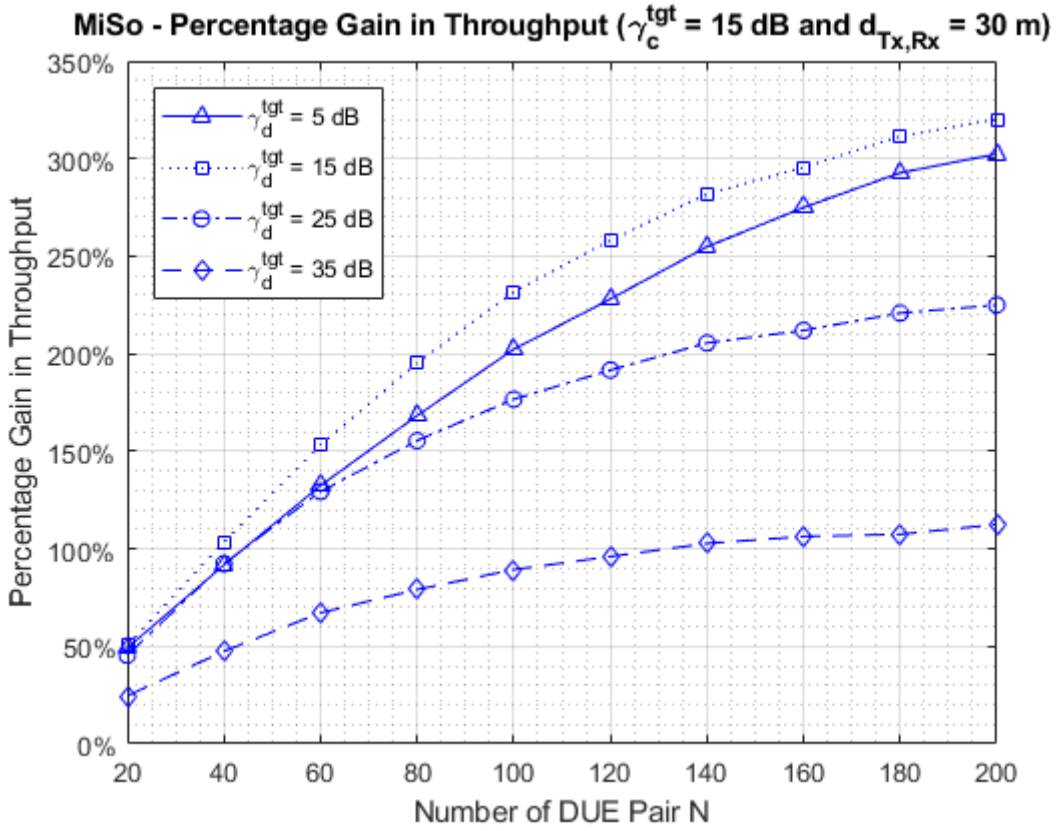

Figure 40. Percentage Gain in System Throughput with Different Values of γ_d^{tgt}.

The resulting plots are presented in the following parts. The plots of the *average number of admitted DUE pairs*, the *percentage gain in system throughput* and the *percentage gain in power efficiency* against the total number of DUE pair in the network for different values of γ_d^{tgt} are shown in Figures 39, 40 and 41 respectively. On average, out of 200

DUE pairs, about 150 DUE pairs were admitted at a DUE SINR value γ_d^{tgt} = 5 dB. The algorithm becomes more stringent, and fewer DUE pairs were admitted and permitted to reuse RB as the values of γ_d^{tgt} grew bigger. At γ_d^{tgt} = 35 dB, the algorithm admitted only as low as 25 DUE pairs out of 200 DUE pairs in the cell. However, at all values of γ_d^{tgt}, the algorithm produced a significant gain in the overall system throughput and power efficiency. As seen from the plot, lower target values with high number of admitted DUE does not necessarily translate to higher power efficiency or throughput gain. From the plots in Figure 40 and 41, the highest percentage gain in throughput and power efficiency values were recorded at γ_d^{tgt} = 15 dB which is neither the lowest or the highest value. This shows the significance of selecting a proper target value for DUEs to obtain an optimum result of maximizing throughput and power efficiency, without affecting the QoS of the communication link negatively.

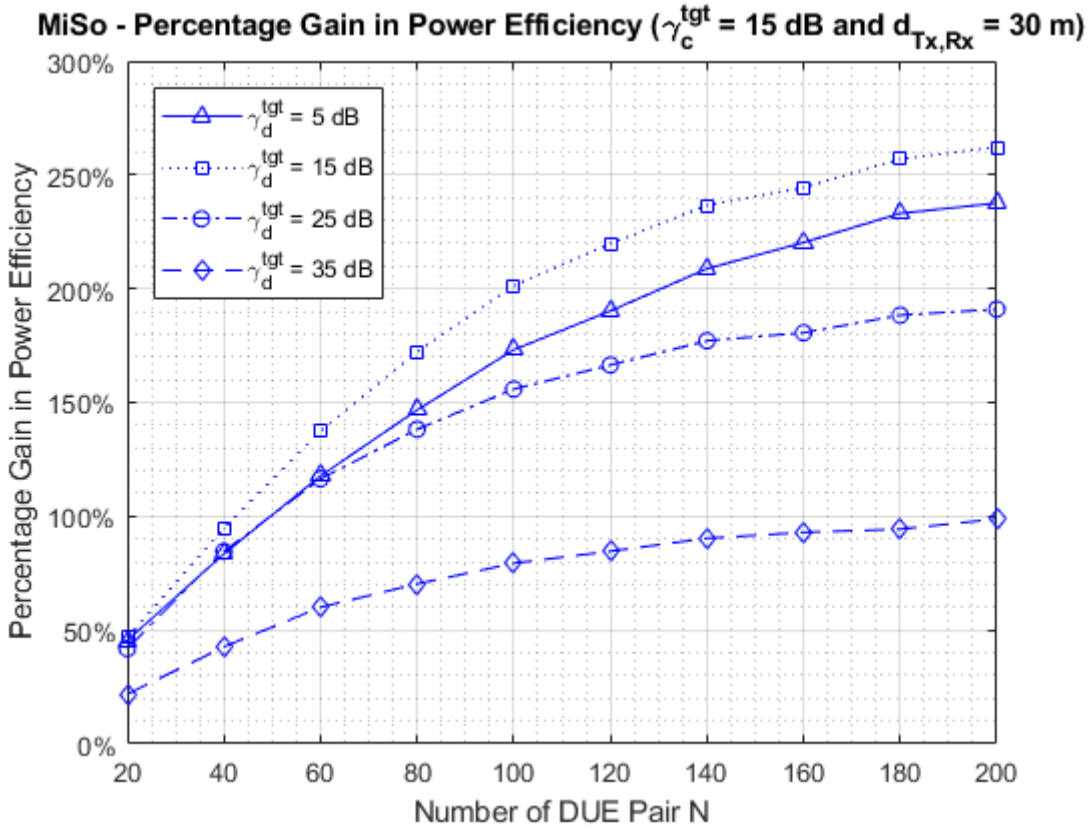

Figure 41. Percentage Gain in Power Efficiency with Different Values of γ_d^{tgt}.

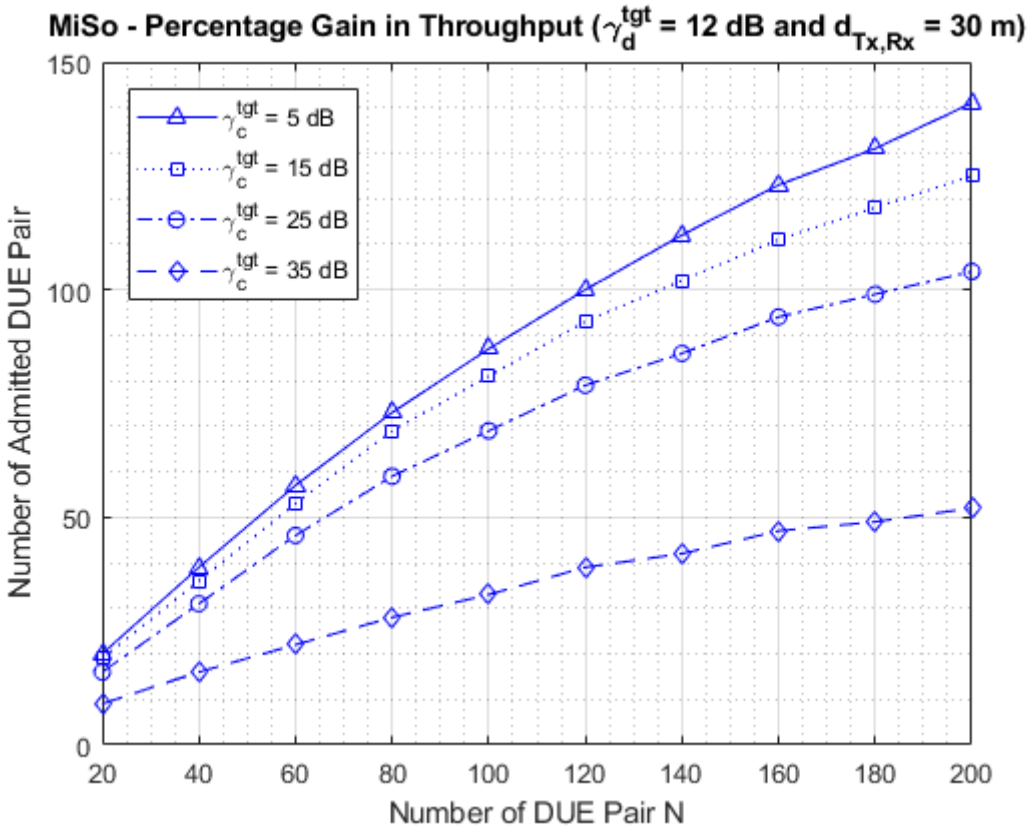

Figure 42. Average Number of Admitted DUE Pairs with Different Values of γ_c^{tgt}.

Figures 42, 43 and 44 shows the plots of the *average number of admitted DUE pairs*, the *percentage gain in system throughput* and the *percentage gain in power efficiency* respectively against the total number of DUE pair in the cell at different values of γ_c^{tgt}. Out of 200 DUE pairs, about 150 DUE pairs were admitted at a CUE SINR value γ_c^{tgt} = 5 dB. Similar to what happened in the case of γ_d^{tgt}, the algorithm becomes stricter, and fewer DUE pairs were admitted and permitted to reuse cellular RB as the values of γ_c^{tgt} grew bigger. At γ_c^{tgt} = 35 dB, the algorithm admitted only 50 DUE pairs out of 200 DUE pairs in the cell.

However, at all values of γ_c^{tgt}, the algorithm produced a significant gain in the overall system throughput and power efficiency. Unlike the case of γ_d^{tgt}, the highest percentage gain in system throughput was recorded when γ_c^{tgt} was in its lowest value of 5 dB as seen

in plot in Figure 43 while the highest percentage power efficiency values were recorded at γ_c^{tgt} = 15 dB which is neither the lowest or the highest value. This demonstrates how the SINR value of CUEs affect the resource allocation and admission control process.

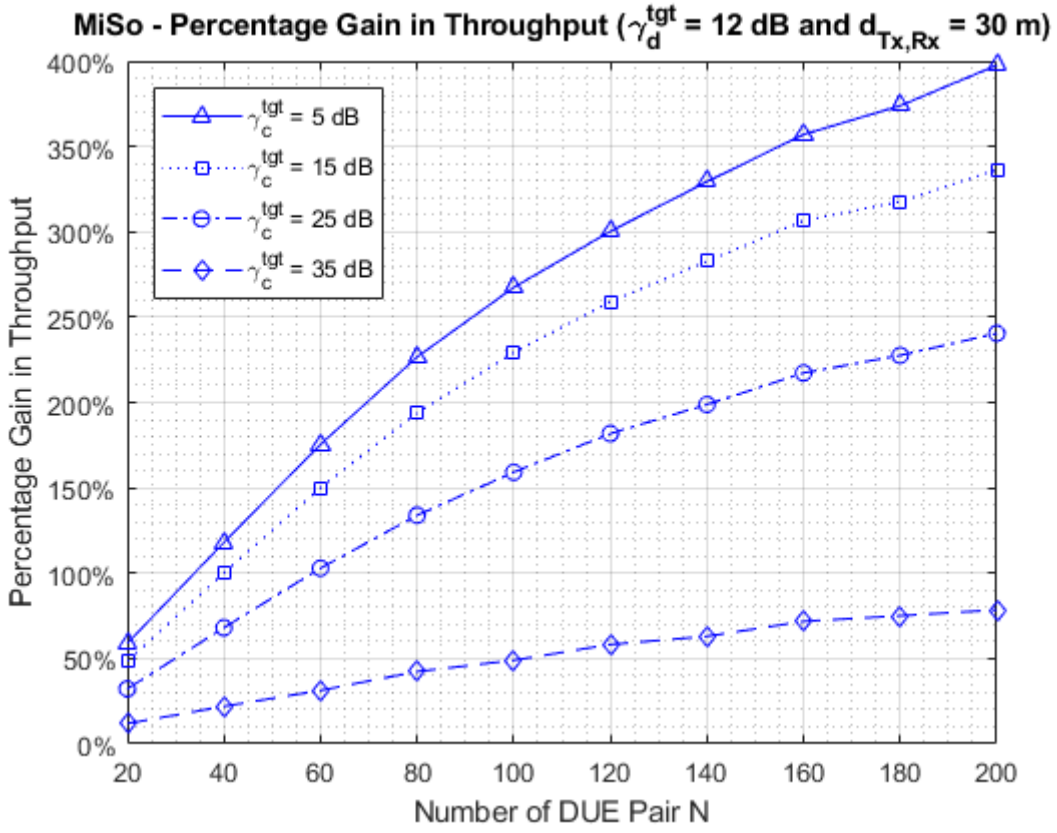

Figure 43. Percentage Gain in System Throughput with Different Values of γ_c^{tgt}.

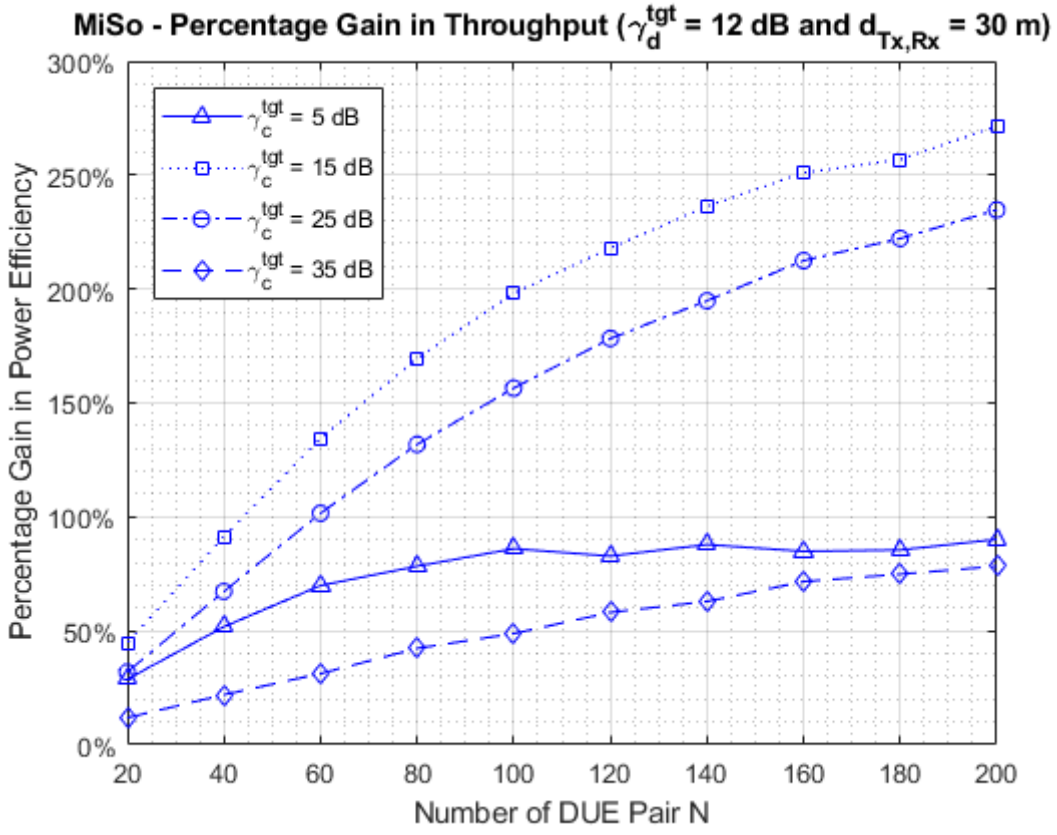

Figure 44. Percentage Gain in Power Efficiency with Different Values of γ_c^{tgt}.

To investigate how the distance between the transmitting DUE and the receiving DUE $d_{Tx,Rx}$ affects the resource allocation, power control and admission control, the algorithm was executed for different values of $d_{Tx,Rx}$ and the results are given in the following plots. The resulting plots of the *average number of admitted DUE pairs*, the *percentage gain in system throughput* and the *percentage gain in power efficiency* against the total number of DUE pair in the network for different values of $d_{Tx,Rx}$ are shown in Figures 45, 46 and 47 respectively.

As seen from the plot, the average number of DUE pairs permitted to reuse cellular RB drops as the distance between the transmitting and receiving DUE increases. Consequently, the percentage gain in system throughput and power efficiency decreases as the distance between transmitting and receiving DUE increases. However, a reasonable number of DUE pairs were admitted for reuse, and significant gain in system throughput

and power efficiency were recorded even when transmitting and receiving DUE were far apart with a separation distance of as long as 70 m. Although, the algorithm was able to admit very few DUE pairs at a distance of 100 m between transmitting and receiving DUEs, negative gain in system throughput and power efficiency were recorded at this distance.

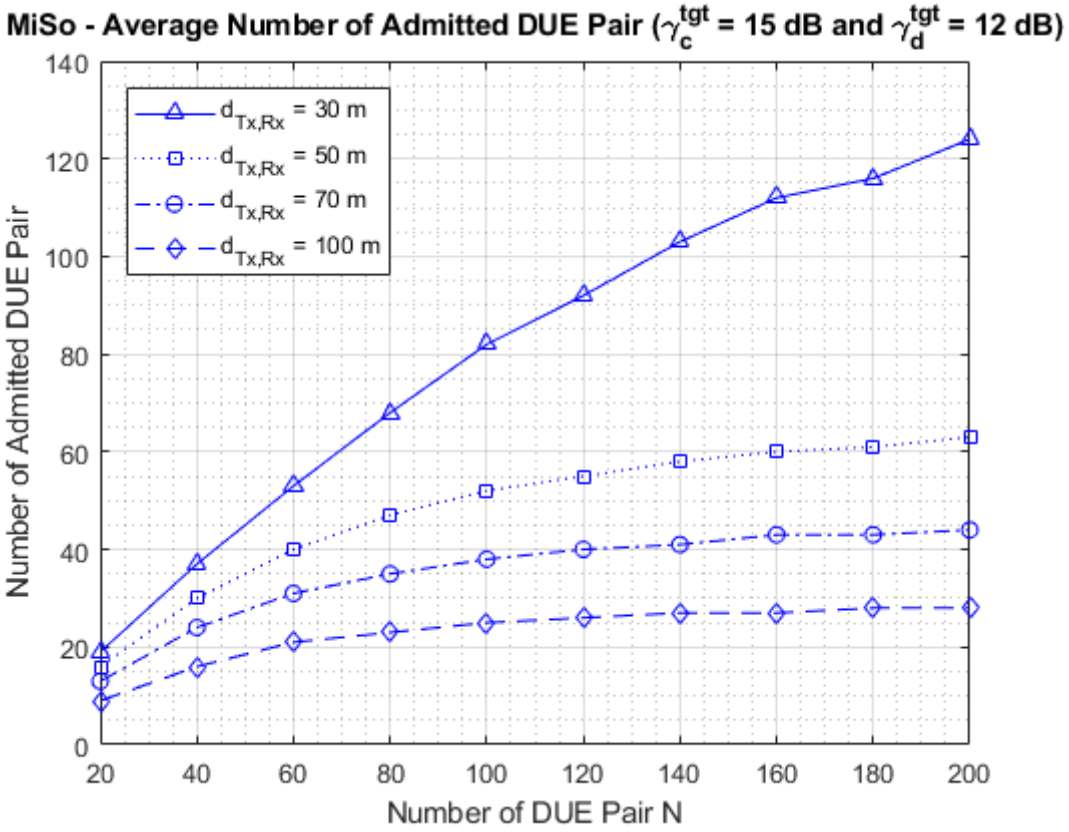

Figure 45. Average Number of Admitted DUE Pairs with Different Values of $d_{Tx,Rx}$.

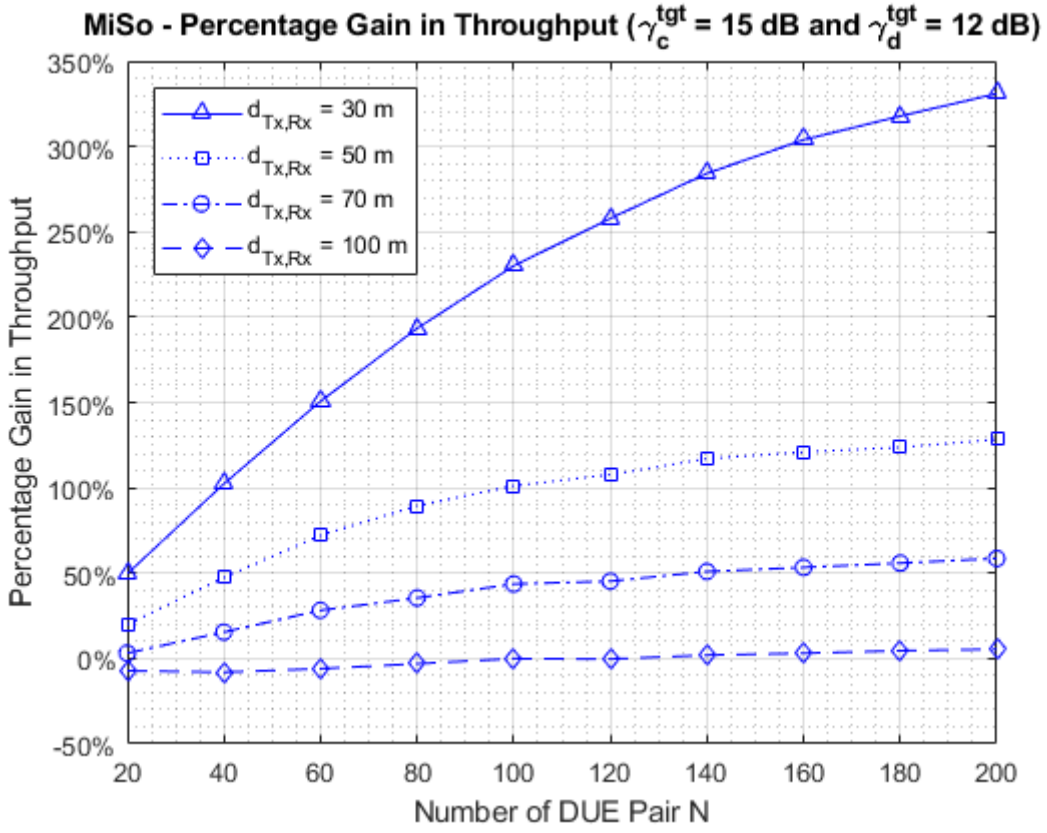

Figure 46. Percentage Gain in System Throughput with Different Values of $d_{Tx,Rx}$.

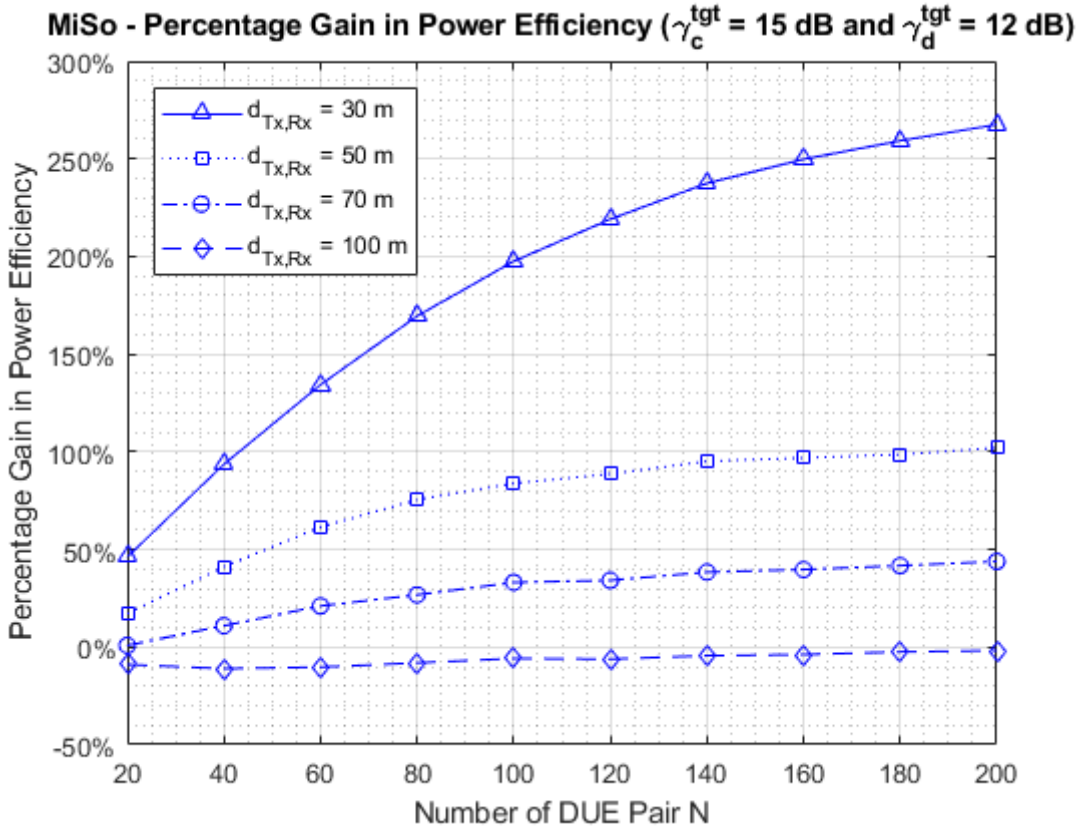

Figure 47. Percentage Gain in Power Efficiency with Different Values of $d_{Tx,Rx}$.

5.3. Comparison of MiSo, GTM+ and GRA Algorithms

The result of performance comparison between MiSo, GTM+ and GRA algorithm is presented in the section. Three *performance metrics* were explored in comparing the performance of these three algorithms. These are the *number of DUE pair admitted* for RB reuse, normalized *overall system throughput*, and *power efficiency* of the system. In this simulation, the distance between the DUE transmitter and receiver was fixed at a specific value with $d_{Tx,Rx}$ = 30 m for all DUE pairs. With respect to this, DUEs and CUEs were randomly placed in the cell. The number of CUE/RB was set to 10 while the number of DUE pair was set at the start to 20 with an increment step of 20 DUEs pair up to as high as 200 DUE pairs. For fairness purpose, in this simulation stage, for algorithms that has no power control included, i.e. GTM+ and GRA algorithm, transmit power of each

DUE is set to 10 dBm. On the other hand, for the MiSo algorithm which has power control, DUEs can transmit using transmit power in the range 0 dBm to 23 dBm (i.e. P^{max} = 23 dBm), with the actual transmit power determined by the Stackelberg Game-based power control. SINR targets of DUEs and CUEs were fixed at a specific value with γ_d^{tgt} = 12 dB for all DUEs and γ_c^{tgt}= 15 dB for all CUEs. To reflect true average performance like the previous simulation stage, this simulation was also repeated 500 times and the average values were plotted as shown in Figures 48, 49, and 50.

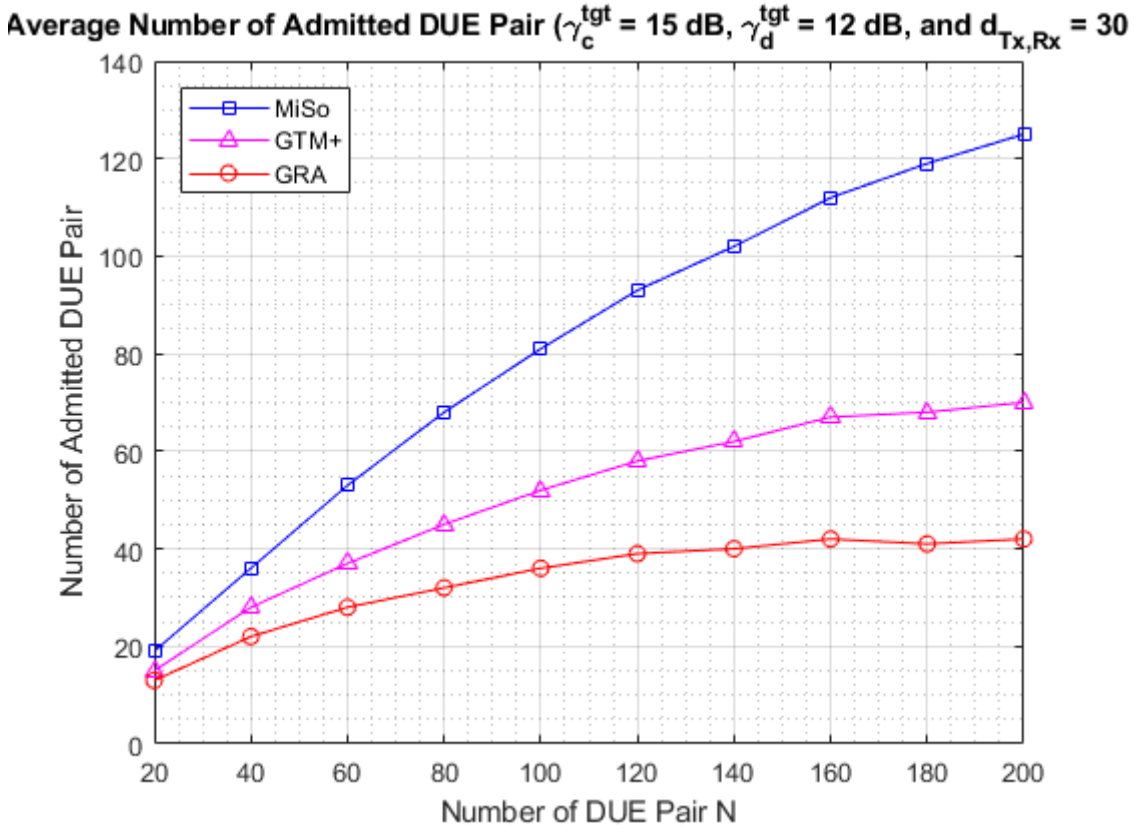

Figure 48. Average Number of Admitted DUE Pairs with MiSo, GTM+ and GRA.

The plot of the *average number of DUE pairs admitted* for reuse of cellular RB against the total number of DUE pairs in the network corresponding to MiSo, GTM+ and GRA algorithms is shown in Figure 48. As seen from the plot, among the three algorithms, MiSo algorithm admitted the highest number of DUE pairs, followed by GTM+ algorithm, and then GRA algorithm with the lowest number of admitted DUE pairs. GRA

algorithm reached its limit of 40 admitted DUE pairs much earlier at around the point where the total number of DUE pair *N* was 120. GTM+ algorithm also reach its admission limit of 70 DUE pairs at around the point where the total number of DUE pair in the network was 160. The values for MiSo, on the other hand, continued to increase even when the total number of DUE pair was as high as 200. In the case of MiSo, the total number of DUE pair admitted for reuse with 10 CUEs reached as high as 125 DUE pairs out of a total of 200 DUE pairs in the network.

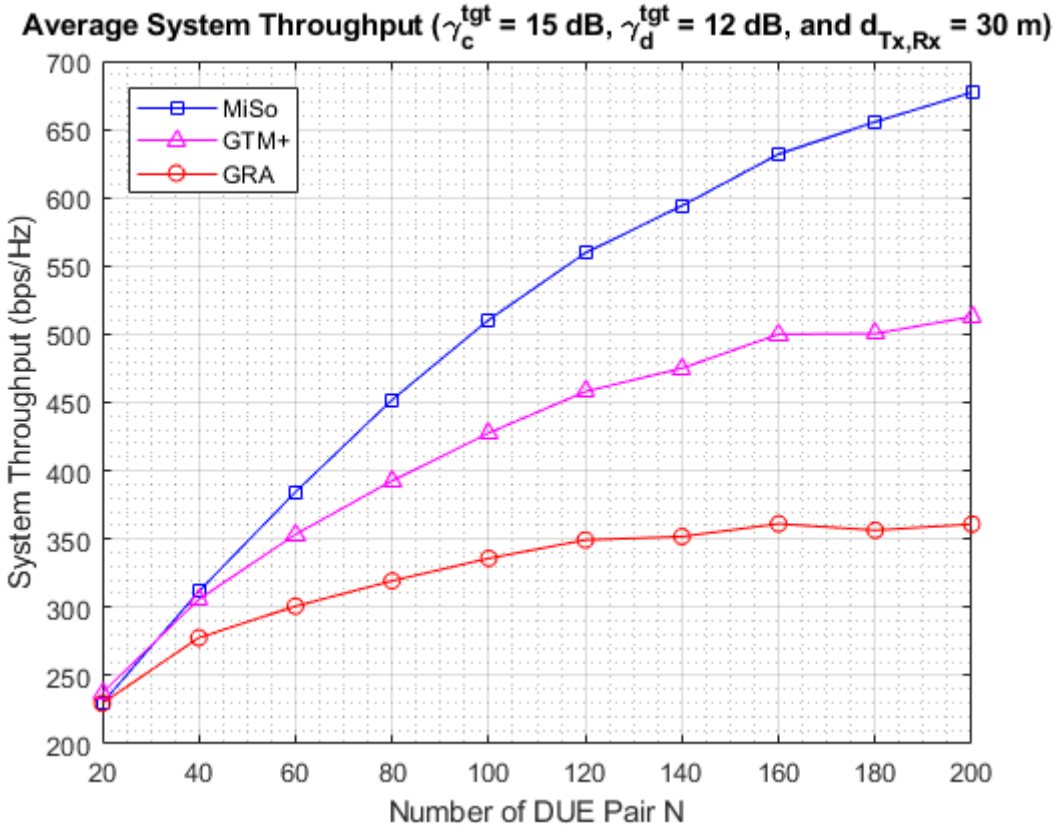

Figure 49. Overall System Throughput with MiSo, GTM+ and GRA.

The plot in Figure 49 shows the values of the *average overall system throughput* attained with different number of DUE pairs in the network for MiSo, GTM+ and GRA. From the plot, Miso has the best performance in terms of throughput, followed by GTM+, and then GRA with the lowest performance out of the three algorithms. For GRA algorithm, the attained system throughput reached a limit of about 350 bps/Hz at the point where *N* is

120. GTM+ algorithm also reached a limit around 500 bps/Hz at the point where N is 160. The overall system throughput in the case of MiSo continued to increase with no limit with a value of 680 bps/Hz at N = 200. The plot of the *average power efficiency* obtained against the total number of DUE pairs in the network corresponding to MiSo, GTM+ and GRA algorithms is shown in Figure 50. Similar to what was experienced in the case of system throughput, the power efficiency values of GRA and GTM+ reached their limits at the point when the total number of DUE pair in the network reached 120 and 160 respectively. Conversely, MiSo algorithm which produced the best performance in terms of power efficiency out of the three algorithms, continuously experienced a significant increase in power efficiency at each increment step of N up to the last value of 200 DUE pair.

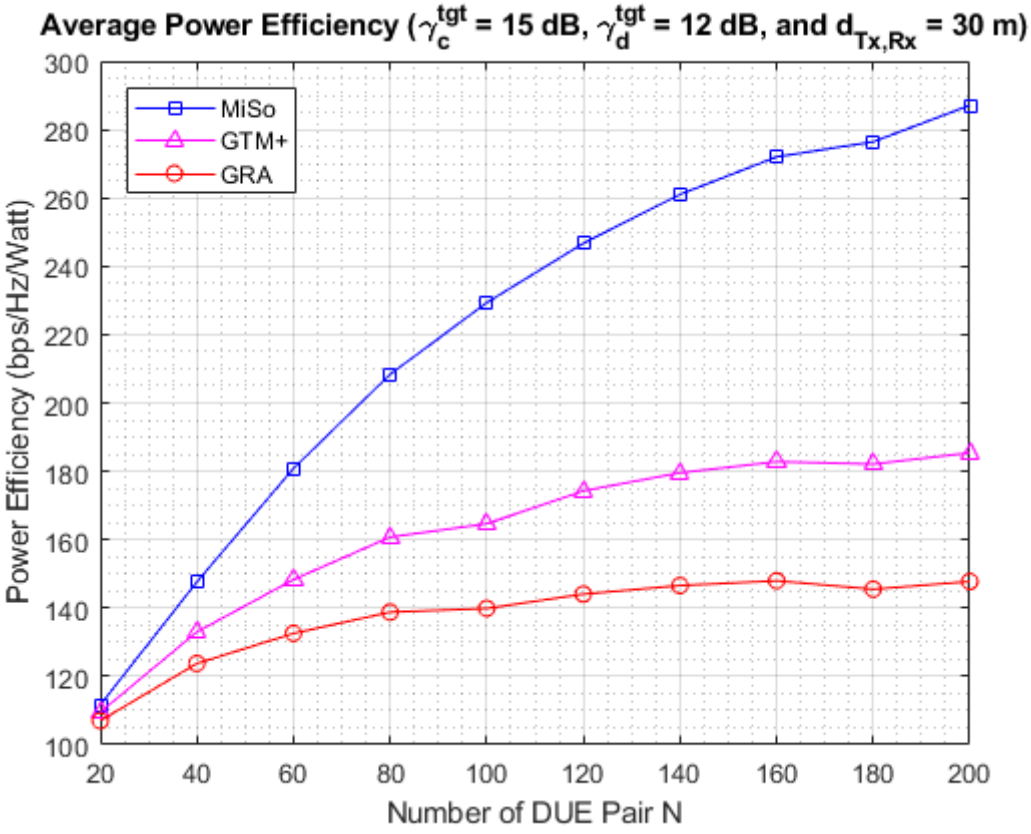

Figure 50. Power Efficiency with MiSo, GTM+ and GRA.

In conclusion, with all the *three-performance metrics* discussed above, it is evident that MiSo algorithm outperforms GRA and GTM+ algorithm, with GRA producing the worst performance out of the three with respect to the performance metrics considered. MiSo produced the best performance because of its power control features. With *power control*, MiSo was able to admit reasonably high number of DUE pairs out of the total number in the network, by limiting interference impose on CUE by DUEs sharing its RB and reducing mutual interference among DUEs sharing the same RB in a reuse group. Consequently, MiSo achieved higher throughput with relatively lower transmit power, resulting in a more power efficient network compared to other algorithms.

6. CONCLUSIONS AND FUTURE RESEARCH WORK

6.1. Conclusions

Due to the unprecedented and unceasing rise in the number of connected users and networked devices, the next-generation 5G cellular networks are envisaged and required to support the enormous number of simultaneously connected users and devices with access to numerous services and applications by providing networks with highly improved data rate, higher capacity, lower end-to-end latency, improved spectral efficiency, and lower power consumption. The requirements and the various technology enablers and new technological trends for the next generation networks have been identified and discussed, highlighting several research and development projects initiated for the realization the goals of 5G networks. More importantly, D2D communication have also been discussed under 3GPP ProSe and the Direct-D2D HT in the METIS Project as one of the key driving force to accomplishing the targets of the next generation networks offering lots of potentials in latency reduction, reducing power consumption and improving spectral efficiency.

Three potential gains of D2D communication were also identified; *proximity gain*, *reuse gain* and *hop gain*. Despite the promising potentials of the technology there are challenges that should be adequately addressed before its implementation. These challenges were also discussed, and solutions were suggested. Concepts of *interference management* in a *multi-sharing* D2D network that reuses cellular *uplink* resources were introduced in this work. Link-level simulation was conducted to demonstrate the gain of D2D transmission over cellular transmission in specific scenarios. System-level simulations were also conducted, implementing MiSo, a joint *admission control*, *resource allocation* and *power control* scheme for a multi-sharing D2D system in a *single cell* environment. The performance of the scheme was evaluated, and comparisons were made between the scheme and two other similar schemes in GTM+ and GRA using system throughput and power efficiency as the major performance metrics.

The results of the simulations conducted ascertained the potential gains of D2D communication. Results of the link-level simulations showed that transmission in D2D mode in certain scenarios offers significant gain in received SINR, user throughput and reduced power consumption over transmission in cellular mode in such scenarios. Moreover, the results of the system-level simulations also indicate the feasibility of deploying D2D communication underlaying 5G networks and its possibility to offer efficient spectrum reuse for improving spectral efficiency and overall network performance when properly implemented. For instance, from the result of MiSo simulation, 10 resource blocks allocated to 10 cellular links can be conveniently be reused or shared simultaneously by 125 D2D links at a reasonable power consumption level without causing deterioration in the QoS of the both the cellular or D2D links. In summary, with the introduction of D2D link that reuse cellular spectrum, the overall result shows an improvement in spectral efficiency, overall network throughput and power efficiency.

6.2. Future Work

This thesis concentrated on interference management in a multi-sharing D2D network that reuses cellular uplink resources. The focus was set on reuse of only uplink resources because downlink resources are more congested, and the interference from the high transmission power of the base station may be uncontrollable and can greatly affect D2D transmission. Moreover, majority of research focuses on uplink reuse and majority of network providers does not allow reuse of downlink resources. However, with few adjustments, the same approach can be followed for implementations where downlink resources are reused instead. Also, the significance of selecting and using an optimum SINR target for both D2D links and cellular link to maximize the realized gain was demonstrated in the result of the simulation. With this stated, SINR target optimization can be jointly implemented with admission control, resource allocation and power control to further maximize the throughput and power efficiency gain with D2D communication.

REFERENCES

3GPP. (2014). *3rd Generation Partnership Project; Technical Specification Group Services and System Aspects; Study on architecture enhancements to support Proximity-based Services (ProSe) (Release 12).* Valbonne, FRANCE: 3GPP Organizational Partners. doi:3GPP TR 23.703 V12.0.0 (2014-02)

Andrews, J. G., Buzzi, S., Choi, W., Hanly, S. V., Lozano, A., Soong, A. C., & Zhang, J. C. (2014). What Will 5G Be? *IEEE Journal on Selected Areas in Communications,* 32:6, 1065–1082. doi:10.1109/JSAC.2014.2328098

Agiwal, M., Roy, A., & Saxena, N. (2016). Next Generation 5G Wireless Networks: A Comprehensive Survey. *IEEE Communications Surveys & Tutorials,* 18:3), 1617–1655.

Agrawal, J., Patel, R., Mor, P., Dubey, P., & Keller, J. M. (2015, November 2). Evolution of Mobile Communication Network: from 1G to 4G. *International Journal of Multidisciplinary and Current Research,* 3:Nov/Dec 2015, 1100–1103. Retrieved from http://ijmcr.com

Al-Falahy, N., & Alani, O. Y. (2017). Technologies for 5G Networks: Challenges and Opportunities. *IT Professional,* 19:1, 12–20. doi:10.1109/MITP.2017.9

Alkurd, R., Shubair, R. M., & Abualhaol, I. (2014). Survey on Device-to-Device communications: Challenges and Design Issues. *2014 IEEE 12th International New Circuits and Systems Conference (NEWCAS)* (pp. 361–364). Trois-Rivieres, QC, Canada: IEEE. doi:10.1109/NEWCAS.2014.6934057

Aydin, O., Valentin, S., Ren, Z., Lakshmana, T. R., Sui, Y., Svensson, T., . . . Klein, A. (2013). *Mobile and wireless communications Enablers for the Twenty-twenty Information Society; Summary on preliminary trade-off investigations and first set of potential network-level solutions.* METIS. doi:ICT-317669-METIS/D4.1

Aziz, D., Kusume, K., Queseth, O., Tullberg, H., Fallgren, M., Schellmann , M., . . . Maternia, M. (2015). *Mobile and wireless communications Enablers for the*

Twenty-twenty Information Society (METIS) Final Project Report - Deliverable D8.4. METIS. doi:ICT-317669-METIS/D8.4

Banelli, P., Buzzi, S., Colavolpe, G., Modenini, A., Rusek, F., & Ugolini, A. (2014). Modulation Formats and Waveforms for 5G Networks: Who Will Be the Heir of OFDM?: An overview of alternative modulation schemes for improved spectral efficiency. *IEEE Signal Processing Magazine*, 31:6, 80–93. doi:10.1109/MSP.2014.2337391

Barreto, A. N., Faria, B., Almeida, E., Rodriguez, I., Lauridsen, M., Amorim, R., & Vieira, R. (2016). 5G – Wireless Communications for 2020. *Journal of Communication and Information Systems*, 31:1, 146–163. doi:10.14209/jcis.2016.14

Boccardi, F., Heath Jr, R. W., Lozano, A., Marzetta, T. L., & Popovski, P. (2014). Five Disruptive Technology Directions for 5G. *IEEE Communications Magazine*, 52:2, 74–80. doi:10.1109/MCOM.2014.6736746

Checko, A., Christiansen, H. L., Yan, Y., Scolari, L., Kardaras, G., Berger, M. S., & Dittmann, L. (2015). Cloud RAN for Mobile Networks—A Technology Overview. *IEEE Communications Surveys & Tutorials*, 17:1, 405–426. doi:10.1109/COMST.2014.2355255

Chen, S., & Zhao, J. (2014). The Requirements, Challenges, and Technologies for 5G of Terrestrial Mobile Telecommunication. *IEEE Communications Magazine*, 52:5, 36–43. doi:10.1109/MCOM.2014.6815891

Ciou, S.-A., Kao, J.-C., Lee, C. Y., & Chen, K.-Y. (2015). Multi-Sharing Resource Allocation for Device-to-Device Communication Underlaying 5G Mobile Networks. *2015 IEEE 26th Annual International Symposium on Personal, Indoor, and Mobile Radio Communications (PIMRC)* (pp. 1509–1514). Hong Kong, China: IEEE. doi:10.1109/PIMRC.2015.7343537

Cisco Systems Inc. (2017). *Cisco Visual Networking Index: Global Mobile Data Traffic Forecast Update, 2016–2021, White Paper.* San Jose, CA: Cisco Systems.

Cisco Systems, Inc. (2017). *The Zettabyte Era: Trends and Analysis.* San Jose, CA: Cisco Systems.

Feng, D., Lu, L., Yuan-Wu, Y., Li, G. Y., Feng, G., & Li, S. (2013). Optimal Resource Allocation for Device-to-Device Communications in Fading Channels. *2013 IEEE Global Communications Conference (GLOBECOM)* (pp. 3673–3678). Atlanta, GA, USA: IEEE. doi:10.1109/GLOCOM.2013.6831644

Fodor, G., Dahlman, E., Mildh, G., Parkvall, S., Reider, N., Miklós, G., & Turányi, Z. (2012). Design Aspects of Network Assisted Device-to-Device Communications. *IEEE Communications Magazine*, 50:3, 170–177. doi:10.1109/MCOM.2012.6163598

Fodor, G., Roger, S., Rajatheva, N., Slimane, S. B., Svensson, T., Popovski, P., . . . Ali, S. (2016). An Overview of Device-to-Device Communications Technology Components in METIS. *IEEE Access,* 4:1, 3288–3299. doi:10.1109/ACCESS.2016.2585188

Gupta, A., & Jha, R. K. (2015). A Survey of 5G Network: Architecture and Emerging Technologies. *IEEE Access: Recent Advances in Software Defined Networking for 5G Networks,* 3, 1206–1232. doi:10.1109/ACCESS.2015.2461602

Haus, M., Waqas, M., Ding, A. Y., Li, Y., Tarkoma, S., & Ott, J. (2017). Security and Privacy in Device-to-Device (D2D) Communication: A Review. *IEEE Communications Surveys & Tutorials,* 19:2, 1054–1079. doi:10.1109/COMST.2017.2649687

Jaloun, M., & Guennoun, Z. (2010). Wireless Mobile Evolution to 4G Network. *Wireless Sensor Network,* 2, 309–317. doi:10.4236/wsn.2010.24042

Jiang , T., & Wu, Y. (2008). An Overview: Peak-to-Average Power Ratio Reduction Techniques for OFDM Signals. *IEEE Transactions on Broadcasting,* 54:2, 257–268. doi:10.1109/TBC.2008.915770

Jimaa, S., Chai, K. K., Chen, Y., & Alfadhl, Y. (2011). LTE-A an Overview and Future Research Areas. *Second International Workshop on the Performance Enhancements in MIMO-OFDM Systems,* (pp. 395–399). Wuhan.

Kanchi, S., Sandilya, S., Bhosale, D., Pitkar, A., & Gondhalekar, M. (2013). Overview of LTE-A Technology. *Global High Tech Congress on Electronics (GHTCE)* (pp. 195–200). Shenzhen: IEEE.

Khan, F., Pi, Z., & Rajagopal, S. (2012). Millimeter-wave Mobile Broadband with Large Scale Spatial Processing for 5G Mobile Communication. *2012 50th Annual Allerton Conference on Communication, Control, and Computing (Allerton)* (pp. 1517–1523). Monticello, IL, USA: IEEE. doi:10.1109/Allerton.2012.6483399

Korhonen, J. (2003). *Introduction to 3G Mobile Communications* (2nd ed.). London: Artech House.

Kumar, A., Liu, Y., Sengupta, J., & Divya. (2010, December). Evolution of Mobile Wireless Communication Networks: 1G to 4G. *International Journal of Electronics & Communication Technology,* 1:1, 68–72. Retrieved October 17, 2017, from www.iject.org

Lee, J., Kim, Y., Lee, H., Ng, B. L., Mazzarese, D., Liu, J., . . . Zhou, Y. (2012). Coordinated Multipoint Transmission and Reception in LTE-Advanced Systems. *IEEE Communications Magazine,* 50:11, 44–40. doi:10.1109/MCOM.2012.6353681

Li, Z., Moisio, M., Uusitalo, M. A., Lundén, P., Wijting, C., Moya, F. S., . . . Venkatasubramanian, V. (2014). Overview on initial METIS D2D concept. *2014 1st International Conference on 5G for Ubiquitous Connectivity (5GU)* (pp. 203–208). Akaslompolo, Finland: IEEE. doi:10.4108/icst.5gu.2014.258096

Lien, S.-Y., Chien, C.-C., Tseng, F.-M., & Ho, T.-C. (2016). 3GPP Device-to-Device Communications for BeyonD 4G Cellular Networks. *IEEE Communications Magazine,* 54:3, 29–35. doi:10.1109/MCOM.2016.7432168

Lin, S.-H., Chen, K.-Y., Kao, J.-C., & Hsiao, Y.-F. (2017). Fast Spectrum Reuse and Power Control for Device-to-Device Communication. *2017 IEEE 85th Vehicular Technology Conference (VTC Spring)* (pp. 1–5). Sydney, NSW, Australia: IEEE. doi:10.1109/VTCSpring.2017.8108252

Lin, X., Andrews, J. G., Ghosh, A., & Ratasuk, R. (2014). An Overview of 3GPP Device-to-Device Proximity Services. *IEEE Communications Magazine*, 52:4, 40–48. doi:10.1109/MCOM.2014.6807945

Oshin, O. I., & Atayero, A. A. (2015). 3GPP LTE: An Overview. *Lecture Notes in Engineering and Computer Science: Proceedings of the World Congress on Engineering (WCE).* 1, pp. 616–621. London, UK.: IAENG. Retrieved from http://www.iaeng.org/publication/WCE2015/

Osseiran, A., Boccardi, F., Braun, V., Kusume, K., Marsch, P., Maternia, M., . . . M. F. (2014, May 2014). Scenarios for 5G Mobile and Wireless Communications: The Vision of the METIS Project. *IEEE Communications Magazine*, 52:5, pp. 26–35. doi:10.1109/MCOM.2014.6815890

Pi, Z., & Khan, F. (2011). An Introduction to Millimeter-Wave Mobile Broadband Systems. *IEEE Communications Magazine*, 49:6, 101–107. doi:10.1109/MCOM.2011.5783993

Pirinen, P. (2014). A Brief Overview of 5G Research Activities. *2014 1st International Conference on 5G for Ubiquitous Connectivity (5GU)* (pp. 17–22). Akaslompolo: IEEE. doi:10.4108/icst.5gu.2014.258061

Popovski, P., Braun, V., Mayer, H.-P., Fertl, P., Ren, Z., Gonzales-Serrano, D., . . . Chatzikokolakis, K. (2013). *Mobile and wireless communications Enablers for the Twenty-twenty Information Society: Scenarios, requirements and KPIs for 5G mobile and wireless system.* METIS. doi:ICT-317669-METIS/D1.1

Premnath , S. N., Jana, S., Croft, J., Gowda, P. L., Clark, M., Kasera, S. K., . . . Krishnamurthy, S. V. (2013). Secret Key Extraction from Wireless Signal Strength in Real Environments. *IEEE Transactions on Mobile Computing*, 12:5, 917–930. doi:10.1109/TMC.2012.63

Reider, N., & Fodor, G. (2012). A distributed power control and mode selection algorithm for D2D communications. *EURASIP Journal on Wireless Communications and Networking*, 1–25. doi:10.1186/1687-1499-2012-266

Salman, H. A., Ibrahim, L. F., & Fayed, Z. (2014). Overview of LTE-Advanced Mobile Network Plan Layout. *2014 5th International Conference on Intelligent Systems, Modelling and Simulation (ISMS)* (pp. 585–590). Langkawi, Malaysia: IEEE. doi:10.1109/ISMS.2014.106

Shen, X. (2015, March 24). Device-to-device communication in 5G cellular networks. *IEEE Network,* 29:2, 2–3. doi:10.1109/MNET.2015.7064895

Sun, H., Sheng, M., Wang, X., Zhang, Y., Liu, J., & Wang, K. (2013). Resource Allocation for Maximizing the Device-to-Device Communications Underlaying LTE-Advanced Networks. *2013 IEEE/CIC International Conference on Communications in China - Workshops (CIC/ICCC)* (pp. 61–64). Xi'an, China: IEEE. doi:10.1109/ICCChinaW.2013.6670568

Tehrani, M. N., Uysal, M., & Yanikomeroglu, H. (2014). Device-to-device communication in 5G cellular networks: challenges, solutions, and future directions. *IEEE Communications Magazine,* 52:5, 86–92. doi:10.1109/MCOM.2014.6815897

Tondare, S. M., Panchal, S. D., & Kushnure, D. T. (2014, April). Evolution of Mobile Wireless Communication Networks: 1G to 4G. *International Journal of Advanced Research in Computer and Communication Engineering,* 3:4, 6163–6166. Retrieved October 17, 2017, from www.ijarcce.com

Young, L. J. (2015). Telecom Experts Plot a Path to 5G. *IEEE Spectrum,* 52:10, 14–15. Retrieved from spectrum.ieee.org/telecom/wireless/telecom-experts-plot-a-path-to-5g

Zarrinkoub, H. (2014). *Understanding LTE with MATLAB: From Mathematical Modeling to Simulation and Prototyping.* Massachusetts, USA: John Wiley & Sons.

Zhang , A., & Lin, X. (2017). Security-Aware and Privacy-Preserving D2D Communications in 5G. *IEEE Network,* 31:4, 70–77. doi:10.1109/MNET.2017.1600290

Zhang, A., Zhou, L., & Wang, L. (2016). *Security-Aware Device-to-Device Communications Underlaying Cellular Networks*. 1st edition. New York: Springer International Publishing. doi:978-3-319-32458-6

APPENDICES

APPENDIX 1. Maximum Independent Set-based and Stackelberg Game-based Power Control and Resource Allocation Algorithm

Algorithm 1: MiSo

Algorithm *MiSo*

Input: M CUEs and N DUE pairs.

Output: RB reuse results $\{\Delta_1, \Delta_2, \Delta_3, \ldots, \Delta_M\}$ and transmit power results $\{P_1, P_2, P_3, \ldots, P_N\}$

// Initialization.

$U \leftarrow \{1, 2, 3, \ldots, M\}$. // U is the set of unmarked groups/CUEs.

Set $\Gamma_1, \Gamma_2, \Gamma_3, \ldots, \Gamma_M$ to be empty sets.

Compute $P_1^{\text{init}}, P_2^{\text{init}}, P_3^{\text{init}}, \ldots, P_N^{\text{init}}$ by Equation 4.9.

Join($\{1, 2, 3, \ldots, M\}$). // Each DUE pair joins a group that maximizes the sheer rate and becomes a candidate.

while $U \neq \emptyset$ **do**

Find the largest unmarked group c. //$c \leftarrow \arg\max_{c' \in U} |\Gamma_{c'}|$

$U \leftarrow U - \{c\}$. // Make group c marked.

// Tier-1 allocation starts here.

Form the modified conflict graph CG_c for group c.

$\Lambda_c \leftarrow$ the maximum independent set of CG_c.

$\Delta_c^1 \leftarrow \Lambda_c$. Then remove one DUE pair at a time from Δ_c^1, until each SINR requirement of $d \in \Delta_c^1$ is satisfied.

$P_d \leftarrow P_d^{\text{init}}$, for each $d \in \Delta_c^1$.

// Tier-2 allocation starts here.

$\Lambda_c^{'} \leftarrow \Lambda_c - \Delta_c^1$. $\quad \Delta_c \leftarrow \Delta_c^1$.

while $\Lambda_c^{'} \neq \emptyset$ *and* $\lambda_{c,\Delta_c}(d^*) > 0$ **do**

Compute M_c and M_d, $d \in \Delta_c$, by Equation 4.14 and Equation 4.15.

for each $d \in \Lambda_c^{'}$ **do**

Compute $P_d^{\min}$ by Equation 4.12, $P_d^{\max}$ by Equation 4.13, and the six possible values of (α_c^*, P_d^*) by Equation 4.18 and Equation 4.19. Among the six, the actual (α_c^*, P_d^*) is the one with largest $U_c(\alpha_c, P_d)$, which is defined in Equation 4.20.

Compute $\lambda_{c,\Delta_c}(d)$ by Equation 4.16.

$d^* = \arg\max_{d \in \Lambda_c^{'}} \lambda_{c,\Delta_c}(d)$// Find the winner d^*.

if $\lambda_{c,\Delta_c}(d^*) > 0$ **then**

$P_{d^*} \leftarrow P_d^*$. // Transmission power of d^* is set to be P_d^*.

Move d^* from $\Lambda_c^{'}$ to Δ_c.

Join($\Gamma_c - \Delta_c$). // Candidates not getting elected join other groups.

Function *Join(D)*

// Each DUE pair in the set D joins the unmarked group that maximizes the share rate.

for each $d \in D$ **do**

$c^* = \arg\max_{c \in U} r_{(c,\, d)}$.

$\Gamma_{c^*} \leftarrow \Gamma_{c^*} \cup \{d\}$.

APPENDIX 2. Greedy Throughput Maximization Plus Algorithm

Algorithm 2: GTM+

Algorithm *GTM+*

Input: N DUE pairs, $M - K$ real CUEs, and K idle RBs.

Output: RB allocation results $\Delta_1, \Delta_2, \Delta_3, \ldots, \Delta_M$.

// Pre-allotment of idle RBs.

Randomly pick K DUE pairs, say $D_{\delta_1}, D_{\delta_2}, D_{\delta_3}, \ldots, D_{\delta_K}$, one for each idle RB. Pretend and treat these DUE pairs as K CUEs which are numerated as CUEs M–K+1, M–K+2, . . . , M.

// Initialization.

$U \leftarrow \{1, 2, 3, \ldots, M\}$. // U is the set of unmarked groups/CUEs.

Set $\Gamma_1, \Gamma_2, \Gamma_3, \ldots, \Gamma_M$ to be empty sets. // Γ_c is the set of DUEs that joins group c.

for each $d \in \{1, 2, 3, \ldots, N\} - \{\delta_1, \delta_2, \delta_3, \ldots, \delta_K\}$ **do**

  $c^* \leftarrow$ WhoGivesMaxUtility(d, U).

  $\Gamma_{c^*} \leftarrow \Gamma_{c^*} \cup \{d\}$. // That is, d joins group c*.

// The main body (consisting of iterations) starts here.

while $U \neq \emptyset$ **do**

  Form the conflict graph $CG_{c'}$ for the largest group $\Gamma_{c'}$ in U. //$c' \leftarrow \arg\max_{c \in U} |\Gamma_c|$

  $\Delta_{c'} \leftarrow$ the maximum weight independent set of $CG_{c'}$.

  for each $d' \in \Delta_{c'}$ **do**

    // Check if DUE pair n does not meet its SINR requirement.

    if $P_{c'} g_{c',d'} + \sum_{d \in \Delta_{c'} - \{d'\}} P_d g_{d,d'} > I_{d'}$ **then**

      Remove d' from $\Delta_{c'}$.

  Sort elements/DUEs in $\Delta_{c'}$ by their interference on c' in descending order.

  // Remove one DUE from $\Delta_{c'}$ at a time until the superposed interference is below maximum tolerable interference $I_{c'}$.

  while $\sum_{d \in \Delta_{c'}} P_d g_{d,B} > I_{c'}$ **do**

    Remove the first element from $\Delta_{c'}$.

  for each $d \in \Gamma_{c'} - \Delta_{c'}$ **do**

    $c^* \leftarrow$ WhoGivesMaxUtility(d, $U - \{c'\}$).

    $\Gamma_{c^*} \leftarrow \Gamma_{c^*} \cup \{d\}$. // d joins group c^*.

  $U \leftarrow U - \{c'\}$. // Make group c' marked.

Function *WhoGivesMaxUtility(d, C)*

  // Return $c^* = \arg\max_{c \in C} \{u_d(c): P_d g_{d,B} \leq I_c\}$.

  MaxUtility $\leftarrow 0$.

  $c^* \leftarrow 0$.

  for each $c \in C$ **do**

    if $P_d g_{d,B} \leq I_c$ **then**

      if $u_d(c) >$ *MaxUtility* **then**

        MaxUtility $\leftarrow u_d(c)$.

        $c^* \leftarrow c$.

  Return c^*.

APPENDIX 3. Greedy Resource Allocation Algorithm

Algorithm 3: GRA

Algorithm *GRA*

Input: Conflict Graph $CG_c=(V_c, E_c)$, $c \in \{1, 2, 3, \ldots, M\}$

Output: A feasible set of admitted D2D pairs Δ

for each $c \in M$ **do**

Update Conflict Graph CG_c.

Choose a D2D pair $d^* \in V_c$ with the minimum interference degree ID_d^c in CG_c, move it from V_c to set Δ_c.

Update the maximum tolerable interference $I_{m,max}$;

Remove all the D2D pairs that have conflict with d^*.

while $I_{m,max} > 0$ **do**

Choose another D2D pair $d^{**} \in V_c$ that has the minimum interference degree ID_d^c in CG_c, for each $d \in \Delta_c \cup \{d^{**}\}$, compute the current SINR and compare with their own SINR requirement.

If all the SINR requirements are satisfied, **then**

Add d^{**} to set Δ_c and update $I_{m,max}$.

Remove all the D2D pairs that have conflict with d^{**}.

else

Remove d^{**} from Δ_c;

Return Δ_c.

Return the set of admitted D2D pairs Δ.